

¹

Doctoral Thesis

²

Microbiota in Human Diseases

³

Jaewoong Lee

⁴

Department of Biomedical Engineering

⁵

Ulsan National Institute of Science and Technology

⁶

2025

7

Microbiota in Human Diseases

8

Jaewoong Lee

9

Department of Biomedical Engineering

10

Ulsan National Institute of Science and Technology

Microbiota in Human Diseases

A thesis/dissertation submitted to
Ulsan National Institute of Science and Technology
in partial fulfillment of the
requirements for the degree of
Doctor of Philosophy

Jaewoong Lee

04.16.2025 of submission

Approved by

Advisor

Semin Lee

Microbiota in Human Diseases

Jaewoong Lee

This certifies that the thesis/dissertation of Jaewoong Lee is approved.

04.16.2025 of submission

Signature

Advisor: Semin Lee

Signature

Taejoon Kwon

Signature

Eunhee Kim

Signature

Kyemyung Park

Signature

Min Hyuk Lim

13

Abstract

14 (Microbiome)

15 (PTB) Section 2 introduces...

16 (Periodontitis) Section 3 describes...

17 (Colon) Setion 4...

18 (Conclusion)

19

20 **This doctoral dissertation is an addition based on the following papers that the author has already
21 published:**

- 22 • Hong, Y. M., **Lee, Jaewoong**, Cho, D. H., Jeon, J. H., Kang, J., Kim, M. G., ... & Kim, J. K. (2023).
23 Predicting preterm birth using machine learning techniques in oral microbiome. *Scientific Reports*,
24 13(1), 21105.

Contents

26	1	Introduction	1
27	2	Predicting preterm birth using random forest classifier in salivary microbiome	8
28	2.1	Introduction	8
29	2.2	Materials and methods	10
30	2.2.1	Study design and study participants	10
31	2.2.2	Clinical data collection and grouping	10
32	2.2.3	Salivary microbiome sample collection	10
33	2.2.4	16s rRNA gene sequencing	10
34	2.2.5	Bioinformatics analysis	11
35	2.2.6	Data and code availability	11
36	2.3	Results	12
37	2.3.1	Overview of clinical information	12
38	2.3.2	Comparison of salivary microbiomes composition	12
39	2.3.3	Random forest classification to predict PTB risk	12
40	2.4	Discussion	20
41	3	Random forest prediction model for periodontitis statuses based on the salivary microbiomes	22
42	3.1	Introduction	22
43	3.2	Materials and methods	24
44	3.2.1	Study participants enrollment	24
45	3.2.2	Periodontal clinical parameter diagnosis	24
46	3.2.3	Saliva sampling and DNA extraction procedure	26
47	3.2.4	Bioinformatics analysis	26
48	3.2.5	Data and code availability	27
49	3.3	Results	29

50	3.3.1	Summary of clinical information and sequencing data	29
51	3.3.2	Diversity indices reveal differences among the periodontitis severities .	29
52	3.3.3	DAT among multiple periodontitis severities and their correlation . .	29
53	3.3.4	Classification of periodontitis severities by random forest models . .	30
54	3.4	Discussion	51
55	4	Metagenomic signature analysis of Korean colorectal cancer	55
56	4.1	Introduction	55
57	4.2	Materials and methods	57
58	4.2.1	Study participants enrollment	57
59	4.2.2	DNA extraction procedure	57
60	4.2.3	Bioinformatics analysis	57
61	4.2.4	Data and code availability	59
62	4.3	Results	60
63	4.3.1	Summary of clinical characteristics	60
64	4.3.2	Gut microbiome compositions	60
65	4.3.3	Diversity indices	61
66	4.3.4	DAT selection	62
67	4.3.5	ML prediction	63
68	4.4	Discussion	80
69	5	Conclusion	81
70	References		82
71	Acknowledgments		98

72

List of Figures

73	1	DAT volcano plot	14
74	2	Salivary microbiome compositions over DAT	15
75	3	Random forest-based PTB prediction model	16
76	4	Diversity indices	17
77	5	PROM-related DAT	18
78	6	Validation of random forest-based PTB prediction model	19
79	7	Diversity indices	37
80	8	Differentially abundant taxa (DAT)	38
81	9	Correlation heatmap	39
82	10	Random forest classification metrics	40
83	11	Random forest classification metrics from external datasets	41
84	12	Rarefaction curves for alpha-diversity indices	42
85	13	Salivary microbiome compositions in the different periodontal statuses	43
86	14	Correlation plots for differentially abundant taxa	44
87	15	Clinical measurements by the periodontitis statuses	45
88	16	Number of read counts by the periodontitis statuses	46
89	17	Proportion of DAT	47

90	18	Random forest classification metrics with the full microbiome compositions and ANCOM-selected DAT compositions	48
91			
92	19	Alpha-diversity indices account for evenness	49
93	20	Gradient Boosting classification metrics	50
94	21	Gut microbiome compositions in genus level	70
95	22	Alpha-diversity indices in genus level	71
96	23	Alpha-diversity indices with recurrence in genus level	72
97	24	Alpha-diversity indices with OS in genus level	73
98	25	Beta-diversity indices in genus level	74
99	26	Beta-diversity indices with recurrence in genus level	75
100	27	Beta-diversity indices with recurrence in genus level	76
101	28	DAT with recurrence in species level	77
102	29	DAT with OS in species level	78
103	30	Random forest classification and regression	79

List of Tables

105	1	Confusion matrix	6
106	2	Standard clinical information of study participants	13
107	3	Clinical characteristics of the study participants	32
108	4	Feature combinations and their evaluations	33
109	5	List of DAT among the periodontally healthy and periodontitis stages	34
110	6	Feature the importance of taxa in the classification of different periodontal statuses.	35
111	7	Beta-diversity pairwise comparisons on the periodontitis statuses	36
112	8	Clinical characteristics of CRC study participants	64
113	9	DAT list for CRC recurrence	65
114	10	DAT list for CRC OS	66
115	11	Random forest classification and their evaluations	68
116	12	Random forest regression and their evaluations	69

List of Abbreviations

- ¹¹⁸ **ACC** Accuracy
- ¹¹⁹ **ACE** Abundance-based coverage estimator
- ¹²⁰ **ASV** Amplicon sequence variant
- ¹²¹ **AUC** Area-under-curve
- ¹²² **BA** Balanced accuracy
- ¹²³ **BMI** Body mass index
- ¹²⁴ **C-section** Cesarean section
- ¹²⁵ **DAT** Differentially abundant taxa
- ¹²⁶ **F1** F1 score
- ¹²⁷ **Faith PD** Faith's phylogenetic diversity
- ¹²⁸ **FN** False negative
- ¹²⁹ **FP** False positive
- ¹³⁰ **FTB** Full-term birth
- ¹³¹ **GA** Gestational age
- ¹³² **MAE** Mean absolute error
- ¹³³ **MSI** Microsatellite instability
- ¹³⁴ **MSI-H** MSI-High
- ¹³⁵ **MSI-L** MSI-Low
- ¹³⁶ **MSS** Microsatellite stable
- ¹³⁷ **MWU test** Mann-Whitney U-test
- ¹³⁸ **OS** Overall survival
- ¹³⁹ **PRE** Precision
- ¹⁴⁰ **PROM** Prelabor rupture of membrane
- ¹⁴¹ **PTB** Preterm birth
- ¹⁴² **qPCR** quantitative-PCR

- ¹⁴³ **RMSE** Root mean squared error
- ¹⁴⁴ **ROC curve** Receiver-operating characteristics curve
- ¹⁴⁵ **rRNA** Ribosomal RNA
- ¹⁴⁶ **SD** Standard deviation
- ¹⁴⁷ **SEN** Sensitivity
- ¹⁴⁸ **SPE** Specificity
- ¹⁴⁹ **t-SNE** t-distributed stochastic neighbor embedding
- ¹⁵⁰ **TN** True negative
- ¹⁵¹ **TP** True positive

152 **1 Introduction**

153 The microbiome refers to the complex community of microorganisms, including bacteria, viruses, fungi,
154 and other microbes, that inhabit various environments within living organisms (Ursell, Metcalf, Parfrey,
155 & Knight, 2012; Gilbert et al., 2018). In humans, the microbiome plays a crucial role in maintaining
156 health (Lloyd-Price, Abu-Ali, & Huttenhower, 2016), influencing processes such as digestion (Lim, Park,
157 Tong, & Yu, 2020), immune response (Thaiss, Zmora, Levy, & Elinav, 2016; Kogut, Lee, & Santin, 2020;
158 C. H. Kim, 2018), and even mental health (Mayer, Tillisch, Gupta, et al., 2015; X. Zhu et al., 2017;
159 X. Chen, D'Souza, & Hong, 2013). These microbial communities are not static nor constant, but rather
160 dynamic ecosystem that interacts with their host and respond to environmental changes. Recent studies
161 have revealed that imbalances in the microbiome, known as dysbiosis, can contribute to a wide range of
162 diseases, including obesity (John & Mullin, 2016; Tilg, Kaser, et al., 2011; Castaner et al., 2018), diabetes
163 (Barlow, Yu, & Mathur, 2015; Hartstra, Bouter, Bäckhed, & Nieuwdorp, 2015; Sharma & Tripathi, 2019),
164 infections (Whiteside, Razvi, Dave, Reid, & Burton, 2015; Alverdy, Hyoju, Weigerinck, & Gilbert, 2017),
165 inflammatory conditions (Francescone, Hou, & Grivennikov, 2014; Peirce & Alviña, 2019; Honda &
166 Littman, 2012), and cancers (Helmink, Khan, Hermann, Gopalakrishnan, & Wargo, 2019; Cullin, Antunes,
167 Straussman, Stein-Thoeringer, & Elinav, 2021; Sepich-Poore et al., 2021; Schwabe & Jobin, 2013). Thus,
168 understanding the composition of the human microbiomes is essential for developing new therapeutic
169 approaches that target these microbial populations to promote health and prevent diseases.

170 The microbiome participates a crucial role in overall health, influencing not only digestion and immune
171 function but also systemic and neurological processes through the brain-gut axis (Martin, Osadchiy,
172 Kalani, & Mayer, 2018; Aziz & Thompson, 1998; R. Li et al., 2024). The gut microbiota interact with
173 the host through metabolic byproducts, immune signaling, and the production of neurotransmitters, *e.g.*
174 serotonin and dopamine, which are essential for brain function and cognition. Disruptions in microbial
175 composition, known as dysbiosis, have been linked to various diseases, including inflammatory bowel
176 disease (Sultan et al., 2021; Baldelli, Scaldaferrri, Putignani, & Del Chierico, 2021), obesity (Kang et al.,
177 2022; Hamjane, Mechita, Nourouti, & Barakat, 2024; Pezzino et al., 2023), diabetes (Cai et al., 2024;
178 X. Li et al., 2021; Y. Li et al., 2023), and cardiovascular diseases (Manolis, Manolis, Melita, & Manolis,
179 2022; Tian et al., 2021). Furthermore, the brain-gut axis, a bidirectional communication system between
180 the gut microbiome composition and the central nervous system, has been implicated in mental disorders,
181 *e.g.* anxiety disorder, depressive disorder, and neurodegenerative diseases. Emerging evidence suggested
182 that alterations in the host microbiome can influence mood, cognitive function, and even behavior through
183 immune modulation, vagus nerve signaling, and microbial metabolites. These findings highlight the
184 microbiome as a critical factor in maintaining host health and suggest that targeted interventions, namely
185 probiotics, antibiotics, dietary modification, and microbiome-based therapies, may hold promise for
186 improving both physical and mental comfort. Hence, understanding the microbial effects could lead to
187 novel therapeutic strategies for a wide range of health conditions.

188 16S ribosomal RNA (rRNA) gene sequencing is one of the most extensively applied methods for
189 characterizing microbial communities by targeting the conserved 16S rRNA gene, which contains both

190 highly conserved and variable regions in bacteria (Tringe & Hugenholtz, 2008; Janda & Abbott, 2007).
191 The conserved regions enable universal primer binding, while the variable regions provide the specificity
192 needed to differentiate microbial taxa. Among these regions, the V3-V4 region is frequently selected for
193 sequencing due to its balance between phylogenetic resolution and sequencing efficiency (Johnson et al.,
194 2019; López-Aladid et al., 2023). Therefore, the V3-V4 region offers sufficient variability to classify a
195 wide range of bacteria taxa while maintaining compatibility with widely used sequencing platforms.

196 On the other hand, PathSeq is a computational pipeline designed for the identification and analysis
197 of microbial sequences within short-read human sequencing data, such as next-generation sequencing
198 (Kostic et al., 2011; Walker et al., 2018). PathSeq's scalable and effective processing of massive amounts
199 of sequencing data allows large-scale microbial profiling possible. PathSeq workflow consists of two
200 main phases: a subtractive phase and an analytic phase. The subtractive phase is removing human-derived
201 reads by aligning them to a human reference genome; and, the analytic phase is mapping remaining reads
202 to microbial reference databases, not only bacterial reference genome, but also archaeal, fungal, and viral
203 reference genomes. This approach allows for the comprehensive detection of microbiome compositions,
204 without a requirement for targeted amplification. PathSeq presents a more comprehensive and objective
205 evaluation of microbiome compositions than conventional microbiome profiling techniques including 16S
206 rRNA gene sequencing, capturing an assortment of microbial species beyond bacteria. Therefore, PathSeq
207 is an effective instrument for metagenomic research, infectious disease study, and microbiome analysis in
208 environmental and clinical contexts because of its capacity to operate with complex sequencing datasets
209 (Ojesina et al., 2013; Park et al., 2024; Tejeda et al., 2021).

210 Diversity indices are essential techniques for evaluating the complexity and variety of microbial
211 communities, in ecological and microbiological research (Tucker et al., 2017; Hill, 1973). Alpha-diversity
212 index attributes to the heterogeneity within a specific community, obtaining the number of different taxa
213 and the distribution of taxa among the individuals, *i.e.*, richness and evenness. On the other hand, beta-
214 diversity index measures the variations in microbiome compositions between the individuals, highlighting
215 differences among the microbiome compositions of the study participants (B.-R. Kim et al., 2017).
216 Altogether, by providing a thorough understanding of microbiome compositions, diversity indices, *e.g.*
217 alpha-diversity and beta-diversity, allow us to investigate factors that affecting community variability and
218 structure.

219 Differentially abundant taxa (DAT) detection is a key analytical approach in microbiome study to
220 identify microbial taxa that significantly differ in abundance between distinct study participant groups.
221 This DAT detection method is particularly valuable for understanding how microbial communities vary
222 across different conditions, such as disease states, environmental factors, and/or experimental treatments.
223 Various statistical and computational techniques, *e.g.* LEfSe (Segata et al., 2011), DESeq2 (Love, Huber,
224 & Anders, 2014), ANCOM (Lin & Peddada, 2020), and ANCOM-BC (Lin, Eggesbø, & Peddada,
225 2022; Lin & Peddada, 2024), are commonly used to assess differential abundance while accounting for
226 compositional and sparsity-related challenges in microbiome composition data (Swift, Cresswell, Johnson,
227 Stilianoudakis, & Wei, 2023; Cappellato, Baruzzo, & Di Camillo, 2022). Thus, identifying DAT can
228 provide insights into microbial biomarkers associated with specific health conditions or disease statuses,

enabling potential applications in diagnostics and therapeutics. However, due to the nature of microbiome composition data and the influence of sequencing depth, appropriate normalization and statistically adjustments are necessary to ensure reliable and stable detection of differentially abundant microbes (Xia, 2023; Pan, 2021). Integrating DAT detection analysis with functional profiling further enhances our understanding of the biological significance of microbial shifts or dysbiosis. As microbiome research advances, improving methodologies for DAT selection remains essential for uncovering meaningful microbial association and their potential roles in human diseases.

Classification is one of the supervised machine learning techniques used to categorized data into predefined classes based on features within the data (Kotsiantis, Zaharakis, & Pintelas, 2006; Sen, Hajra, & Ghosh, 2020). In other words, the method learns the relationship between input features and their corresponding output classes through the process of training a classification model using labeled data. Classification models are essential for advising choices in a wide range of applications, including medical diagnostics (Omondiagbe, Veeramani, & Sidhu, 2019). Thus, researchers could uncover sophisticated connections in input features and corresponding classes and produce reliable prediction by utilizing machine learning classification.

Random forest classification is one of the ensemble machine learning methods that constructs several decision trees during training and aggregates their results to provide classification predictions (Breiman, 2001; Geurts, Ernst, & Wehenkel, 2006). A portion of the features and classes—known as bootstrapping (Jiang & Simon, 2007; Champagne, McNairn, Daneshfar, & Shang, 2014; J.-H. Kim, 2009) and feature bagging (Bryll, Gutierrez-Osuna, & Quek, 2003; Alelyani, 2021; Yaman & Subasi, 2019)—are utilized to construct each tree in the forest. The majority vote from each tree determines the final classification, which lowers the possibility of overfitting in comparison to a single decision tree. Furthermore, random forest classifier offers several advantages, including its robustness to outliers and its ability to calculate the feature importance.

Furthermore, k -fold cross-validation is a widely applied resampling technique that enhances the reliability and robustness of machine learning models by iteratively evaluating their performance across multiple data partitions (Wong & Yeh, 2019; Ghojogh & Crowley, 2019). Instead of relying on a single train-test split, k -fold cross-validation divides the dataset into equally sized k folds, where the machine learning model is trained on $k - 1$ folds and tested on the remaining fold in an iterative manner. This process is repeated k times, with each fold serving as the test set once, and the final performance is averaged across all iterations to provide a more generalizable estimate of model metrics. By reducing the risk of overfitting and minimizing variance in performance evaluation, k -fold cross-validation ensures that the machine learning model is not overly dependent on a specific train-test split. By applying k -fold cross-validation, researchers can ensure that their machine learning models are both robust and reliable, leading to more accurate and reproducible results (Fushiki, 2011).

Evaluating the performance of a machine learning classification model is essential to ensure its reliability and effectiveness in real-world solutions and applications (Novaković, Veljović, Ilić, Papić, & Tomović, 2017; Hossin & Sulaiman, 2015; Hand, 2012). A confusion matrix is a tabular representation of predictions of classification, showing the counts of true positives (TP), true negatives (TN), false positives

(FP), and false negatives (FN) (Table 1). From this matrix, evaluations can be derived: accuracy (ACC; Equation 1), balanced accuracy (BA; Equation 2), F1 score (F1; Equation 3), sensitivity (SEN; Equation 4), specificity (SPE; Equation 5), and precision (PRE; Equation 6). These metrics are in [0, 1] range and high metrics are good metrics. The confusion matrix also helps in identifying specific types of errors, such as a tendency to produce false positive or false negatives, offering valuable insights for improving the classification model. By combining the confusion matrix with other evaluation metrics, researchers can comprehensively assess the classification metrics and refine it for real-world solutions and applications.

The receiver-operating characteristics (ROC) curve is a graphical representation used to evaluate the performance of a classification model by plotting the sensitivity against (1-specificity) at multiple threshold setting (Gonçalves, Subtil, Oliveira, & de Zea Bermudez, 2014; Obuchowski & Bullen, 2018; Centor, 1991). The ROC curve illustrates the trade-off between detecting true positives while minimizing false positives, suggesting determining the optimal decision threshold for classification. A key metric derived from the ROC curve is the area-under-curve (AUC), which quantifies overall ability of the classification model to discriminate between positive and negative predictions. An AUC value of 0.5 indicates a model performing no better than random chance, while value closer to 1.0 suggests high predictive accuracy. Thus, by analyzing the AUC value of the ROC curve, researchers can compare different models and select the better classification model that offers the best balance between sensitivity and specificity for a given application.

Regression is a powerful predictive machine learning approach used to analyze complex relationships between variables and make continuous value predictions (Maulud & Abdulazeez, 2020; Yildiz, Bilbao, & Sproul, 2017). Beside classification, which assigns discrete labels, regression models estimate numerical outcomes based on input features, making them particularly useful in biological research and clinical applications for predicting disease risk, patient outcomes, and biomarker selection. By leveraging high-throughput biological techniques and clinical information, regression model enables the discovery of hidden patterns and the development of precision medicine strategies. As computational methods advance, integrating regression models with metagenomic data can improve predictive accuracy and facilitate data-driven therapeutic guide in healthcare.

Evaluating the performance of machine learning regression models requires assessing their prediction errors using appropriate metrics. Mean absolute error (MAE; Equation 7) and root mean squared error (RMSE; Equation 8) are commonly used measures for quantifying the accuracy of regression models. By optimizing regression models based on MAE and RMSE, researchers can improve prediction accuracy and enhance the reliability of machine learning regression models.

This dissertation present a comprehensive, multi-disease human microbiome analysis, bridging the association between preterm birth (PTB) (Section 2), periodontitis (Section 3), and colorectal cancer (CRC) (Section 4) through a unified metagenomic approach. While previous studies have examined the role and characteristics of human microbiome in these diseases individually, this dissertation uniquely integrates human microbiome-driven insights across these diseases to identify shared and disease-specific microbial signatures. By applying high-throughput metagenomic sequencing, microbial diversity analysis, and advanced bioinformatics techniques, this dissertation aims to uncover novel microbiome-based

307 biomarkers and mechanistic insights into how microbial communities influence these conditions. These
308 findings contribute to a broader understanding of microbiome-mediated disease interactions and pave the
309 way for personalized medicine strategies, including microbiome-targeted diagnostics and therapeutics.

Table 1: Confusion matrix

		Predicted	
		Positive	Negative
Actual	Positive	True positive (TP)	False negative (FN)
	Negative	False positive (FP)	True negative (TN)

$$310 \quad ACC = \frac{TP + TN}{TP + FN + FP + TN} \quad (1)$$

$$311 \quad BA = \frac{1}{2} \times \left(\frac{TP}{TP + FP} + \frac{TN}{TN + FN} \right) \quad (2)$$

$$312 \quad F1 = \frac{2 \times TP}{2 \times TP + FP + FN} \quad (3)$$

$$313 \quad SEN = \frac{TP}{TP + FP} \quad (4)$$

$$314 \quad SPE = \frac{TN}{TN + FN} \quad (5)$$

$$315 \quad PRE = \frac{TP}{TP + FP} \quad (6)$$

$$316 \quad MAE = \sum_{i=1}^n |Prediction_i - Real_i| / n \quad (7)$$

$$RMSE = \sqrt{\sum_{i=1}^n (Prediction_i - Real_i)^2 / n} \quad (8)$$

317 **2 Predicting preterm birth using random forest classifier in salivary mi-**
318 **crobiome**

319 **This section includes the published contents:**

320 Hong, Y. M., **Lee, Jaewoong**, Cho, D. H., Jeon, J. H., Kang, J., Kim, M. G., ... & Kim, J. K. (2023).
321 Predicting preterm birth using machine learning techniques in oral microbiome. *Scientific Reports*, 13(1),
322 21105.

323 **2.1 Introduction**

324 Preterm birth (PTB), characterized by the delivery of neonates prior to 37 weeks of gestation, is one
325 of the major cause to neonatal mortality and morbidity (Blencowe et al., 2012). Multiple pregnancies
326 including twins, short cervical length, and infection on genitourinary tract are known risk factor for
327 PTB (Goldenberg, Culhane, Iams, & Romero, 2008). Nevertheless, the extent to which these aspects
328 affect birth outcomes is still up for debate. Henceforth, strategies to boost gestation and enhance delivery
329 outcomes can be more conveniently implemented when pregnant women at high risk of PTB are identified
330 early (Iams & Berghella, 2010).

331 Prediction models that can be utilized as a foundation for intervention methods still have an unac-
332 ceptable amount of classification evaluations, including accuracy, sensitivity, and specificity, despite a
333 great awareness of the risk factors that trigger PTB (Sotiriadis, Papatheodorou, Kavvadias, & Makrydi-
334 mas, 2010). Several attempts have been made to predict PTB through integrating data such as human
335 microbiome composition, inflammatory markers, and prior clinical data with predictive machine learn-
336 ing methods (Berghella, 2012). Because it is affordable and straightforward to use, fetal fibronectin is
337 commonly used in medical applications. However, with a sensitivity of only 56% that merely similar to
338 random prediction, it has a low classification evaluation (Honest et al., 2009). Due to the difficulty and
339 imprecision of the method in general, as well as the requirement for a qualified specialist cervical length
340 measuring is also restricted (Leitich & Kaider, 2003).

341 Preterm prelabor rupture of membranes (PROM) brought on by gestational inflammation and infection
342 contribute to about 70% of PTB cases (Romero, Dey, & Fisher, 2014). Nevertheless, as antibiotics and
343 anti-inflammatory therapeutic strategies were ineffective to decrease PTB occurrence rates, the pathology
344 of PTB has not been entirely elucidated by inflammatory and infectious pathways (Romero, Hassan, et al.,
345 2014). Recent researches on maternal microbiomes were beginning to examine unidentified connections
346 of PTB as a consequence of developmental processes in molecular biological technology (Fettweis et al.,
347 2019).

348 However, as anti-inflammatory and antibiotic therapies were insufficient to lower PTB occurrence
349 rates, infectious and inflammatory processes are insufficient to exhaustively clarify the pathogenesis and
350 pathophysiology of PTB. It has been hypothesized that the microbiota linked to PTB originate from either
351 a hematogenous pathway or the female genitourinary tract increasing through the vagina and/or cervix
352 (Han & Wang, 2013). Vaginal microbiome compositions have been found in women who eventually

353 acquire PTB, and recent studies have tried to predict PTB risk using cervico-vaginal fluid (Kindinger et
354 al., 2017). Even though previous investigation have confirmed the potential relationships between the
355 vaginal microbiome compositions and PTB, these studies are only able to clarify an upward trajectory.

356 Multiple unfavorable birth outcomes, including PROM and PTB, have been linked to periodontitis
357 as an independence risk factor, according to numerous epidemiological researches (Offenbacher et al.,
358 1996). It is expected that the oral microbiome will be able to explain additional hematogenous pathways
359 in light of these precedents; however, the oral microbiome composition of fetuses is limited understood.

360 Hence, in order to identify the salivary microbiome linked to PTB and to establish a machine learning
361 prediction model of PTB determined by oral microbiome compositions, this study examined the salivary
362 microbiome compositions of PTB study participants with a full-term birth (FTB) study participants.

363 **2.2 Materials and methods**

364 **2.2.1 Study design and study participants**

365 Between 2019 and 2021, singleton pregnant women who received treatment to Jeonbuk National University Hospital for childbirth were the participants of this study. This study was conducted according to the
366 Declaration of Helsinki (Goodyear, Krleza-Jeric, & Lemmens, 2007). The Institutional Review Board
367 authorized this study (IRB file No. 2019-01-024). Participants who were admitted for elective cesarean
368 sections (C-sections) or induction births, as well as those who had written informed consent obtained
369 with premature labor or PROM, were eligible.
370

371 **2.2.2 Clinical data collection and grouping**

372 Questionnaires and electronic medical records were implemented to gather information on both previous
373 and current pregnancy outcomes. The following clinical data were analyzed:

- 374 • maternal age at delivery
- 375 • diabetes mellitus
- 376 • hypertension
- 377 • overweight and obesity
- 378 • C-section
- 379 • history PROM or PTB
- 380 • gestational week on delivery
- 381 • birth weight
- 382 • sex

383 **2.2.3 Salivary microbiome sample collection**

384 Salivary microbiome samples were collected 24 hours before to delivery using mouthwash. The standard
385 methods of sterilizing were performed. Medical experts oversaw each stage of the sample collecting
386 procedure. Participants received instruction not to eat, drink, or brush their teeth for 30 minutes before
387 sampling salivary microbiome. Saliva samples were gathered by washing the mouth for 30 seconds with
388 12 mL of a mouthwash solution (E-zен Gargle, JN Pharm, Pyeongtaek, Gyeonggi, Korea). The samples
389 were tagged with the anonymous ID for each participant and kept in low temperature (4 °C) until they
390 underwent further processing. Genomic DNA was extracted using an ExgeneTM Clinic SV kit (GeneAll
391 Biotechnology, Seoul, Korea) following with the manufacturer instructions and store at -20 °C.

392 **2.2.4 16s rRNA gene sequencing**

393 Salivary microbiome samples were transported to the Department of Biomedical Engineering of the
394 Ulsan National Institute of Science and Technology . 16S rRNA sequencing was then carried out using a
395 commissioned Illumina MiSeq Reagent Kit v3 (Illumina, San Diego, CA, USA). Library methods were
396 utilized to amplify the V3-V4 areas. 300 base-pair paired-end reads were produced by sequencing the

397 pooled library using a v3 \times 600 cycle chemistry after the samples had been diluted to a final concentration
398 of 6 pM with a 20% PhiX control.

399 **2.2.5 Bioinformatics analysis**

400 The independent *t*-test was utilized to evaluate the differences of continuous values between from the
401 PTB participants than the FTB participants; χ^2 -square test was applied to decide statistical differences of
402 categorical values. Clinical measurement comparisons were conducted using SPSS (version 20.0) (Spss
403 et al., 2011). At $p < 0.05$, statistical significance was taken into consideration.

404 QIIME2 (version 2022.2) was implemented to import 16S rRNA gene sequences from salivary
405 microbiome samples of study participants for additional bioinformatics processing (Bolyen et al., 2019).
406 DADA2 was used to verify the qualities of raw sequences (Callahan et al., 2016). The remain sequences
407 were clustered into amplicon sequence variants (ASVs). Diversity indices, namely Faith PD for alpha
408 diversity index (Faith, 1992) and Hamming distance for beta diversity index (Hamming, 1950), were
409 calculated. MWU test (Mann & Whitney, 1947), and PERMANOVA multivariate test were evaluated for
410 measuring statistical significance (Anderson, 2014; Kelly et al., 2015).

411 Taxonomic assignment were implemented with HOMD (version 15.22) (T. Chen et al., 2010).
412 Afterward, DESeq2 was implemented to identify differentially abundant taxa (DAT) that could dis-
413 tinguish between salivary microbiome from PTB and FTB participants (Love et al., 2014). Taxa with
414 $|\log_2 \text{FoldChange}| > 1$ and $p < 0.05$ were considered as statistically significant.

415 The taxa for predicting PTB using salivary microbiome data were determined using a random forest
416 classifier (Breiman, 2001). Through stratified *k*-fold cross-validation (*k* = 5) that preserves the existence
417 rate of PTB and FTB participants, consistency and trustworthy classification were ensured (Wong & Yeh,
418 2019).

419 **2.2.6 Data and code availability**

420 All sequences from the 59 study participants have been published to the Sequence Read Archives
421 (project ID PRJNA985119): <https://dataview.ncbi.nlm.nih.gov/object/PRJNA985119>. Docker
422 image that employed throughout this study is available in the DockerHub: https://hub.docker.com/r/fumire/helixco_premature. Every code used in this study can be found on GitHub: https://github.com/CompbioLabUnist/Helixco_Premature.

425 **2.3 Results**

426 **2.3.1 Overview of clinical information**

427 In the beginning, 69 volunteer mothers were recruited for this study. However, due to insufficient clinical
428 information or twin pregnancies, 10 participants were excluded from the study participants. Demographic
429 and clinical information of the study participants are displayed in Table 2. Because PROM is one of the
430 leading factors of PTB, it was prevalent in the PTB group than the FTB group. Other maternal clinical
431 factors did not significantly differ between the FTB and PTB groups. There were no cases in both groups
432 that had a history of simultaneous periodontal disease or cigarette smoking.

433 **2.3.2 Comparison of salivary microbiomes composition**

434 The salivary microbiome composition was composed of 13953804 sequences from 59 study participants,
435 with 102305.95 ± 19095.60 and 64823.41 ± 15841.65 (mean \pm SD) reads/sample before and following
436 the quality-check stage, accordingly. There was not a significant distinction between the PTB and FTB
437 groups with regard to on alpha diversity nor beta diversity metrics (Figure 4).

438 DESeq2 was used to select 32 DAT that distinguish between the PTB and FTB groups out of the 465
439 species that were examined (Love et al., 2014): 26 FTB-enriched DAT and six PTB-enriched DAT. Seven
440 PROM-related DAT were removed from these 32 PTB-related DAT to lessen the confounding effect of
441 PROM (Figure 5). Therefore, there were a total of 25 PTB-related DAT: 22 FTB-enriched DAT and three
442 PTB-enriched DAT (Figure 1).

443 A significant negative correlation was found using Pearson correlation analysis between GW and
444 differences between PTB-enriched DAT and FTB-enriched DAT ($r = -0.542$ and $p = 7.8e-6$; Figure 5).

445 **2.3.3 Random forest classification to predict PTB risk**

446 To classify PTB according to DAT, random forest classifiers were constructed. The nine most significant
447 DAT were used to obtain the best BA (0.765 ± 0.071 ; Figure 3a). Moreover, random forest classification
448 model determined each DAT's importance (Figure 3b). We conducted a validation procedure on nine
449 twin pregnancies that were excluded in the initial study design in order to confirm the reliability and
450 dependability of our random forest-based PTB prediction model (Figure 6). Comparable to the PTB
451 prediction model on the 59 initial singleton study participants, the validation classification on PTB risk of
452 these twin participants have an accuracy of 87.5%.

Table 2: Standard clinical information of study participants.

Continuous variable for independent *t*-test. Categorical variable for Pearson's χ^2 -square test. Continuous variable: mean \pm SD. Categorical variable: count (proportion)

	PTB (n=30)	FTB (n=29)	p-value
Maternal age (years)	31.8 \pm 5.2	33.7 \pm 4.5	0.687
C-section	20 (66.7%)	24 (82.7%)	0.233
Previous PTB history	4 (13.3%)	1 (3.4%)	0.353
PROM	12 (40.0%)	1 (3.4%)	0.001
Pre-pregnant overweight	8 (26.7%)	7 (24.1%)	1.000
Gestational weight gain (kg)	9.0 \pm 5.9	11.5 \pm 4.6	0.262
Diabetes	2 (6.7%)	2 (6.9%)	1.000
Hypertension	11 (36.7%)	4 (13.8%)	0.072
Gestational age (weeks)	32.5 \pm 3.4	38.3 \pm 1.1	\leq 0.001
Birth weight (g)	1973.4 \pm 686.6	3283.4 \pm 402.7	\leq 0.001
Male	14 (46.7%)	13 (44.8%)	1.000

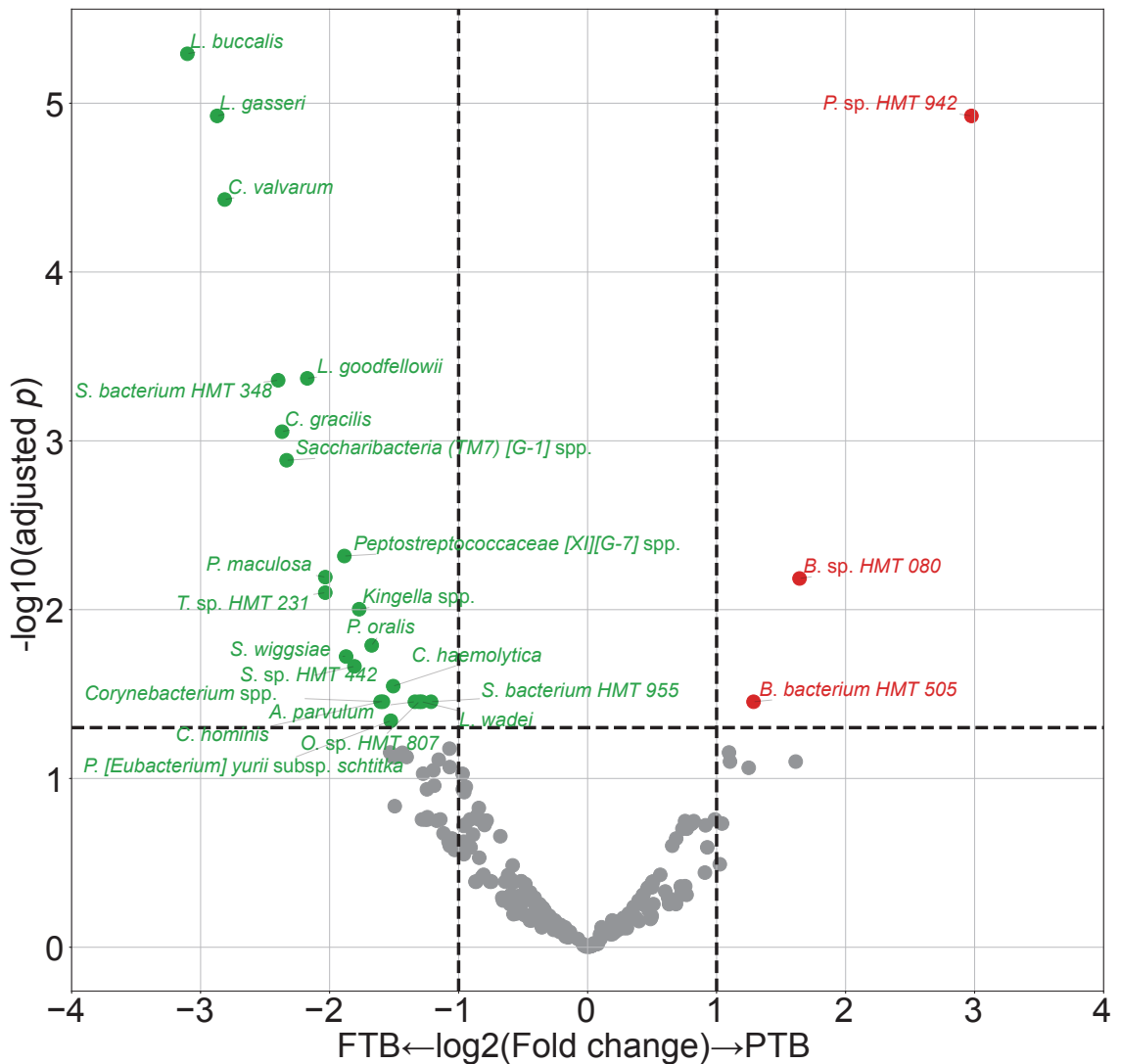


Figure 1: DAT volcano plot.

Red dots represent PTB-enriched DAT, while green dots represent FTB-enriched DAT.

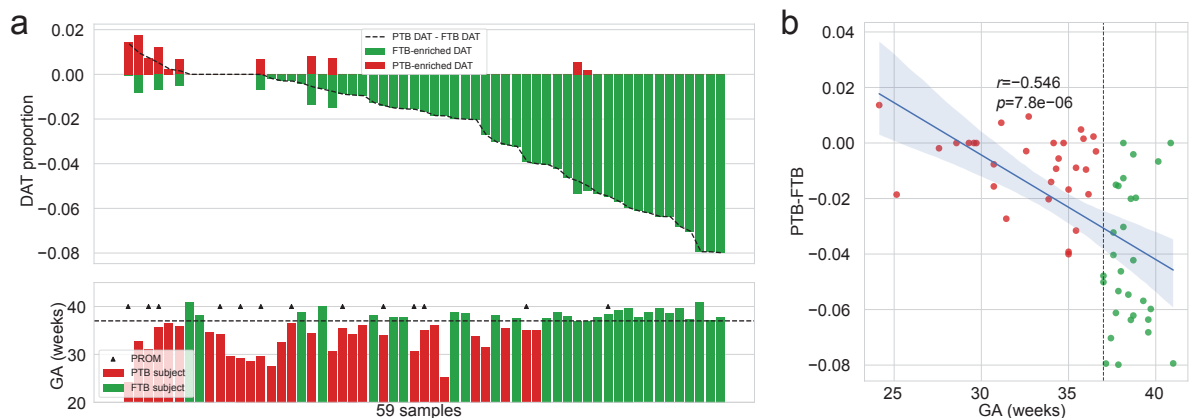


Figure 2: **Salivary microbiome compositions over DAT.**

(a) Frequencies of DAT of study subjects. The study participants are arranged in respect of (PTB-enriched DAT – FTB-enriched DAT). The study participants' GA is displayed in accordance with the upper panel's order (PTB: red bar, FTB: green bar. PROM: arrow head.) **(b)** Correlation plot with GA and (PTB-enriched DAT – FTB-enriched DAT). Strong negative correlation is found with Pearson correlation.

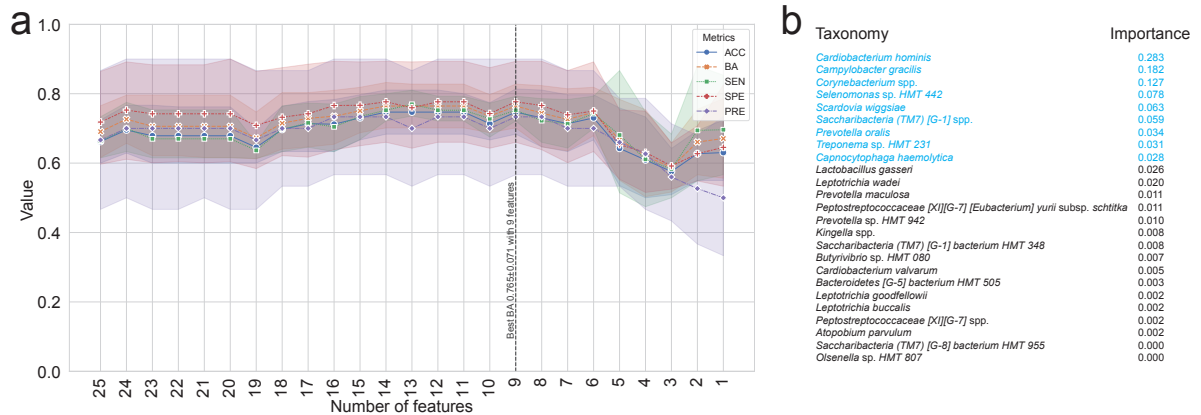


Figure 3: **Random forest-based PTB prediction model.**

(a) Machine learning evaluations upon number of features (DAT). Random Forest classifier has the best BA (0.765 ± 0.071 ; Mean \pm SD) with the nine most important DAT. **(b)** Importance of DAT.

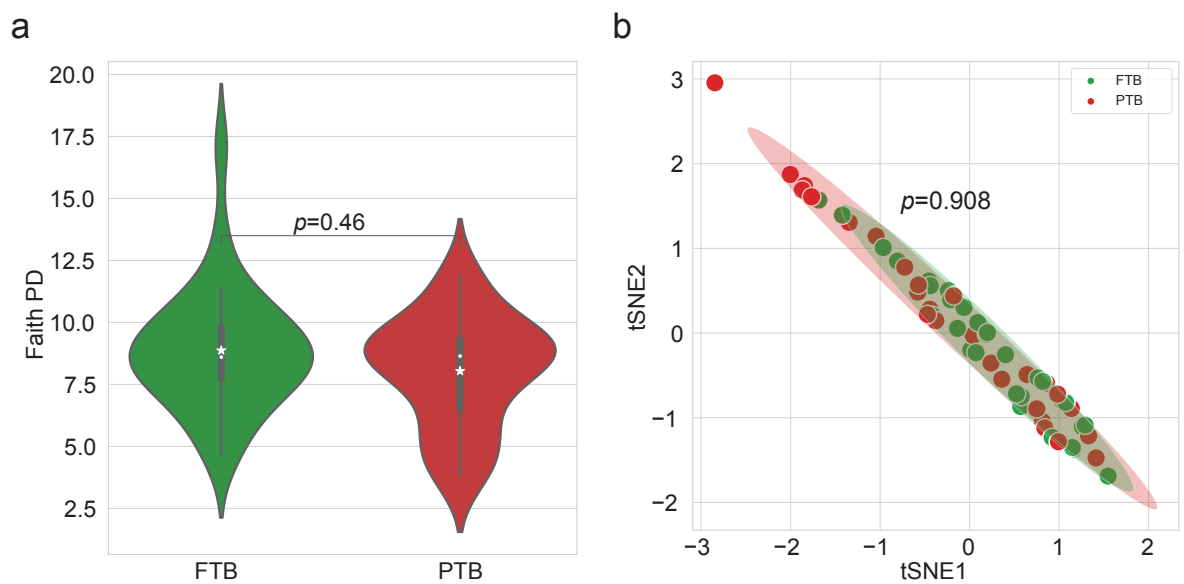


Figure 4: **Diversity indices.**

(a) Alpha diversity index (Faith PD). There is no statistically significant difference between the PTB and FTB group (MWU test $p = 0.46$). **(b)** t-SNE plot with beta diversity index (Hamming distance). There is no statistically significant difference between the PTB and FTB group (PERMANOVA test $p = 0.908$)

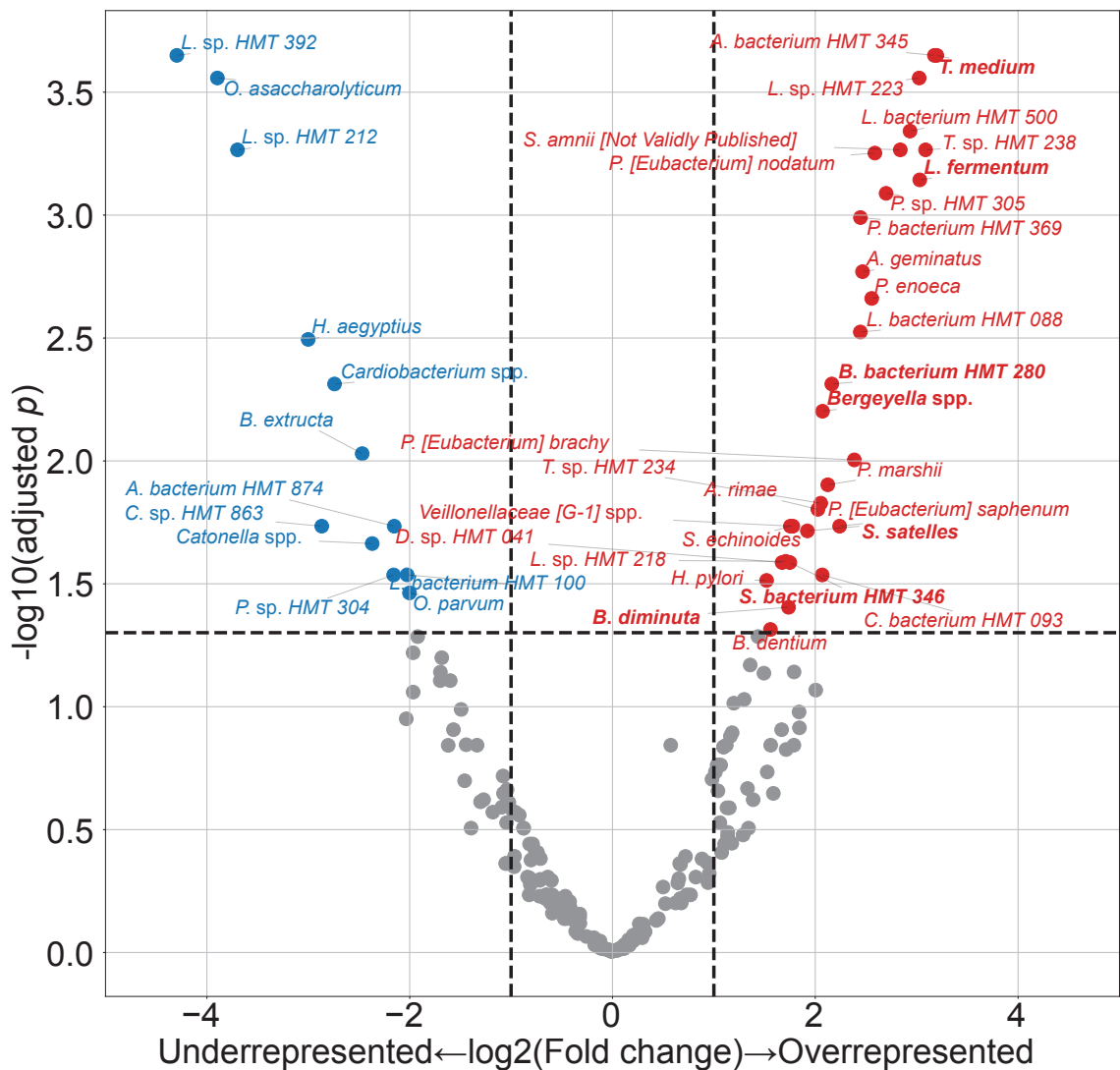


Figure 5: **PROM-related DAT**.

Only seven of these 42 PROM-related DAT overlapped with PTB-related DAT (bold text). Blue dots represented PROM-underrepresented DAT, while red dots represented PROM-overrepresented DAT.

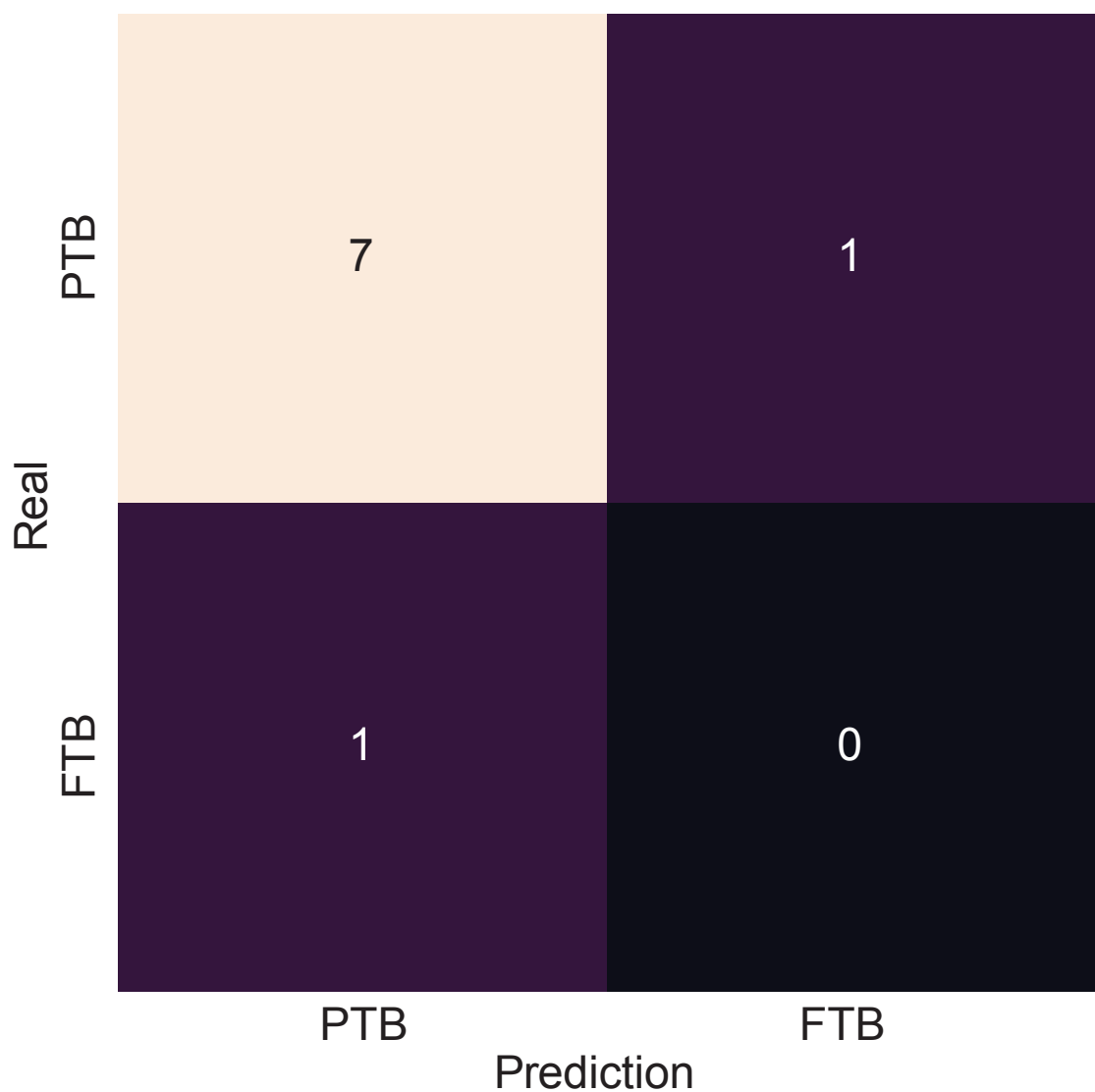


Figure 6: Validation of random forest-based PTB prediction model.

Nine twin pregnancies (eight PTB subjects and a FTB subject) that were excluded in the initial study subjects were subjected to a validation procedure. The random forest-based PTB prediction model shows 87.5% accuracy, comparable to the PTB classification evaluations on the singleton study subjects (0.714 ± 0.061 . Mean \pm SD)

453 **2.4 Discussion**

454 In this study, we employed salivary microbiome compositions to develop the random forest-based PTB
455 prediction models to estimate PTB risks. Previous reports have indicated bidirectional associations
456 between pregnancy outcomes and salivary microbiome compositions (Han & Wang, 2013). Nevertheless,
457 the salivary microbiome composition is not yet elucidated. Salivary microbial dysbiosis, including gingival
458 inflammation and periodontitis, have been connected to unfavorable pregnancy outcomes, such as PTB
459 (Ide & Papapanou, 2013). However, the techniques utilized in recent research that primarily focus on
460 recognized infections have led to inconsistent outcomes.

461 One of the most common salivary taxa that has been examined is *Fusobacterium nucleatum*, that is a
462 Gram-negative, anaerobic, and filamentous bacteria (Han, 2015; Brennan & Garrett, 2019; Bolstad, Jensen,
463 & Bakken, 1996). *Fusobacterium nucleatum* can be separated from not only the salivary microbiome
464 but also the vaginal microbiome (Vander Haar, So, Gyamfi-Bannerman, & Han, 2018; Witkin, 2019). In
465 both animal and human investigation, *Fusobacterium nucleatum* infection has been linked to risk of PTB
466 (Doyle et al., 2014). According to recent researches, the placenta women who give birth prematurely may
467 include additional salivary microbiome dysbiosis, such as *Bergeyella* spp. and *Porphyromonas gingivalis*
468 (León et al., 2007; Katz, Chegini, Shiverick, & Lamont, 2009). Although *Bergeyella* spp. were one of the
469 PROM-overrepresented DAT (Figure 5), it was excluded in the final 25 PTB-related DAT. Furthermore,
470 *Porphyromonas gingivalis* and *Campylobacter gracilis* were pathogens of periodontitis in sub-gingival
471 microbiome (Yang et al., 2022). *Lactobacillus gasseri* was also one of the FTB-enriched DAT (Figure
472 1), and it is well established that early PTB risk can be reduced by *Lactobacillus gasseri* in the vaginal
473 microbiome (Basavaprabhu, Sonu, & Prabha, 2020; Payne et al., 2021).

474 With DAT comprising 22 FTB-enriched DAT and three PTB-enriched DAT (Figure 1), we discovered
475 that the FTB study participants had the majority of the essential DAT that distinguished between the PTB
476 and FTB groups. Thus, we hypothesize that the pathogenesis and pathophysiology of PTB may have been
477 triggered by an absence of species with protective characteristics. The association between unfavorable
478 pregnancy outcomes and a dysfunctional microbiome has been explained through two distinct processes.
479 According to the first hypothesis, periodontal pathogens originating in the gingival biofilm might spread
480 from the infected salivary microbiome over the placenta microbiome, invade the intra-amniotic fluid
481 and fetal circulation, and then have a direct impact on the fetoplacental unit, leading to bacteremia
482 (Hajishengallis, 2015). Based on the second hypothesis, inflammatory mediators and endotoxins that
483 generated by the sub-gingival inflammation and derived from dental plaque of periodontitis may spread
484 throughout the body and reach the fetoplacental unit (Stout et al., 2013; Aagaard et al., 2014). Despite
485 belonging to the same species, some subgroups of the salivary microbiome may influence pregnancy
486 outcomes in both favorable and adverse manners. Following this line of argumentation, the salivary
487 microbiome composition or their dysbiosis are more significant than the existence of particular bacteria.

488 Notably, microbial alteration that take place throughout pregnancy may be expected results of a healthy
489 pregnancy. Those pregnancy-related vulnerabilities to dental problem like periodontitis can be explained
490 by three factors. Because of hormone-driven gingival hyper-reactivity to the salivary microbiome in the

491 oral biofilm including sub-gingival biofilm, these conditions are prevalent in pregnant women. For insight
492 at the relationship between the salivary microbiome compositions and PTB, further studies with pathway
493 analysis are warranted.

494 Our study confirmed that salivary microbiome composition could provide potential biomarkers for
495 predicting pregnancy complications including PTB risks using random forest-based classification models,
496 despite a limited number of study participants and a tiny validation sample size. Another limitation of our
497 study was 16S rRNA gene sequencing. In other words, unlike the shotgun sequencing, 16S rRNA gene
498 sequencing only focused on bacteria, not viruses nor fungi. We did not delve into other variables like
499 nutrition status and socioeconomic statuses of study participants that might affect the salivary microbiome
500 composition.

501 Notwithstanding these limitations, this prospective examination showed the promise of the random
502 forest-based PTB prediction models based on mouthwash-derived salivary microbiome composition.
503 Before applying the methods developed in this study in a clinical context, more multi-center and extensive
504 research is warranted to validate our findings.

505 **3 Random forest prediction model for periodontitis statuses based on the**
506 **salivary microbiomes**

507 **3.1 Introduction**

508 Saliva microbial dysbiosis brought on by the accumulation of plaque results in periodontitis, a chronic
509 inflammatory disease of the tissue that surrounds the tooth (Kinane, Stathopoulou, & Papapanou, 2017).
510 Loss of periodontal attachment is a consequence of periodontitis, which may lead to irreversible bone loss
511 and, eventually, permanent tooth loss if left untreated. A new classification criterion of periodontal diseases
512 was created in 2018, about 20 years after the 1999 statements of the previous one (Papapanou et al.,
513 2018). Even with this evolution, radiographic and clinical markers of periodontitis progression remain the
514 primary methods for diagnosing periodontitis (Papapanou et al., 2018). Such tools, nevertheless, frequently
515 demonstrate the prior damage from periodontitis rather than its present condition. Certain individuals have
516 a higher risk of periodontitis, a higher chance of developing severe generalized periodontitis, and a worse
517 response to common salivary bacteria control techniques utilized to prevent and treat periodontitis. As a
518 result, the 2017 framework for diagnosing periodontitis additionally allows for the potential development
519 of biomarkers to enhance diagnosis and treatment of periodontitis (Tonetti, Greenwell, & Kornman, 2018).
520 Instead of only depending on the progression of periodontitis, a new etiological indication based on the
521 current state must be introduced in order to enable appropriate intervention through early detection of
522 periodontitis. Thus, the current clinical diagnostic techniques that rely on periodontal probing can be
523 uncomfortable for patients with periodontitis (Canakci & Canakci, 2007).

524 Due to the development of salivaomics, in this manner, the examination of saliva has emerged as
525 a significant alternative to the conventional ways of identifying periodontitis (Altingöz et al., 2021;
526 Melguizo-Rodríguez, Costela-Ruiz, Manzano-Moreno, Ruiz, & Illescas-Montes, 2020). Given that saliva
527 sampling is non-invasive, painless, and accessible to non-specialists, it may be a valuable instrument for
528 diagnosing periodontitis (Zhang et al., 2016). Furthermore, much research has suggested that periodontitis
529 could be a trigger in the development and exacerbation of metabolic syndrome (Morita et al., 2010; Nesbitt
530 et al., 2010). Consequently, alteration in these levels of salivary microbiome markers may serve as high
531 effective diagnostic, prognostic, and therapeutic indicators for periodontitis and other systemic diseases
532 (Miller, Ding, Dawson III, & Ebersole, 2021; Čižmárová et al., 2022). The pathogenesis of periodontitis
533 typically comprises qualitative as well as quantitative alterations in the salivary microbial community,
534 despite that it is a complex disease impacted by a number of contributing factors including age, smoking
535 status, stress, and nourishment (Abusleme, Hoare, Hong, & Diaz, 2021; Lafaurie et al., 2022). Depending
536 on the severity of periodontitis, the salivary microbial community's diversity and characteristics vary
537 (Abusleme et al., 2021), indicating that a new etiological diagnostic standards might be microbial
538 community profiling based on clinical diagnostic criteria. As a consequence, salivary microbiome
539 compositions have been characterized in numerous research in connection with periodontitis. High-
540 throughput sequencing, including 16S rRNA gene sequencing, has recently used in multiple studies to
541 identify variations in the bacterial composition of sub-gingival plaque collections from periodontal healthy

542 individuals and patients with periodontitis (Altabtbaei et al., 2021; Iniesta et al., 2023; Nemoto et al., 2021).
543 This realization has rendered clear that alterations in the salivary microbial community—especially, shifts to
544 dysbiosis—are significant contributors to the pathogenesis and development of periodontitis (Lamont, Koo,
545 & Hajishengallis, 2018). Yet most of these research either focused only on the microbiome alterations in
546 sub-gingival plaque collection, comprised a limited number of periodontitis study participants, or did not
547 account for the impact of multiple severities of periodontitis.

548 For the objective of diagnosing periodontitis, previous research has developed machine learning-based
549 prediction models based on oral microbiome compositions, such as the sub-gingival microbial dysbiosis
550 index (T. Chen, Marsh, & Al-Hebshi, 2022; Chew, Tan, Chen, Al-Hebshi, & Goh, 2024), which have
551 demonstrated good diagnostic evaluation and could be applied to individual saliva collection. Despite
552 offering valuable details, these indicators are frequently restricted by their limited emphasis on classifying
553 the multiple severities of periodontitis. Furthermore, many of these machine learning models currently in
554 practice are trained solely upon the existence of periodontitis rather than on the multiple severities of
555 periodontitis.

556 Recently, we employed multiplex quantitative-PCR (qPCR) and machine learning-based classification
557 model to predict the severity of periodontitis based on the amount of nine pathogens of periodontitis from
558 saliva collections (E.-H. Kim et al., 2020). On the other hand, the fact that we focused merely at nine
559 pathogens for periodontitis and neglected the variety bacterial species associated to the various severities
560 of periodontitis constrained the breadth of our investigation. By developing a machine learning model
561 that could classify multiple severities of periodontitis based on the salivary microbiome composition,
562 this study aims to fill these knowledge gaps and produce more accurate and therapeutically useful
563 guidance to evaluate progression of periodontitis. Hence, in order to examine the salivary microbiome
564 composition of both healthy controls and patients with periodontitis in multiple stages, we applied
565 16S rRNA gene sequencing. Furthermore, employing the 2018 classification criteria, we sought to find
566 biomarkers (species) for the precise prediction of periodontitis severities (Papapanou et al., 2018; Chapple
567 et al., 2018).

568 **3.2 Materials and methods**

569 **3.2.1 Study participants enrollment**

570 Between 2018-08 and 2019-03, 250 study participants—100 healthy controls, 50 patients with stage I
571 periodontitis, 50 patients with stage II periodontitis, and 50 patients with stage III periodontitis—visited
572 visited the Department of Periodontics at Pusan National University Dental Hospital. The Institutional
573 Review Board of the Pusan National University Dental Hospital accepted this study protocol and design
574 (IRB No. PNUDH-2016-019). Every study participants provided their written informed authorization after
575 being fully informed about this study's objectives and methodologies. Exclusion criteria for the study
576 participants are followings:

- 577 1. People who, throughout the previous six months, underwent periodontal therapy, including root
578 planing and scaling.
- 579 2. People who struggle with systemic conditions that may affect periodontitis developments, such as
580 diabetes.
- 581 3. People who, throughout the previous three months, were prescribed anti-inflammatory medications
582 or antibiotics.
- 583 4. Women who were pregnant or breastfeeding.
- 584 5. People who have persistent mucosal lesions, *e.g.* pemphigus or pemphigoid, or acute infection, *e.g.*
585 herpetic gingivostomatitis.
- 586 6. Patient with grade C periodontitis or localized periodontitis (< 30% of teeth involved).

587 **3.2.2 Periodontal clinical parameter diagnosis**

588 A skilled periodontist conducted each clinical procedure. Six sites per tooth were used to quantify
589 gingival recession and probing depth: mesiobuccal, midbuccal, distobuccal, mesiolingual, midlingual,
590 and distolingual (Huang et al., 2007). A periodontal probe (Hu-Friedy, IL, USA) was placed parallel to
591 the major axis of the tooth at each tooth location in order to gather measurements. The cementoenamel
592 junction of the tooth was analyzed to determine the clinical attachment level, and the deepest point of
593 probing was taken to determine the periodontal pocket depth from the marginal gingival level of the
594 tooth. Plaque index was measured by probing four surfaces per tooth: mesial, distal, buccal, and palatal
595 or lingual. Plaque index was scored by the following criteria:

- 596 0. No plaque present.
- 597 1. A thin layer of plaque that adheres to the surrounding tissue of the tooth and free gingival margin.
598 Only through the use of a periodontal probe on the tooth surface can the plaque be existed.
- 599 2. Significant development of soft deposits that are visible within the gingival pocket, which is a
600 region between the tooth and gingival margin.

601 3. Considerable amount of soft matter on the tooth, the gingival margin, and the gingival pocket.

602 The arithmetic average of the plaque indices collected from every tooth was determined to calculate
603 plaque index of each study participant. By probing four surfaces per tooth, mesial, distal, buccal, and
604 palatal or lingual, to assess gingival bleeding, the gingival index was scored by the following criteria:

605 0. Normal gingiva: without inflammation nor discoloration.

606 1. Mild inflammation: minimal edema and slight color changes, but no bleeding on probing.

607 2. Moderate inflammation: edema, glazing, redness, and bleeding on probing.

608 3. Severe inflammation: significant edema, ulceration, redness, and spontaneous bleeding.

609 The arithmetic average of the gingival indices collected from every tooth was determined to calculate
610 gingival index of each study participant. The relevant data was not displayed, despite that furcation
611 involvement and bleeding on probing were thoroughly utilized into account during the diagnosis process.

612 Periodontitis was diagnosed in respect to the 2018 classification criteria (Papapanou et al., 2018;
613 Chapple et al., 2018). An experienced periodontist diagnosed the periodontitis severity by considering
614 complexity, depending on clinical examinations including radiographic images and periodontal probing.

615 Periodontitis is categorized into healthy, stage I, stage II, and stage III with the following criteria:

616 • Healthy:

617 1. Bleeding sites < 10%

618 2. Probing depth: \leq 3 mm

619 • Stage I:

620 1. No tooth loss because of periodontitis.

621 2. Inter-dental clinical attachment level at the site of the greatest loss: 1-2 mm

622 3. Radiographic bone loss: < 15%

623 • Stage II:

624 1. No tooth loss because of periodontitis.

625 2. Inter-dental clinical attachment level at the site of the greatest loss: 3-4 mm

626 3. Radiographic bone loss: 15-33%

627 • Stage III:

628 1. Teeth loss because of periodontitis: \leq 3 teeth

629 2. Inter-dental clinical attachment level at the site of the greatest loss: \geq 5 mm

630 3. Radiographic bone loss: > 33%

631 **3.2.3 Saliva sampling and DNA extraction procedure**

632 All study participants received instructions to avoid eating, drinking, brushing, and using mouthwash for
633 at least an hour prior to the saliva sample collection process. These collections were conducted between
634 09:00 and 11:00. Mouth rinse was collected by rinsing the mouth for 30 seconds with 12 mL of a solution
635 (E-zen Gargle, JN Pharm, Korea). All saliva samples were tagged with anonymous ID and stored at -4 °C.

636 Bacteria DNA was extracted from saliva samples using an Exgene™Clinic SV DNA extraction kit
637 (GeneAll, Seoul, Korea), and quality and quantity of bacterial DNA was measured using a NanoDrop
638 spectrophotometer (Thermo Fisher Scientific, Wilmington, DE, USA). Hyper-variable regions (V3-V4)
639 of the 16S rRNA gene were amplified using the following primer:

- 640 • Forward: 5'-TCGTCGGCAGCGTCAGATGTGTATAAGAGACAGCCTACGGGNNGCWGCAG-3'
641 • Reverse: 5'-GTCTCGTGGGCTCGGAGATGTGTATAAGAGACAGGACTACHVGGGTATCTAATCC-3'

642 The standard protocols of the Illumina 16S Metagenomic Sequencing Library Preparation were
643 followed in the preparation of the libraries. The PCR conditions were as follows:

- 644 1. Heat activation for 30 seconds at 95 °C.
645 2. 25 cycles for 30 seconds at 95 °C.
646 3. 30 seconds at 55 °C.
647 4. 30 seconds at 72 °C.

648 NexteraXT Indexed Primer was applied to amplification 10 µL of the purified initial PCR products for
649 the final library creation. The second PCR used the same conditions as the first PCR conditions but with
650 10 cycles. 16S rRNA gene sequencing was performed via 2×300 bp paired-end sequencing at Macrogen
651 Inc. (Macrogen, Seoul, Korea) using Illumina MiSeq platform (Illumina, San Diego, CA, USA).

652 **3.2.4 Bioinformatics analysis**

653 We computed alpha-diversity and beta-diversity indices to quantify the divergence of phylogenetic
654 information. Following alpha-diversity indices were calculated using the scikit-bio Python package
655 (version 0.5.5) (Rideout et al., 2018), and these alpha-diversity indices were compared using the MWU
656 test:

- 657 • Abundance-based Coverage Estimator (ACE) (Chao & Lee, 1992)
658 • Chao1 (Chao, 1984)
659 • Fisher (Fisher, Corbet, & Williams, 1943)
660 • Margalef (Magurran, 2021)
661 • Observed ASVs (DeSantis et al., 2006)
662 • Berger-Parker *d* (Berger & Parker, 1970)
663 • Gini (Gini, 1912)

- Shannon (Weaver, 1963)
- Simpson (Simpson, 1949)

Aitchison index for a beta-diversity index was calculated using QIIME2 (version 2020.8) (Aitchison, Barceló-Vidal, Martín-Fernández, & Pawlowsky-Glahn, 2000; Bolyen et al., 2019). We employed the t-SNE algorithm to illustrate multi-dimensional data from the beta-diversity index computation (Van der Maaten & Hinton, 2008). The beta-diversity index was compared using the PERMANOVA test (Anderson, 2014; Kelly et al., 2015) and MWU test.

DAT between multiple periodontitis stages were identified by ANCOM (Lin & Peddada, 2020). The log-transformed absolute abundances of DAT were analyzed by hierarchical clustering in order to identify sub-groups with similar abundance patterns on periodontitis severities. Additionally, we examined the relative proportions among the 20 DAT in order to reduce the effect of salivary bacteria that differ insignificantly across the multiple severities of periodontitis.

Differentially abundant taxa (DAT) among multiple periodontitis severities were selected from the salivary microbiome compositions by ANCOM (Lin & Peddada, 2020). In contrast to conventional techniques that examine raw abundance counts, ANCOM applies log-ratio between taxa to account for the salivary microbiome composition data. The log-transformed abundances of DAT were subjected to hierarchical clustering to discover subgroups of DAT with similar patterns on periodontitis severities. Furthermore, we examined the relative proportion among the DAT in order to reduce the effects of other salivary bacteria that differ non-significantly across the multiple periodontitis severities.

As previously stated (E.-H. Kim et al., 2020), we used stratified k -fold cross-validation ($k = 10$) by severity of periodontitis to achieve consistent and trustworthy classification results (Wong & Yeh, 2019). Additionally, we utilized various features with confusion matrices and their derivations to evaluate the classification outcomes in order to identify which features optimize classification evaluations and decrease sequencing efforts. Using the DAT discovered by ANCOM, we iteratively removed the least significant taxa from the input features (taxa) of the random forest (Breiman, 2001) and gradient boosting (Friedman, 2002) classification models using the backward elimination method. Random forest classifier builds multiple decision trees independently using bootstrapped samples and aggregates their predictions, enhancing stability and reducing overfitting problems. In contrast, Gradient boosting constructs trees sequentially, where each new tree improves the errors of the previous ones using gradient descent, leading to higher classification evaluations.

We investigated external datasets from Spanish individuals (Iniesta et al., 2023) and Portuguese individuals (Relvas et al., 2021) to confirm that our random forest classification was consistent. To ascertain repeatability and dependability, the external datasets were processed using the same pipeline and parameters as those used for our study participants.

3.2.5 Data and code availability

All sequences from the 250 study participants have been published to the Sequence Read Archives (project ID PRJNA976179): <https://www.ncbi.nlm.nih.gov/Traces/study/?acc=PRJNA976179>. Docker

701 image that employed throughout this study is available in the DockerHub: <https://hub.docker.com/>
702 repository/docker/fumire/periodontitis_16s. Every code used in this study can be found on
703 GitHub: https://github.com/CompbioLabUnist/Periodontitis_16S.

704 **3.3 Results**

705 **3.3.1 Summary of clinical information and sequencing data**

706 Among clinical information of the study participants, clinical attachment level, probing depth, plaque
707 index, and gingival index, were significantly increased with periodontitis severity (Kruskal-Wallis test
708 $p < 0.001$), while sex were observed no significant difference (Table 2). Notably, clinical attachment level
709 and probing depth have significant differences among the periodontitis severities (MWU test $p < 0.01$;
710 Figure 15). Additionally, 71461.00 ± 11792.30 and 45909.78 ± 11404.65 reads per sample were obtained
711 before and after filtering low-quality reads and trimming extra-long tails, respectively (Figure 16). In 250
712 study subjects, we have found a total of 425 bacterial taxa (Figure 13).

713 **3.3.2 Diversity indices reveal differences among the periodontitis severities**

714 Rarefaction curves showed that the sequencing depth was sufficient (Figure 12). Alpha-diversity indices
715 indicated significant differences between the healthy and the periodontitis stages (MWU test $p < 0.01$;
716 Figure 7a-e); however, there were no significant differences between the periodontitis stages. This
717 emphasizes how essential it is to classify the salivary microbiome compositions and distinguish between
718 the stages of periodontitis using machine learning approaches.

719 The confidence ellipses of the tSNE-transformed beta-diversity index (Aitchison index) indicated
720 distinct distributions among the periodontitis severities (PERMANOVA $p \leq 0.001$; Figure 7f). Aitchison
721 index demonstrated significant differences every pairwise of the periodontitis severities (PERMANOVA
722 test $p \leq 0.001$; Table 7). Significant differences in the distances between periodontitis severities further
723 demonstrated the uniqueness of each severity of periodontitis (MWU test $p \leq 0.05$; Figure 7g-j).

724 **3.3.3 DAT among multiple periodontitis severities and their correlation**

725 Of the 425 total taxa that identified in the salivary microbiome composition (Figure 13), 20 DAT were
726 identified (Table 5). Three separate subgroups were formed from the participants-level abundances of the
727 DAT using a hierarchical clustering methodology (Figure 8a):

- 728 • Group 1
 - 729 1. *Treponema* spp.
 - 730 2. *Prevotella* sp. HMT 304
 - 731 3. *Prevotella* sp. HMT 526
 - 732 4. *Peptostreptococcaceae [XI][G-5]* saphenum
 - 733 5. *Treponema* sp. HMT 260
 - 734 6. *Mycoplasma faecium*
 - 735 7. *Peptostreptococcaceae [XI][G-9]* brachy
 - 736 8. *Lachnospiraceae [G-8]* bacterium HMT 500
 - 737 9. *Peptostreptococcaceae [XI][G-6]* nodatum
 - 738 10. *Fretibacterium* spp.

- 739 • Group 2
- 740 1. *Porphyromonas gingivalis*
- 741 2. *Campylobacter showae*
- 742 3. *Filifactor alocis*
- 743 4. *Treponema putidum*
- 744 5. *Tannerella forsythia*
- 745 6. *Prevotella intermedia*
- 746 7. *Porphyromonas* sp. HMT 285

- 747 • Group 3
- 748 1. *Actinomyces* spp.
- 749 2. *Corynebacterium durum*
- 750 3. *Actinomyces graevenitzii*

751 Ten DAT that were significant enriched in stage II and stage III, but deficient in healthy formed Group
 752 1 (Figure 8). Furthermore, in comparison to the healthy, the seven DAT of Group 2 were significantly
 753 enriched in each of the stages of periodontitis. On the other hand, three DAT in Group 3 were deficient in
 754 stage II and stage III, but significantly enriched in healthy. The relative proportions of the DAT further
 755 supported these findings (Figure 8b), suggesting that the DAT is primarily linked to periodontitis rather
 756 than other salivary bacteria.

757 Correlation analysis from the DAT showed that DAT from Group 3 was negatively correlated with
 758 Group 1 and Group 2 (Figure 9), and strong correlations were observed the nine pairs of DAT (Figure 14).

759 3.3.4 Classification of periodontitis severities by random forest models

760 To confirm that using selected DAT bacterial profiles could have enhanced sequencing expenses without
 761 losing the classification evaluations, we built the random forest classification models based on DAT and
 762 full microbiome compositions (Figure 18). DAT based classifier showed non-significant different or better
 763 evaluations, by removing confounding taxa.

764 Based on the proportion of DAT, random forest classifier were trained to classify the periodontitis
 765 severities (Table 6). We conducted multi-label classification for the multiple periodontitis severities,
 766 namely healthy, stage I, stage II, and stage III. In this setting, we classified multiple periodontitis
 767 severities with the highest BA of 0.779 ± 0.029 (Table 4). AUC ranged between 0.81 and 0.94 (Figure
 768 10b).

769 Since timely detection in dentistry is demanding (Tonetti et al., 2018), we implemented a random
 770 forest classification for both healthy and stage I. Remarkably, the random forest classifier had the highest
 771 BA at 0.793 ± 0.123 (Table 4). In this setting, this model showed high AUC value for the classifying of
 772 stage I from healthy (AUC=0.85; Figure 10d).

773 Based on the findings that the salivary microbiome composition in stage II is more comparable to
 774 those in stage III than to other severities (Figure 7f and Figure 7j), we combined stage II and stage III to

775 perform a multi-label classification.

776 To examine alternative classification algorithms in comparison to random forest classification, we
777 selected gradient boost algorithm because it is another algorithm of the few classification algorithms
778 that can provide feature importances, which is essential for identifying key taxa contributing to the
779 classification of periodontitis severities. Thus, we assessed gradient boosting algorithms (Figure 20).
780 However, the classification evaluations obtained from gradient boosting have non-significant differences
781 compared to random forest classification.

782 Finally, to confirm the reliability and consistency of our random forest classifier, we validated our
783 classification model using openly accessible 16S rRNA gene sequencing from Spanish participants
784 (Iniesta et al., 2023) and Portuguese participants (Relvas et al., 2021) (Figure 11). Although some
785 evaluations, *e.g.* SPE, were low, the other were comparable.

Table 3: Clinical characteristics of the study participants.

Significant differences were assessed using the Kruskal-Wallis test. NA: Not applicable.

Index	Healthy	Stage I	Stage II	Stage III	p-value
Age (year)	33.83±13.04	43.30±14.28	50.26±11.94	51.08±11.13	6.18E-17
Gender (Male)	44 (44.0%)	22 (44.0%)	25 (50.0%)	25 (50.0%)	NA
Smoking (Never)	83 (83.0%)	36 (72.0%)	34 (68.0%)	29 (58.0%)	NA
Smoking (Ex)	12 (12.0%)	7 (14.0%)	9 (18.0%)	10 (20.0%)	NA
Smoking (Current)	2 (2.0%)	7 (14.0%)	7 (14.0%)	10 (20.0%)	NA
Number of teeth	28.03±2.23	27.36±1.80	26.72±2.89	25.74±4.34	8.07E-05
Attachment level (mm)	2.45±0.29	2.75±0.38	3.64±0.83	4.54±1.14	1.82E-35
Probing depth (mm)	2.42±0.29	2.61±0.40	3.27±0.76	3.95±0.88	6.43E-28
Plaque index	17.66±16.21	35.46±23.75	54.40±23.79	58.30±25.25	3.23E-22
Gingival index	0.09±0.16	0.44±0.46	0.85±0.52	1.06±0.52	2.59E-32

Table 4: Feature combinations and their evaluations

Classification performance with the most important taxon, the two most important taxa, and taxa with the best-balanced accuracy. *P.gingivalis* and *Act.* are *Porphyromonas gingivalis* and *Actinomyces* spp., respectively.

Classification	Features	ACC	AUC	BA	F1	PRE	SEN	SPE
Healthy vs. Stage I vs. Stage II vs. Stage III	<i>P.gingivalis</i>	0.758±0.051	0.716±0.177	0.677±0.068	0.839±0.034	0.839±0.034	0.516±0.102	
	<i>P.gingivalis+Act.</i>	0.792±0.043	0.822±0.105	0.723±0.057	0.861±0.029	0.861±0.029	0.584±0.086	
Top 5 taxa		0.834±0.022	0.870±0.079	0.779±0.029	0.889±0.015	0.889±0.015	0.668±0.033	
Healthy vs. Stage I	<i>Act.</i>	0.687±0.116	0.725±0.145	0.647±0.159	0.762±0.092	0.760±0.128	0.781±0.116	0.513±0.224
	<i>Act.+P.gingivalis</i>	0.733±0.119	0.831±0.081	0.713±0.122	0.797±0.097	0.797±0.126	0.798±0.082	0.627±0.191
Top 9 taxa		0.800±0.103	0.852±0.103	0.793±0.123	0.849±0.080	0.850±0.112	0.857±0.090	0.730±0.193
Healthy vs. Stage I vs. Stages II/III	<i>P.gingivalis</i>	0.776±0.042	0.736±0.196	0.748±0.047	0.832±0.031	0.832±0.031	0.664±0.062	
	<i>P.gingivalis+Act.</i>	0.843±0.035	0.876±0.109	0.823±0.039	0.882±0.026	0.882±0.026	0.764±0.052	
Top 6 taxa		0.885±0.036	0.914±0.027	0.871±0.038	0.914±0.027	0.914±0.025	0.828±0.051	
Healthy vs. Stages I/II/III	<i>P.gingivalis</i>	0.792±0.114	0.856±0.105	0.819±0.088	0.776±0.089	0.840±0.092	0.756±0.175	0.883±0.054
	<i>P.gingivalis+Act.</i>	0.828±0.121	0.926±0.074	0.847±0.116	0.797±0.123	0.800±0.126	0.830±0.191	0.864±0.074
Top 4 taxa		0.860±0.078	0.953±0.049	0.885±0.066	0.832±0.079	0.840±0.128	0.864±0.157	0.905±0.070

Table 5: List of DAT among healthy status and periodontitis stages

No.	Taxonomy	ANCOM W score
1	<i>Porphyromonas gingivalis</i>	424
2	<i>Actinomyces</i> spp.	424
3	<i>Filifactor alocis</i>	421
4	<i>Prevotella intermedia</i>	419
5	<i>Treponema putidum</i>	418
6	<i>Tannerella forsythia</i>	415
7	<i>Porphyromonas</i> sp. HMT 285	412
8	<i>Peptostreptococcaceae [XI][G-6] nodatum</i>	412
9	<i>Fretibacterium</i> spp.	411
10	<i>Mycoplasma faecium</i>	411
11	<i>Prevotella</i> sp. HMT 304	411
12	<i>Lachnospiraceae [G-8] bacterium</i> HMT 500	409
13	<i>Treponema</i> spp.	408
14	<i>Prevotella</i> sp. HMT 526	401
15	<i>Peptostreptococcaceae [XI][G-9] brachy</i>	400
16	<i>Peptostreptococcaceae [XI][G-5] saphenum</i>	398
17	<i>Campylobacter showae</i>	395
18	<i>Treponema</i> sp. HMT 260	393
19	<i>Corynebacterium durum</i>	393
20	<i>Actinomyces graevenitzii</i>	387

Table 6: Feature the importance of taxa in the classification of different periodontal statuses
 Taxa are ranked in descending order of importance; from most important to least important.

Condition	Healthy vs. Stage I vs. Stage II vs. Stage III			Healthy vs. Stage I			Healthy vs. Stage I vs. Stage II/III			Healthy vs. Stage I/II/III		
	Rank	Taxa	Importance	Taxa	Importance	Taxa	Importance	Taxa	Importance	Taxa	Importance	
1	<i>Porphyromonas gingivalis</i>	0.297	<i>Actinomyces spp.</i>	0.195	<i>Porphyromonas gingivalis</i>	0.360	<i>Porphyromonas gingivalis</i>	0.426	<i>Porphyromonas gingivalis</i>	0.461		
2	<i>Actinomyces spp.</i>	0.195	<i>Actinomyces graevenitzii</i>	0.054	<i>Actinomyces spp.</i>	0.125	<i>Actinomyces spp.</i>	0.244	<i>Actinomyces spp.</i>	0.257		
3	<i>Prevotella intermedia</i>	0.054	<i>Actinomyces graevenitzii</i>	0.052	<i>Porphyromonas sp. HMT 285</i>	0.055	<i>Actinomyces graevenitzii</i>	0.049	<i>Actinomyces graevenitzii</i>	0.059		
4	<i>Actinomyces graevenitzii</i>	0.052	<i>Lachnospiraceae (G-8) bacterium HMT 500</i>	0.050	<i>Porphyromonas sp. HMT 285</i>	0.062	<i>Corynebacterium durum</i>	0.046	<i>Corynebacterium durum</i>	0.035		
5	<i>Filifactor alocis</i>	0.050	<i>Campylobacter showae</i>	0.042	<i>Campylobacter showae</i>	0.052	<i>Filifactor alocis</i>	0.036	<i>Filifactor alocis</i>	0.032		
6	<i>Campylobacter showae</i>	0.042	<i>Porphyromonas sp. HMT 285</i>	0.040	<i>Corynebacterium durum</i>	0.052	<i>Prevotella intermedia</i>	0.033	<i>Campylobacter showae</i>	0.023		
7	<i>Porphyromonas sp. HMT 285</i>	0.040	<i>Treponema spp.</i>	0.032	<i>Treponema spp.</i>	0.038	<i>Tannerella forsythia</i>	0.025	<i>Porphyromonas sp. HMT 285</i>	0.022		
8	<i>Corynebacterium durum</i>	0.032	<i>Tannerella forsythia</i>	0.026	<i>Tannerella forsythia</i>	0.037	<i>Prevotella intermedia</i>	0.023	<i>Prevotella intermedia</i>	0.022		
9	<i>Treponema spp.</i>	0.032	<i>Prevotella intermedia</i>	0.025	<i>Prevotella intermedia</i>	0.029	<i>Treponema spp.</i>	0.021	<i>Treponema spp.</i>	0.022		
10	<i>Tannerella forsythia</i>	0.026	<i>Prevotella intermedia</i>	0.025	<i>Peptostreptococcaceae (XII)(G-9) brachy</i>	0.026	<i>Peptostreptococcaceae (XII)(G-9) brachy</i>	0.018	<i>Peptostreptococcaceae (XII)(G-9) brachy</i>	0.015		
11	<i>Treponema putidum</i>	0.025	<i>Freibacterium spp.</i>	0.023	<i>Peptostreptococcaceae (XII)(G-9) brachy</i>	0.018	<i>Lachnospiraceae (G-8) bacterium HMT 500</i>	0.014	<i>Lachnospiraceae (G-8) bacterium HMT 500</i>	0.010		
12	<i>Freibacterium spp.</i>	0.023	<i>Peptostreptococcaceae (XII)(G-9) brachy</i>	0.021	<i>Peptostreptococcaceae (XII)(G-9) brachy</i>	0.018	<i>Peptostreptococcaceae (XII)(G-6) nodatum</i>	0.011	<i>Tannerella forsythia</i>	0.009		
13	<i>Peptostreptococcaceae (XII)(G-9) brachy</i>	0.021	<i>Treponema putidum</i>	0.019	<i>Treponema putidum</i>	0.014	<i>Treponema putidum</i>	0.010	<i>Freibacterium spp.</i>	0.009		
14	<i>Treponema sp. HMT 260</i>	0.019	<i>Prevotella sp. HMT 526</i>	0.018	<i>Prevotella sp. HMT 526</i>	0.011	<i>Prevotella sp. HMT 526</i>	0.009	<i>Prevotella sp. HMT 526</i>	0.006		
15	<i>Prevotella sp. HMT 526</i>	0.018	<i>Peptostreptococcaceae (XII)(G-6) nodatum</i>	0.018	<i>Peptostreptococcaceae (XII)(G-6) nodatum</i>	0.008	<i>Freibacterium spp.</i>	0.008	<i>Peptostreptococcaceae (XII)(G-6) nodatum</i>	0.004		
16	<i>Peptostreptococcaceae (XII)(G-6) nodatum</i>	0.018	<i>Prevotella sp. HMT 304</i>	0.017	<i>Peptostreptococcaceae (XII)(G-6) nodatum</i>	0.008	<i>Treponema sp. HMT 260</i>	0.008	<i>Treponema sp. HMT 260</i>	0.004		
17	<i>Prevotella sp. HMT 304</i>	0.017	<i>Mycoplasma faecium</i>	0.014	<i>Mycoplasma faecium</i>	0.004	<i>Prevotella sp. HMT 304</i>	0.005	<i>Mycoplasma faecium</i>	0.003		
18	<i>Mycoplasma faecium</i>	0.014	<i>Prevotella sp. HMT 304</i>	0.014	<i>Peptostreptococcaceae (XII)(G-5) saphenum</i>	0.003	<i>Peptostreptococcaceae (XII)(G-5) saphenum</i>	0.005	<i>Peptostreptococcaceae (XII)(G-5) saphenum</i>	0.002		
19	<i>Peptostreptococcaceae (XII)(G-5) saphenum</i>	0.014	<i>Lachnospiraceae (G-8) bacterium HMT 500</i>	0.013	<i>Peptostreptococcaceae (XII)(G-5) saphenum</i>	0.003	<i>Prevotella sp. HMT 304</i>	0.004	<i>Prevotella sp. HMT 304</i>	0.001		
20	<i>Lachnospiraceae (G-8) bacterium HMT 500</i>	0.013										

Table 7: Beta-diversity pairwise comparisons on the periodontitis statuses

Statistically significant (p-value) was determined by the PERMANOVA test.

Group 1	Group 2	p-value
Healthy	Stage I	0.001
Healthy	Stage II	0.001
Healthy	Stage III	0.001
Stage I	Stage II	0.001
Stage I	Stage III	0.001
Stage II	Stage III	0.737

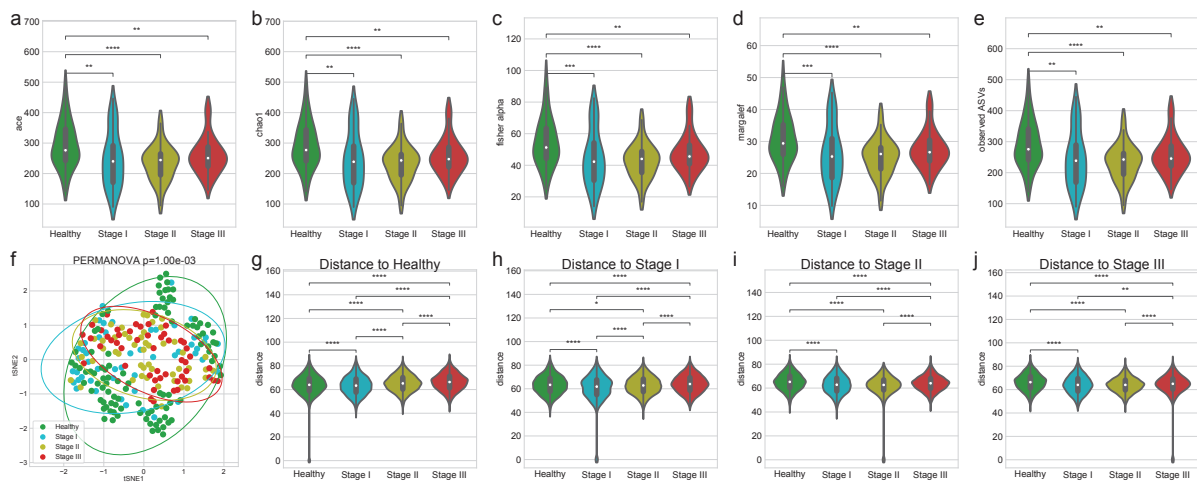


Figure 7: Diversity indices.

Alpha-diversity indices (a-e) indicate that healthy controls have increased heterogeneity than periodontitis stages as measured by: (a) ACE (b) Chao1 (c) Fisher alpha (d) Margalef, and (e) observed ASVs. (f) The beta-diversity index (weighted UniFrac) was visualized using a tSNE-transformed plot. The confidence ellipses are shown to display the distribution of each periodontitis stage. The distance to each stage demonstrated that each periodontitis stage was distinguished from the other periodontitis stages: (g) distance to Healthy (h) distance to Stage I (i) distance to Stage II, and (j) distance to Stage III. Statistical significance determined by the MWU test and the PERMANOVA test: $p < 0.05$ (*), $p < 0.01$ (**), $p < 0.001$ (***) $\text{, and } p \leq 0.0001$ (****).

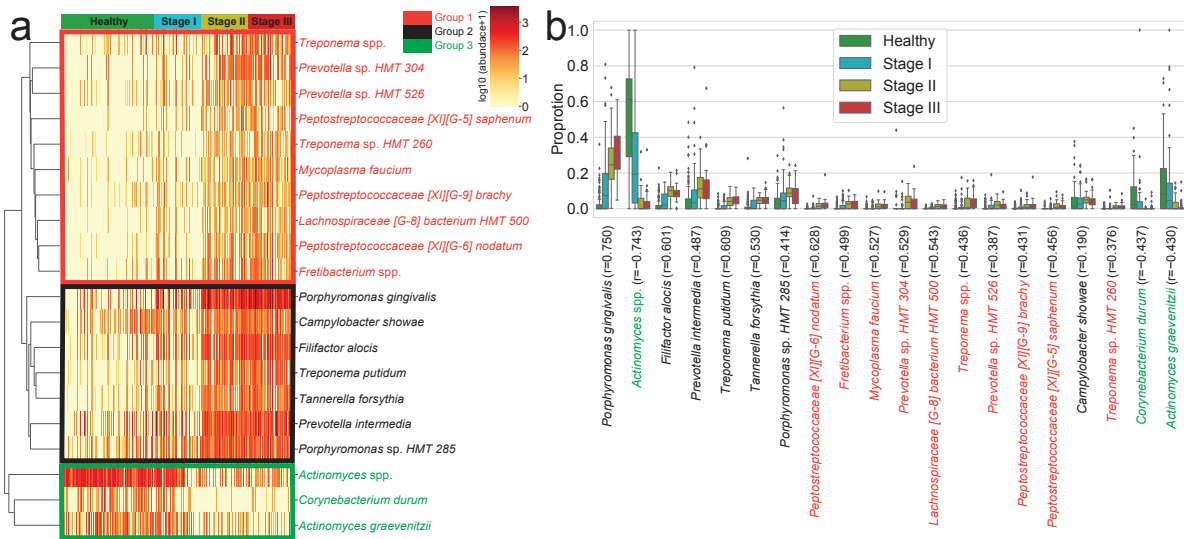


Figure 8: **Differentially abundant taxa (DAT).**

DAT that were identified by ANCOM. **(a)** Heatmap of clustered DAT with similar distribution among subjects. Group 1, Group 2, and Group 3 are marked in red, black, and green, respectively. **(b)** Box plots showing the proportions of DAT. Taxa were sorted by their importance according to ANCOM.

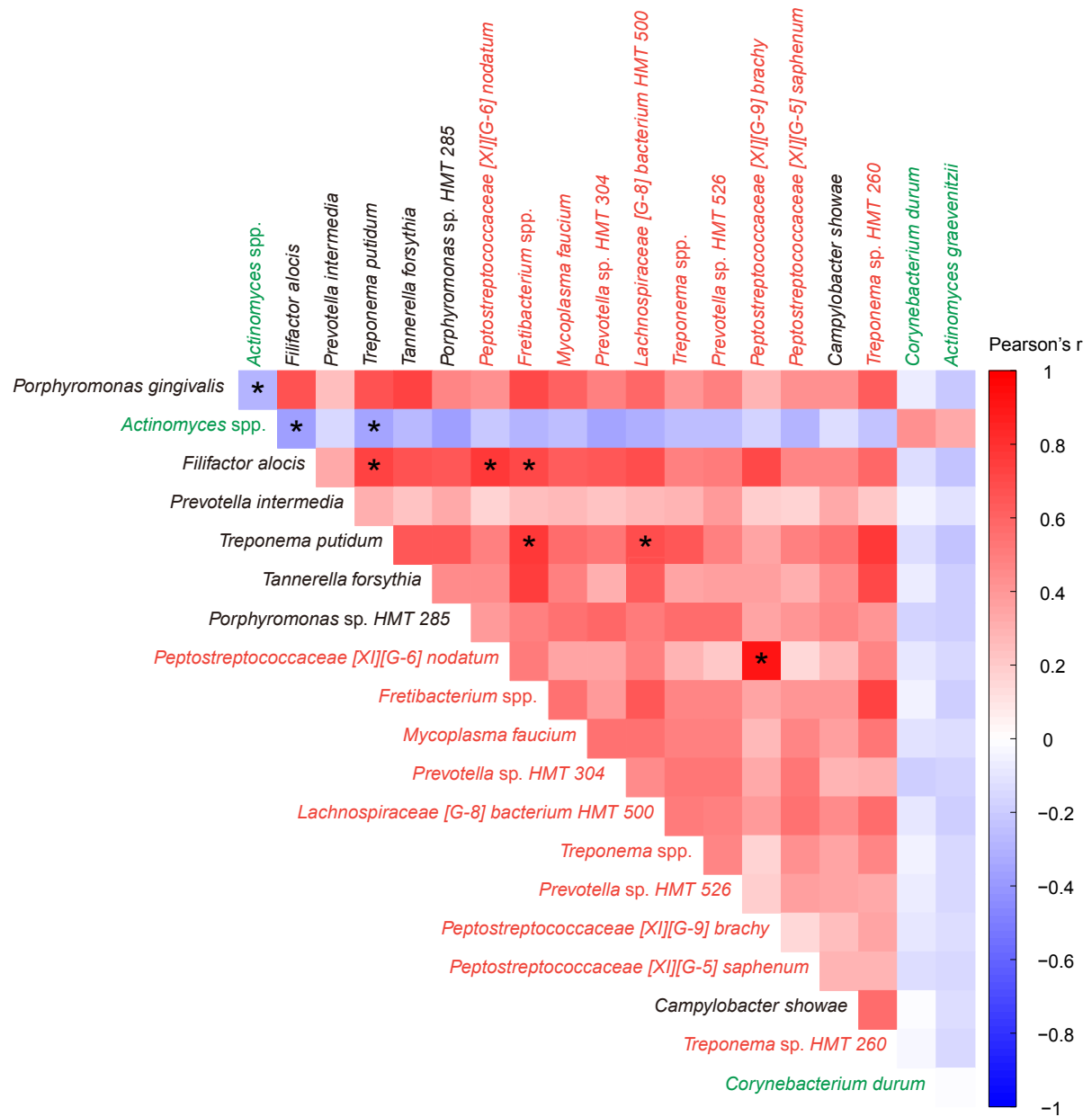


Figure 9: Correlation heatmap.

Pearson's correlations between DAT in healthy status and periodontitis stages. Statistical significance was determined by strong correlation, i.e., $|\text{coefficient}| \geq 0.5$ (*).

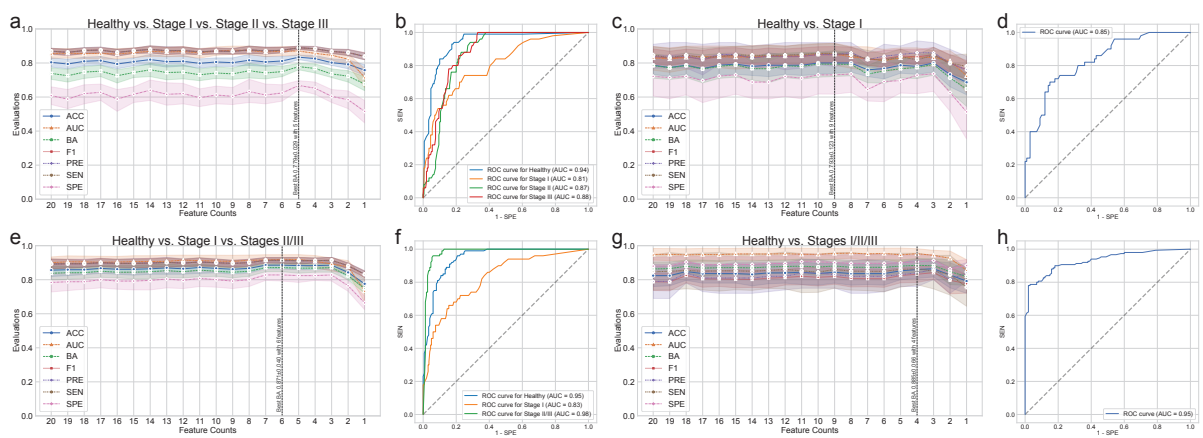


Figure 10: Random forest classification metrics.

The classification metrics in the random forest classifications were as follows: ACC, AUC, BA, F1, PRE, SEN, and SPE. **(a)** Classification performance for healthy vs. stage I vs. stage II vs. stage III. **(b)** ROC curve for the highest BA of (a). **(c)** Classification performance for healthy vs. stage I. **(d)** ROC curve on the highest BA of (c). **(e)** Classification performance for healthy vs. stage I vs. stages II/III. **(f)** ROC curve for the highest BA of (e). **(g)** Classification performance for healthy vs. stages I/II/III. **(h)** ROC curve for the highest BA of (h).

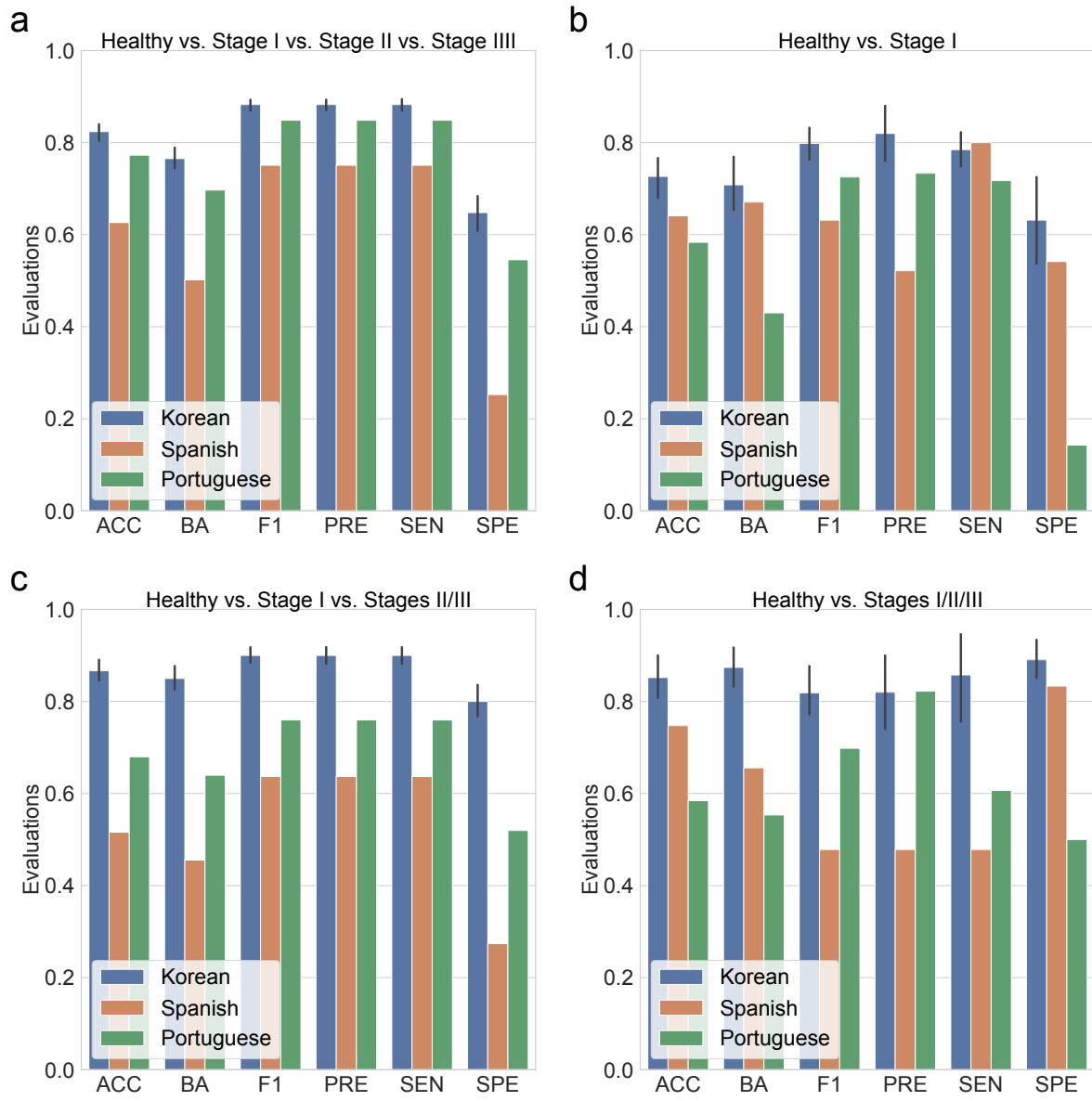


Figure 11: **Random forest classification metrics from external datasets.**

The classification metrics in the random forest classifications were as follows: ACC, AUC, BA, F1, PRE, SEN, and SPE. **(a)** Classification performance for healthy vs. stage I vs. stage II vs. stage III. **(b)** Classification performance for healthy vs. stage I. **(c)** Classification performance for healthy vs. stage I vs. stages II/III. **(d)** Classification performance for healthy vs. stages I/II/III.

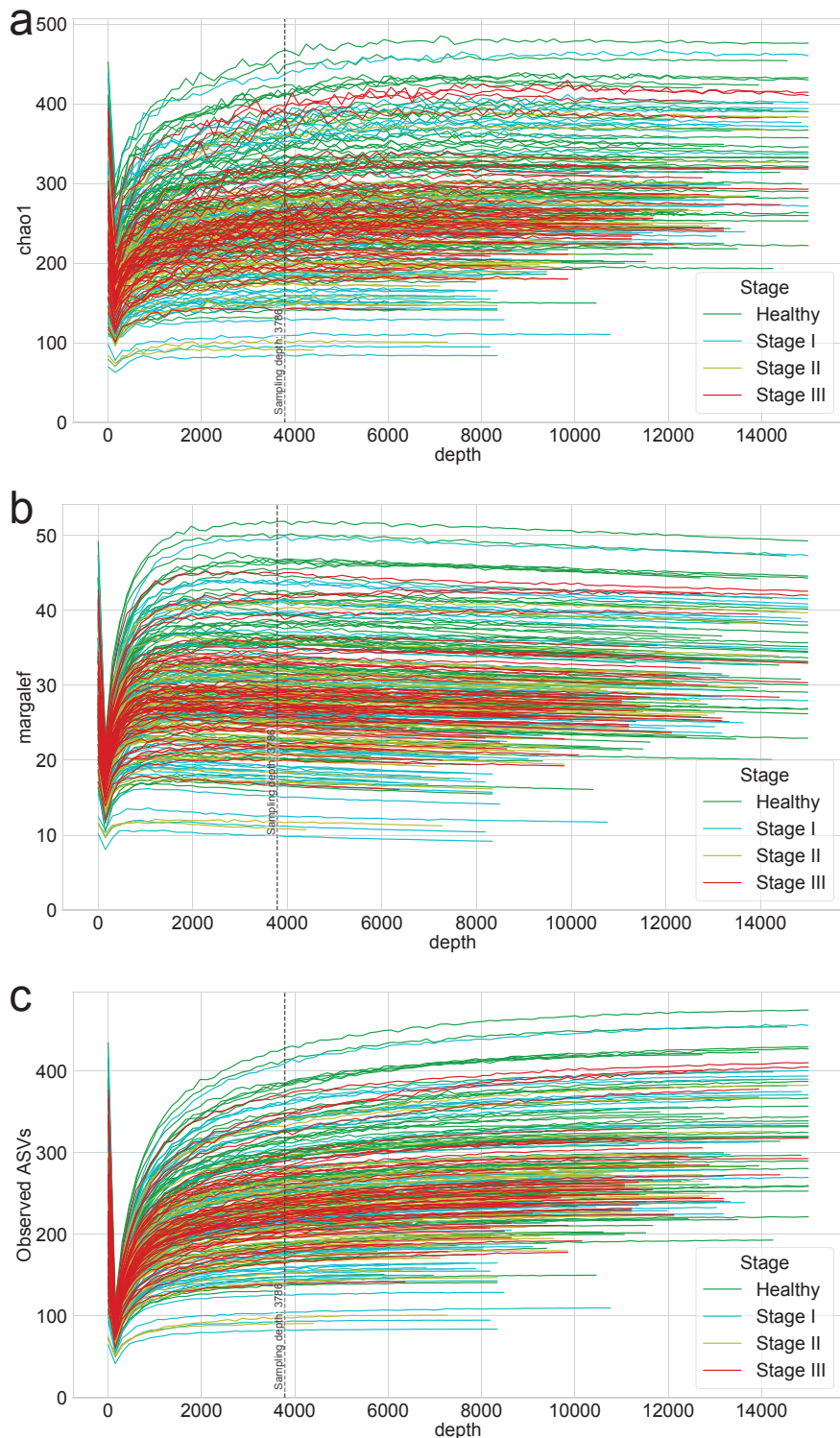


Figure 12: Rarefaction curves for alpha-diversity indices.

Rarefaction of (a) chao1 (b) margalef, and (c) observed ASVs were generated to measure species richness and determine the sampling depth of each sample.

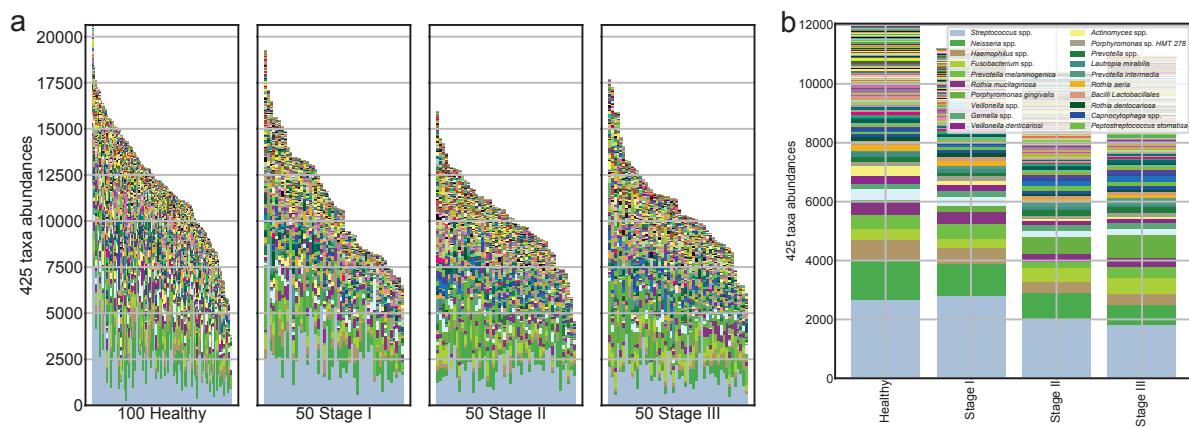


Figure 13: Salivary microbiome compositions in the different periodontal statuses.

Stacked bar plot of the absolute abundance of bacterial species for all samples (**a**) and the mean absolute abundance of bacterial species in the healthy, stage I, stage II, and stage III groups (**b**).

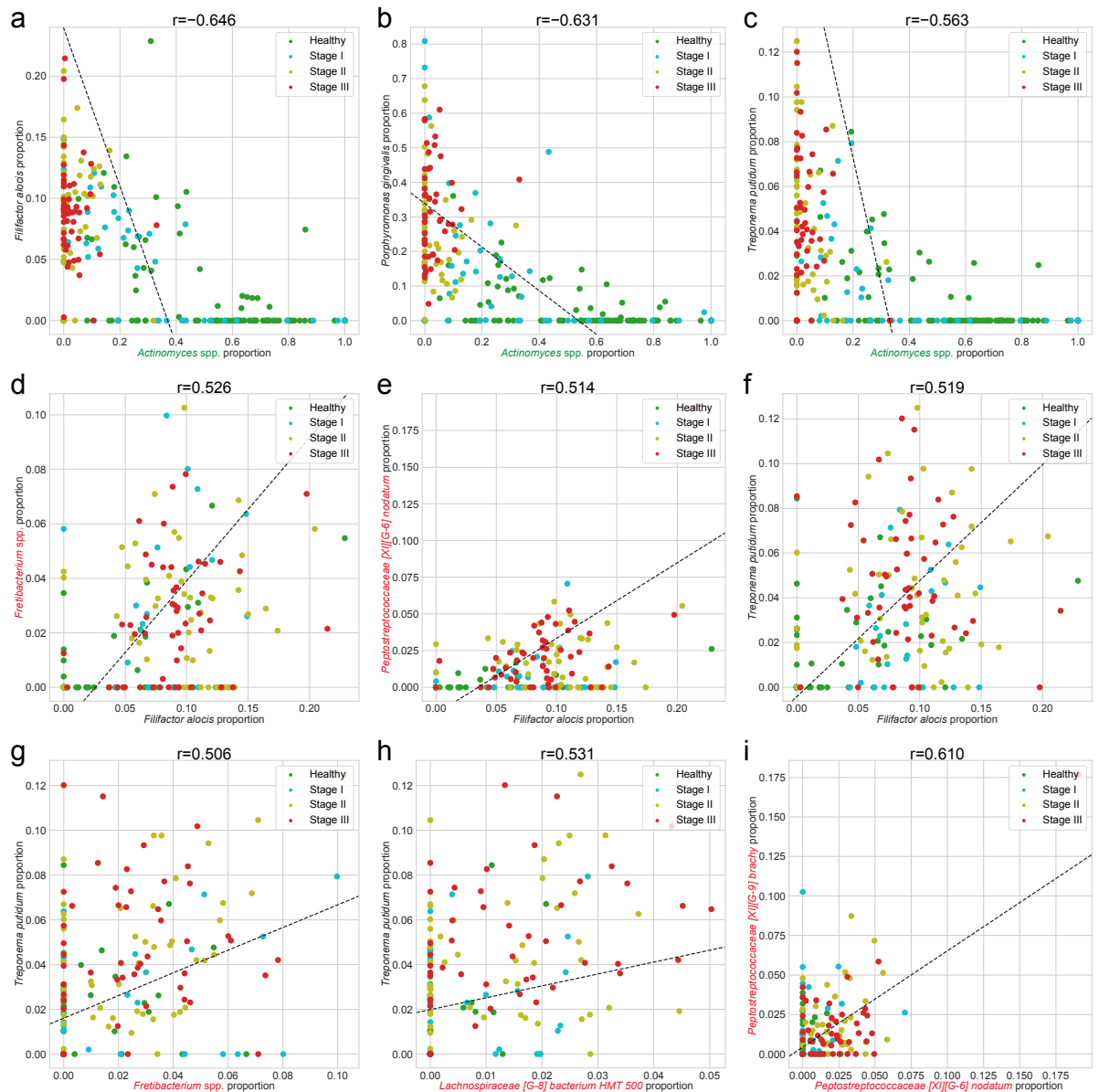


Figure 14: Correlation plots for differentially abundant taxa.

We selected the combinations of DAT with absolute Spearman correlation coefficients greater than 0.5. The color represents periodontal healthy periodontal statuses (green: healthy, cyan: stage I, yellow: stage II, and red: stage III).

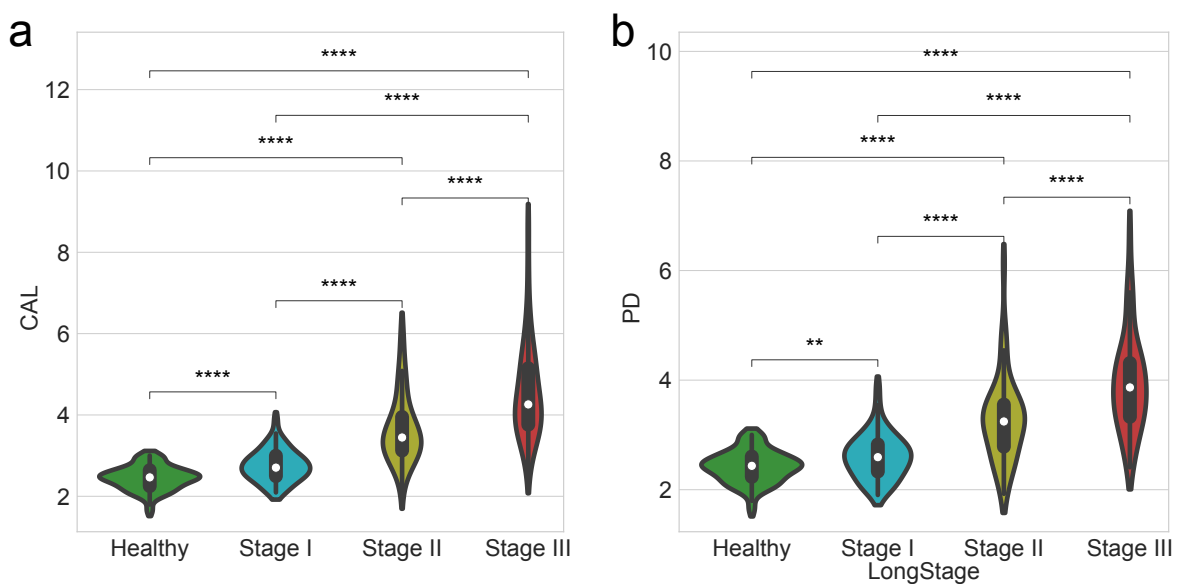


Figure 15: **Clinical measurements by the periodontitis statuses.**

Comparisons of clinical measurement among healthy controls and patients with various periodontitis stages. **(a)** Clinical attachment level (CAL) **(b)** Probing depth (PD). Statistical significance determined by the MWU test: $p < 0.01$ (**) and $p < 0.0001$ (****).

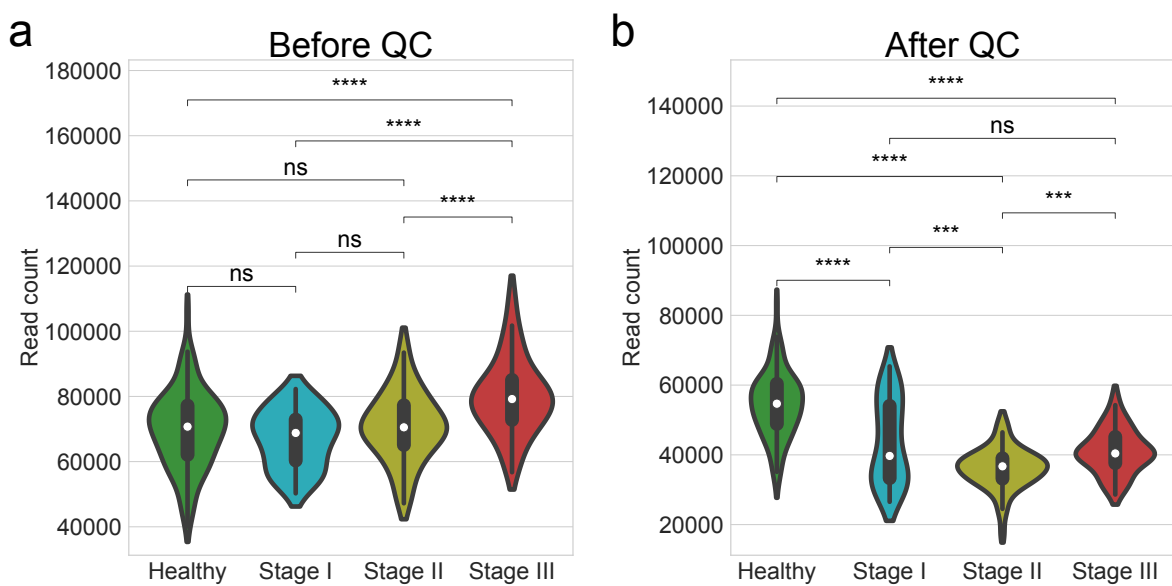


Figure 16: **Number of read counts by the periodontitis statuses.**

Comparisons of the number of read counts among healthy controls and patients with various periodontitis stages. **(a)** Before quality check **(b)** After quality check. Statistical significance determined by the MWU test: $p \geq 0.05$ (ns), $p < 0.05$ (*), $p < 0.01$ (**), $p < 0.001$ (***) $,$ and $p < 0.0001$ (****).

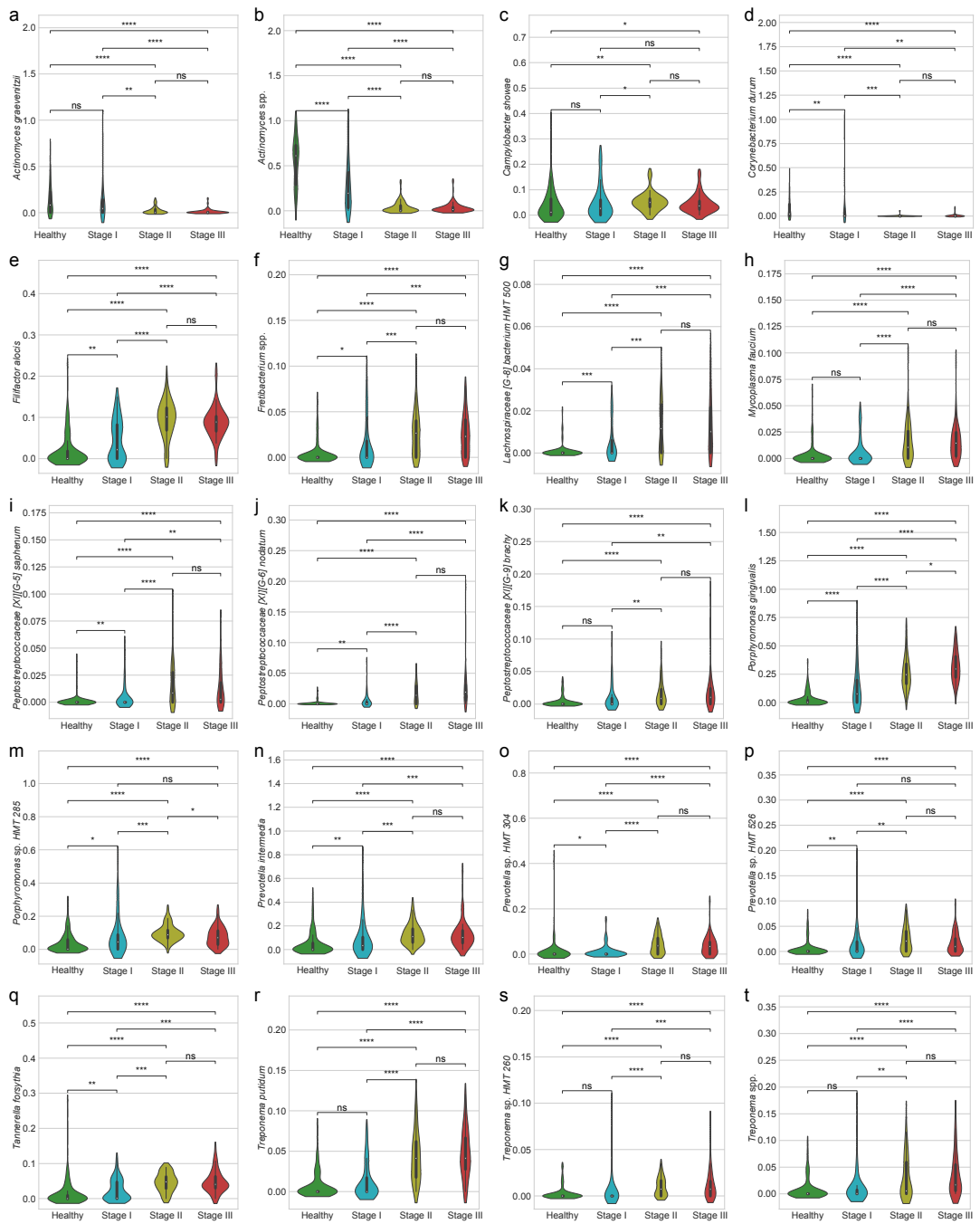


Figure 17: Proportion of DAT.

(a) *Actinomyces graevenitzii* (b) *Actinomyces* spp. (c) *Campylobacter showae* (d) *Corynebacterium durum* (e) *Filifactor alocis* (f) *Fretibacterium* spp. (g) *Lachnospiraceae [G-8] bacterium HMT 500* (h) *Mycoplasma faecium* (i) *Peptostreptococcaceae [XI][G-5] saphenum* (j) *Peptostreptococcaceae [XI][G-6] nodatum* (k) *Peptostreptococcaceae [XI][G-9] brachy* (l) *Porphyromonas gingivalis* (m) *Porphyromonas* sp. HMT 285 (n) *Prevotella intermedia* (o) *Prevotella* sp. HMT 304 (p) *Prevotella* sp. HMT 526 (q) *Tannerella forsythia* (r) *Treponema putidum* (s) *Treponema* sp. HMT 260 (t) *Treponema* spp. Statistical significance determined by the MWU test: $p \geq 0.05$ (ns), $p < 0.05$ (*), $p < 0.01$ (**), $p < 0.001$ (***), and $p < 0.0001$ (****).

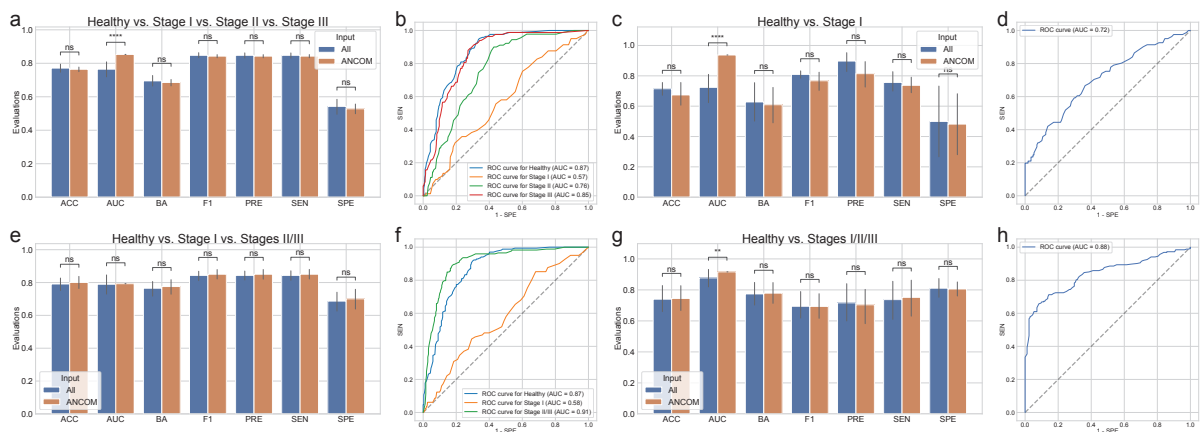


Figure 18: Random forest classification metrics with the full microbiome compositions and ANCOM-selected DAT compositions.

The classification metrics in the random forest classifications were as follows: ACC, AUC, BA, F1, PRE, SEN, and SPE. **(a)** Classification performance for healthy vs. stage I vs. stage II vs. stage III. **(b)** ROC curve for the highest BA of (a). **(c)** Classification performance for healthy vs. stage I. **(d)** ROC curve on the highest BA of (c). **(e)** Classification performance for healthy vs. stage I vs. stages II/III. **(f)** ROC curve for the highest BA of (e). **(g)** Classification performance for healthy vs. stages I/II/III. **(h)** ROC curve for the highest BA of (g). Statistical significance determined by the MWU test: $p \geq 0.05$ (ns), $p < 0.01$ (**), and $p < 0.0001$ (****).

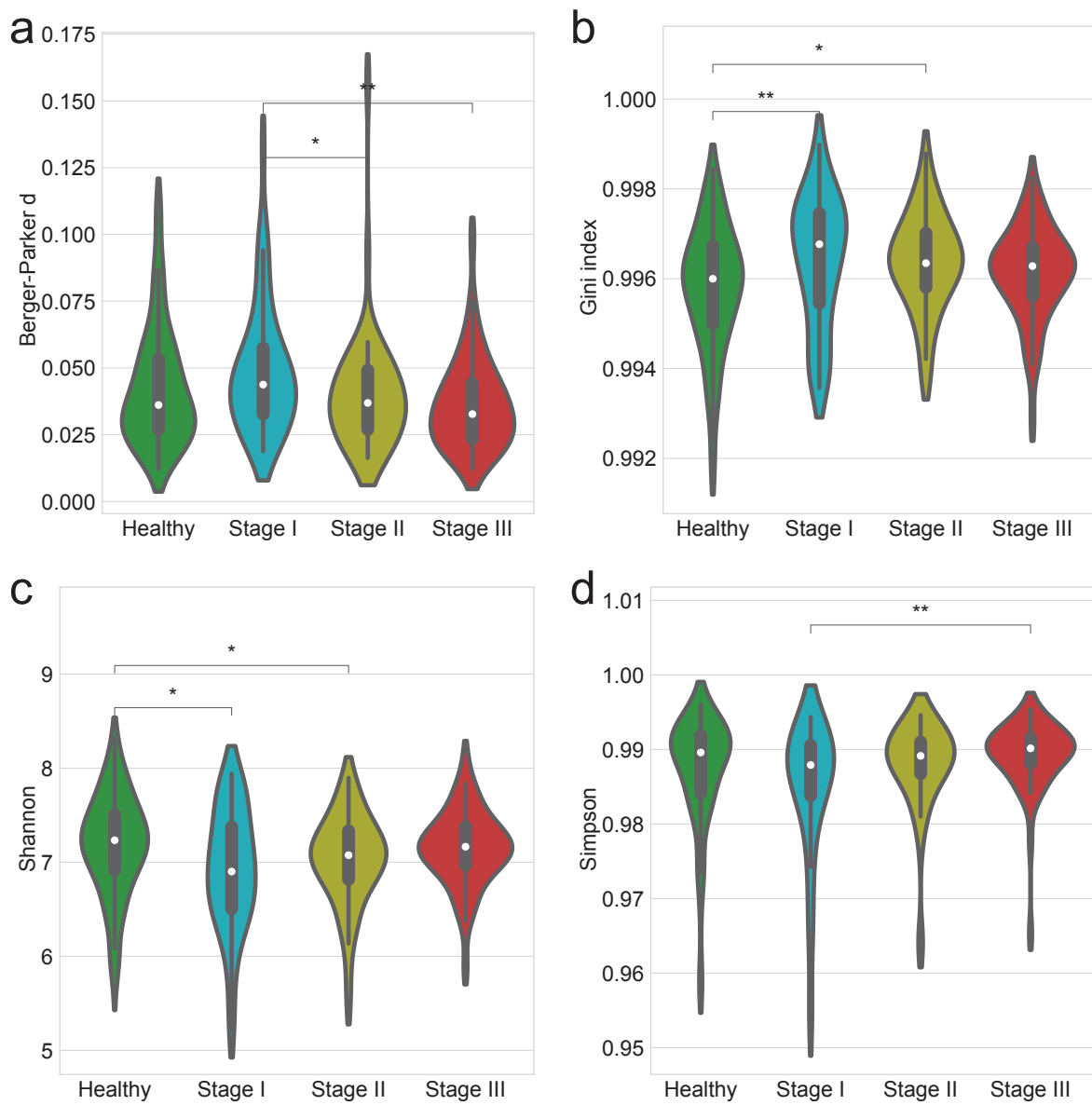


Figure 19: Alpha-diversity indices account for evenness.

Alpha-diversity indices (**a-d**) indicate that the heterogeneity between the periodontitis stages as measured by: **(a)** Berger-Parker *d* **(b)** Gini **(c)** Shannon **(d)** Simpson. Statistical significance determined by the MWU test: $p < 0.05$ (*) and $p < 0.01$ (**)

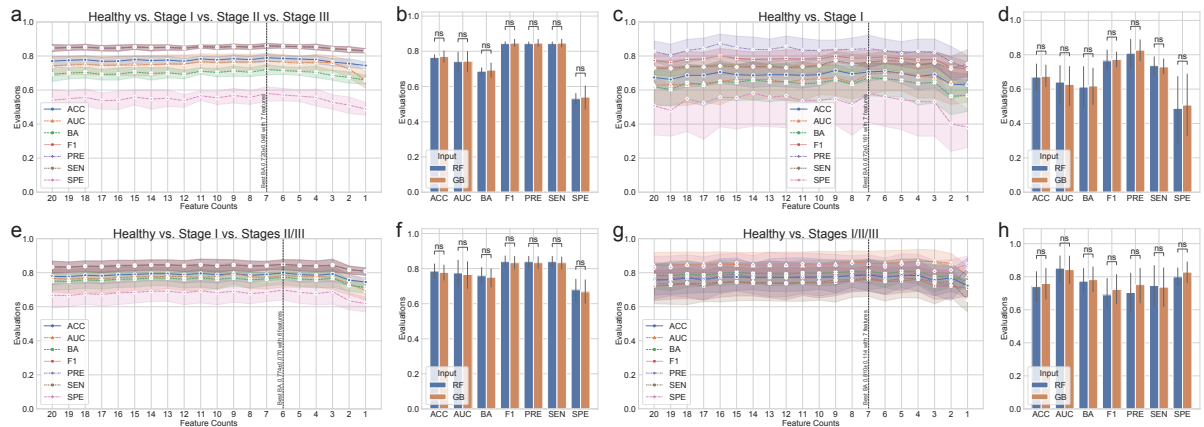


Figure 20: Gradient Boosting classification metrics.

The classification metrics in the random forest classifications were as follows: ACC, AUC, BA, F1, PRE, SEN, and SPE. The feature counts mean that the classification model trained on the most important n features as the Table 5. **(a)** Comparison of Random forest (RF) and Gradient boosting (GB) for healthy vs. stage I vs. stage II vs. stage III. **(b)** Comparison of RF and GB for the highest BA of (a). **(c)** Classification performance for healthy vs. stage I. **(d)** Comparison of RF and GB for healthy vs. stage I vs. stages II/III. **(e)** Comparison of RF and GB for the highest BA of (d). **(f)** Comparison of RF and GB for Healthy vs. Stage I vs. Stages II/III. **(g)** Classification performance for healthy vs. stages I/II/III. **(h)** Comparison of RF and GB for Healthy vs. Stages I/II/III. MWU test: $p \geq 0.05$ (ns)

786 **3.4 Discussion**

787 In order to investigate at potential alterations in the salivary microbiome compositions based on periodontal
788 statuses, including healthy, stage I, stage II, and stage III, we employed 16S rRNA gene sequencing to
789 perform a cross-sectional periodontitis analysis. In this study, the 2018 periodontitis classification served
790 as the basis for the classification of periodontitis severities (Papapanou et al., 2018). There were notable
791 variations in the salivary microbiome composition among the multiple severities of periodontitis (Figure
792 13). Furthermore, our random forest classification model based on the proportions of DAT in the salivary
793 microbiome compositions across study participants to predict multiple periodontitis statuses with high
794 AUC of 0.870 ± 0.079 (Table 4).

795 Previous research identified the red complex as the primary pathogens of periodontitis (Listgarten,
796 1986): *Porphyromonas gingivalis*, *Tannerella forsythia*, and *Treponema denticola*. Other studies, however,
797 have shown that periodontal pathogens communicate with other bacteria in the salivary microbiome
798 networks to generate dental plaque prior to the pathogenesis and development of periodontitis (Lamont &
799 Jenkinson, 2000; Rosan & Lamont, 2000; Yoshimura, Murakami, Nishikawa, Hasegawa, & Kawaminami,
800 2009).

801 Using subgingival plaque collections, recent researches have suggested a connection between the
802 periodontitis severity and the salivary microbiome compositions (Altabtbaei et al., 2021; Iniesta et al.,
803 2023; Nemoto et al., 2021). Therefore, we have examined the salivary microbiome compositions of
804 patients with multiple severities of periodontitis and periodontally healthy controls, extending on earlier
805 studies.

806 According to our findings, the salivary microbiome compositions have 425 taxa (Figure 13). We
807 computed the alpha-diversity indices to determine the variability within each salivary microbiome
808 composition, including ace (Chao & Lee, 1992), chao1 (Chao, 1984), fisher alpha (Fisher et al., 1943),
809 margalef (Magurran, 2021), observed ASVs (DeSantis et al., 2006), Berger-Parker *d* (Berger & Parker,
810 1970), Gini (Gini, 1912), Shannon (Weaver, 1963), and Simpson (Simpson, 1949) (Figure 7 and Figure
811 19). Alpha-diversity indices suggested that the microbial richness of periodontally healthy controls was
812 higher than that of patients with periodontitis (Figure 7a-e and Figure 19). These results are in line with
813 findings with that patients with advanced periodontitis, namely stage II and stage III, have less diversified
814 communities than periodontally healthy controls (Jorth et al., 2014). Recognizing that the periodontitis
815 severity increases the amount of *Porphyromonas gingivalis*, the salivary microbiome compositions from
816 periodontally healthy controls conserved microbial networks dominated by *Streptococcus* spp. (Figure
817 13). *Porphyromonas gingivalis* is one of the known periodontal pathogen that could cause dysbiosys
818 in the salivary microbiomes, suggesting in the pathophysiology of periodontitis. Despite this finding,
819 earlier research found that subgingival microbiome of patients with periodontitis had a greater alpha-
820 diversity index (observed ASVs) than that of healthy controls (Iniesta et al., 2023), might due to the
821 different sampling sites between saliva and subgingival plaque. On the other hand, another research
822 has addressed significant discrepancies in alpha-diversity indices from subgingival plaque, saliva, and
823 tongue biofilms from healthy controls and periodontitis patients, resulting the highest alpha-diversity

824 index in saliva collections (Belstrøm et al., 2021). Moreover, early-stage periodontitis, namely stage I,
825 did not determine statistically significant differences in alpha-diversity indices compared to advanced
826 periodontitis, including stage II and stage III (Figure 7a-e). Accordingly, saliva collection of stage I
827 periodontitis may exhibit heterogeneity, indicating a midpoint condition between a healthy state and
828 advanced periodontitis (stage II and stage III). Likewise, gingivitis is often associated with low abundances
829 of the majority of periodontal pathogens, including *Porphyromonas gingivalis*, *Tannerella forsythia*, and
830 *Treponema denticola* (Abusleme et al., 2021). Compared to healthy controls, patients with stage I
831 periodontitis have higher detection rates of *Porphyromonas gingivalis* and *Tannerella forsythia* (Tanner et
832 al., 2006, 2007).

833 Therefore, we calculated beta-diversity indices to analyze the differences between the study partici-
834 pants. The distances for the multiple stages of periodontitis, including stage I, stage II, and stage III, as
835 well as healthy controls (Figure 4g-j and Table 7), suggesting notable differences among the multiple
836 periodontitis severities. In other words, the composition of the salivary microbiome compositions varies
837 depending on the periodontitis stages, so that supporting the findings from a previous study (Iniesta et al.,
838 2023). Taken together that it is nearly impossible to fully restore the attachment level after it has been lost
839 due to the progression and development of periodontitis, the ability to rapidly screen for periodontitis in
840 its early phases using saliva collections would be highly beneficial for effective disease management and
841 treatment.

842 Of the total of 425 taxa in the salivary microbiome composition that have been identified (Figure 13),
843 ANCOM was applied to select 20 taxa as the DAT that indicated notable abundance variation among
844 the periodontitis severities (Figure 8 and Table 5). Three sub-groups were formed from the DAT using
845 hierarchical clustering (Figure 8a). Surprisingly, two of the red complex pathogens (Rôças, Siqueira Jr,
846 Santos, Coelho, & de Janeiro, 2001), *Porphyromonas gingivalis* and *Tannerella forsythia*, were classified
847 in Group 2 and were more prevalent in stage II and stage III periodontitis compared to healthy controls.
848 *Campylobacter showae* was additionally placed in Group 2 of the orange complex pathogens (Gambin et
849 al., 2021). Furthermore, some of the DAT in Group 2 have reported their crucial roles in pathogenesis
850 and development of periodontitis: *Filifactor alocis* (Aruni et al., 2015), *Treponema putidum* (Wyss et
851 al., 2004), *Tannerella forsythia* (Stafford, Roy, Honma, & Sharma, 2012; W. Zhu & Lee, 2016), and
852 *Prevotella intermedia* (Karched, Bhardwaj, Qudeimat, Al-Khabbaz, & Ellepolo, 2022). Taken together,
853 this indicates that DAT in Group 2 is essential to periodontitis. The portion of some Group 1 DAT,
854 including *Peptostreptococcaceae[XI][G-5] saphenum*, *Peptostreptococcaceae[XI][G-6] nodatum*, and
855 *Peptostreptococcaceae[XI][G-9] brachy*, in healthy controls and patients with periodontitis significantly
856 differed, according to earlier research (Lafaurie et al., 2022). These outcomes support our research,
857 implying that Group 1 DAT are also essential to the etiology and progression of periodontitis. However,
858 in contrast to patients with periodontitis, Group 3 DAT, namely *Corynebacterium durum* and *Actinomyces*
859 *graevenitzii*, were enriched in healthy controls, which is consistent with earlier research (Redanz et al.,
860 2021; Nibali et al., 2020).

861 In our correlation analysis (Figure 9), we have discovered strongly negative correlations (coefficient \leq
862 -0.5) between DAT of Group 3 and these of Group 1 and Group 2; we have also identified nine DAT

pairs with strong correlations (coefficient $\leq -0.5 \vee$ coefficient ≥ 0.5) (Figure 14). Interestingly, there were strongly negative correlations (coefficient ≤ -0.5) between Group 2 DAT and *Actinomyces* spp., taxa which belong to Group 3: *Filifactor alocis* (Figure 14a), *Porphyromonas gingivalis* (Figure 14b), and *Treponema putidum* (Figure 14c). Taken together that pathogens, including *Filifactor alocis* (Aja, Mangar, Fletcher, & Mishra, 2021; Hiranmayi, Sirisha, Rao, & Sudhakar, 2017), *Porphyromonas gingivalis* (Rôças et al., 2001), and *Treponema putidum* (Wyss et al., 2004), become dominant taxa in patients with stage III periodontitis. On the other hand, commensal salivary bacteria, such as *Actinomyces* spp., gradually declined. Additionally, several DAT from Group 1 and Group 2 exhibited strong positive correlations (coefficient ≥ 0.5) (Figure 14d-i). It has been established that all of these DAT from Group 1 and Group 2 are periodontal pathogens: *Filifactor alocis* (Aja et al., 2021; Hiranmayi et al., 2017), *Fretibacterium* spp. (Teles, Wang, Hajishengallis, Hasturk, & Marchesan, 2021), *Lachnospiraceae[G-8] bacterium HMT 500* (Lafaurie et al., 2022), *Peptostreptococcaceae[XI][G-6] nodatum* (Lafaurie et al., 2022; Haffajee, Teles, & Socransky, 2006), *Peptostreptococcaceae[XI][G-9] brachy* (Lafaurie et al., 2022), and *Treponema putidum* (Wyss et al., 2004). Thus, these fundamental roles of identified periodontal pathogens in the pathophysiology and progression of periodontitis are further supported by these strong positive correlations (coefficient ≥ 0.5), suggesting that advanced periodontitis, i.e., stage III, might arise from the additional DAT from Group 1 and Group 2.

Moreover, to predict periodontitis statuses from salivary microbiome composition, we have constructed machine-learning classification models based on random forest for four classification settings:

1. healthy vs. stage I vs. stage II vs. stage III
2. healthy vs. stage I
3. healthy vs. stage I vs. stages II/III
4. healthy vs. stages I/II/III

Porphyromonas gingivalis and *Actinomyces* spp. were the two most important taxa (feature) in all classification settings (Table 6). This finding aligns with a recent study that identifies *Actinomyces* spp. as the most prevalent bacteria in both the healthy gingivitis controls, while *Porphyromonas gingivalis* is recognized as the most predominant taxon within the periodontitis subjects, based on analyses of subgingival plaque samples (Nemoto et al., 2021). We have previously developed machine learning models for the classification of periodontitis, with the objective of predicting the severities of chronic periodontitis by analyzing the copy numbers of nine known salivary bacteria species. We classified healthy controls and patients with periodontitis utilizing bacterial combinations in conjunction with a random forest model (E.-H. Kim et al., 2020):

- AUC: 94%
- BA: 84%
- SEN: 95%
- SPE: 72%

Another study established a machine-learning model for the classification of periodontitis, employing 266 species derived from the buccal microbiome (Na et al., 2020):

- AUC: 92%

- 902 • BA: 84%
903 • SEN: 94%
904 • SPE: 74%
- 905 By separating patients with periodontitis from healthy controls using only four DAT, *e.g.* *Actinomyces*
906 *graevenitzii*, *Actinomyces* spp., *Corynebacterium durum*, and *Porphyromonas gingivalis*, our machine
907 learning model performed better than previously published models (Figure 10, Table 4, and Table 6):
- 908 • AUC: $95.3\% \pm 4.9\%$
909 • BA: $88.5\% \pm 6.6\%$
910 • SEN: $86.4\% \pm 15.7\%$
911 • SPE: $90.5\% \pm 7.0\%$
- 912 This result showed that by detecting Group 3 bacteria that were substantially abundant in health
913 controls than patients with periodontitis, our study increased BA by at least 5% and SPE by at least 17%.
- 914 Furthermore, we have validated our machine-learning prediction model using openly accessible 16S
915 rRNA gene sequencing data from Portuguese (Iniesta et al., 2023) and Spanish participants (Relvas et
916 al., 2021) in order to ensure the consistency of our random forest classification model (Figure 11). Our
917 classification models employed in this study were primarily developed and assessed on Korean study par-
918 ticipants, which may limit their generalizability to other ethnic groups with different salivary microbiome
919 compositions (Premaraj et al., 2020; Renson et al., 2019). Therefore, the evaluations of this periodonti-
920 tis classification models can be affected by ethnic-specific variances and differences, highlighting the
921 necessity for additional validation and adjustment across a spectrum of ethnic backgrounds.
- 922 Regarding the clinical characteristics and potential confounders influencing the analysis of salivary
923 microbiome compositions connected with periodontitis severity, this study had a number of limitations
924 that were pointed out. We did not offer clinical information, such as the percentage of teeth, the percentage
925 of bleeding on probing, nor dental furcation involvement, even though we did gather information on
926 attachment level, probing depth, plaque index, and gingival index (Renvert & Persson, 2002); this might
927 have it challenging to present thorough and in-depth data about periodontal health. Moreover, the broad age
928 range may make it tougher to evaluate the relationship between age and periodontitis statuses, providing
929 the necessity for future studies to consider into account more comprehensive clinical characteristics
930 associated with periodontitis. Additionally, potential confounders—*e.g.* body mass index (Bombin, Yan,
931 Bombin, Mosley, & Ferguson, 2022) and e-cigarette use (Suzuki, Nakano, Yoneda, Hirofushi, & Hanioka,
932 2022)—which might have affected dental health and salivary microbiome composition were disregarding
933 consideration in addition to smoking status and systemic diseases. Thus, future research incorporating
934 these components would offer a more thorough knowledge of how lifestyle factors interact and affect the
935 salivary microbiome composition and periodontal health. Throughout, resolving these limitations will
936 advance our understanding in pathogenesis and development of periodontitis, offering significant novel
937 insights on the causal connection between systemic diseases and the salivary microbiome compositions.

938 **4 Metagenomic signature analysis of Korean colorectal cancer**

939 **4.1 Introduction**

940 Colorectal cancer (CRC) is one of the most prevalent and life-threatening malignancies worldwide
941 (Kuipers et al., 2015; Center, Jemal, Smith, & Ward, 2009; N. Li et al., 2021), with its incidence
942 influenced by a combination of genetic (Zhuang et al., 2021; Peltomaki, 2003), environmental (O'Sullivan
943 et al., 2022; Raut et al., 2021), and lifestyle factors (X. Chen et al., 2021; Bai et al., 2022; Zhou et
944 al., 2022; X. Chen, Li, Guo, Hoffmeister, & Brenner, 2022). Established risk factors include a often
945 diet in red and processed meats (Kennedy, Alexander, Taillie, & Jaacks, 2024; Abu-Ghazaleh, Chua,
946 & Gopalan, 2021), obesity (Mandic, Safizadeh, Niedermaier, Hoffmeister, & Brenner, 2023; Bardou
947 et al., 2022), cigarette smoking (X. Chen et al., 2021; Bai et al., 2022), alcohol consumption (Zhou et
948 al., 2022; X. Chen et al., 2022), and a sedentary lifestyle (An & Park, 2022), all of which contribute to
949 chronic inflammation, mutagenesis, and metabolic regulation. Additionally, underlying conditions, e.g.
950 Lynch syndrome (Vasen, Mecklin, Khan, & Lynch, 1991; Hampel et al., 2008) and familial adenomatous
951 polyposis (Inra et al., 2015; Burt et al., 2004), significantly increase risk of CRC due to persistent mucosal
952 inflammation and somatic mutations that promote tumorigenesis.

953 The gut microbiome plays a fundamental role in maintaining host health by helping digestion
954 (Joscelyn & Kasper, 2014; Cerqueira, Photenhauer, Pollet, Brown, & Koropatkin, 2020), regulating
955 metabolism (Dabke, Hendrick, Devkota, et al., 2019; Utzschneider, Kratz, Damman, & Hullarg, 2016;
956 Magnúsdóttir & Thiele, 2018), adjusting immune function (Kau, Ahern, Griffin, Goodman, & Gordon,
957 2011; Shi, Li, Duan, & Niu, 2017; Broom & Kogut, 2018), and even coordinating neurological processes
958 by the brain-gut axis (Martin et al., 2018; Aziz & Thompson, 1998; R. Li et al., 2024). Comprising
959 these gut microbiota, including, archaea, bacteria, fungi, and viruses, the gut microbiome contributes
960 to the synthesis of essential vitamins, and production of fatty acids, which influence intestinal integrity
961 and immune responses. Thus, well-balanced gut microbiome composition modulates systemic immune
962 function by interacting with gut-associated lymphoid tissue, shaping immune tolerance and response
963 to infections. Hence, emerging evidence suggests that dysbiosis in the gut microbiome composition are
964 associated not only a narrow range of diseases, e.g. diarrhea and enteritis (Paganini & Zimmermann,
965 2017; Gao, Yin, Xu, Li, & Yin, 2019) but also a wide range of diseases, e.g. obesity, diabetes, and cancers
966 (Barlow et al., 2015; Hartstra et al., 2015; Helmink et al., 2019; Cullin et al., 2021).

967 Recent studies have highlighted the crucial role of the gut microbiome in tumorigenesis and progres-
968 sion of CRC (Song, Chan, & Sun, 2020; Rebersek, 2021), with dysbiosis emerging as a potential risk
969 factor. Dysbiosis in gut microbiome compositions can promote tumorigenesis of many cancers, including
970 CRC, through several signaling cascades, including inflammation, mutagenesis, and altered metabolism
971 in host. Certain bacteria species, such as *Fusobacterium* genus (Hashemi Goradel et al., 2019; Bullman et
972 al., 2017; Flanagan et al., 2014), *Bacteroides* genus (Ulger Toprak et al., 2006; Boleij et al., 2015), and
973 *Escherichia coli* (Swidsinski et al., 1998; Bonnet et al., 2014), have been associated with development
974 and progression of CRC by producing pro-inflammatory signals, generating toxins including mutagens,

975 and disrupting the intestinal barriers including mucous surface. In contrast, beneficial bacteria, such as
976 *Lactobacillus* genus (Ghorbani et al., 2022; Ghanavati et al., 2020) and *Bifidobacterium* genus (Le Leu,
977 Hu, Brown, Woodman, & Young, 2010; Fahmy et al., 2019), are regarded to apply protective roles by
978 maintaining homeostasis of gut microbiome compositions and regulating immune responses including
979 inflammation.

980 Furthermore, identifying metagenome biomarkers in Korean CRC patients is essential, as the gut
981 microbiome compositions significantly vary by ethnicity due to genetic, dietary, and environmental
982 factor (Fortenberry, 2013; Merrill & Mangano, 2023; Parizadeh & Arrieta, 2023). Additionally, ethnicity-
983 specific microbiome composition signatures may affect the reliability of previously established biomarkers
984 derived from predominantly Western CRC cohorts (Network et al., 2012), necessitating population-
985 specific investigations. By identifying metagenomic biomarkers tailored to Korean CRC patients, we
986 can improve early detection rate of early-stage CRC, develop more accurate risk of CRC, and explore
987 microbiome-targeted therapies that consider host-microbiome interactions within the Korean population.

988 Accordingly, this study aims to identify microbiome-based biomarkers specific to CRC within
989 the Korean population, addressing the critical demand for ethnicity-specific microbiome research. By
990 leveraging metagenomic sequencing and advanced computational biology analysis, this study seeks to
991 uncover novel microbial signatures associated with Korean CRC patients. As part of the larger "Multi-
992 genomic analysis for biomarker development in colon cancer" project (NTIS No. 1711055951), this study
993 investigates microbial signatures within next-generation sequencing data to enhance precision medicine
994 approaches for CRC and to develop robust microbiome-based biomarkers for early detection, prognosis,
995 and therapeutic stratification, complementing genomic and epigenomic markers. Hence, this research
996 represents a crucial step toward personalized cancer diagnostic and therapeutic strategies tailored to the
997 Korean population.

998 **4.2 Materials and methods**

999 **4.2.1 Study participants enrollment**

1000 To achieve metagenomic observations of CRC, a total of 211 Korean CRC patients were enrolled (Table
1001 8). The tissue samples were collected from both the tumor lesion and its corresponding adjacent normal
1002 lesion to enable comparative metagenomic analyses. Tumor tissue samples were obtained from confirmed
1003 CRC lesions, ensuring adequate representation of CRC-associated microbial alterations. Adjacent normal
1004 tissues were collected from non-cancerous regions away from the tumor margin to serve as a control
1005 for baseline molecular and microbial composition. Moreover, clinical information was collected for all
1006 study participants included in this study to investigate potential associations between gut microbiome
1007 compositions and clinical outcomes. Key clinical characteristics recorded included overall survival (OS)
1008 and recurrence. These clinical parameters were integrated with metagenomic data to explore potential
1009 microbiome-based biomarkers for CRC prognosis and progression. Ethical approval was obtained for
1010 clinical data collection, and all patient information was anonymized to ensure confidentiality in accordance
1011 with institutional guidelines.

1012 **4.2.2 DNA extraction procedure**

1013 Tissue samples were immediately processed under sterile conditions to prevent contamination and
1014 preserved in low temperature (-80°C) storage for downstream DNA extraction and whole-genome
1015 sequencing. Furthermore, produced sequencing data were provided by the "Multi-genomic analysis
1016 for biomarker development in colon cancer" project (NTIS No. 1711055951) in mapped BAM format,
1017 aligned to the hg38 human reference genome. The preprocessing pipeline utilized by the main project
1018 included high-throughput whole-genome sequencing using standardized alignment algorithm, BWA
1019 (H. Li & Durbin, 2009). In addition to the mapped human sequences, our whole-genome sequencing
1020 data retained unmapped sequences, which contain potential microbial reads that were not aligned to the
1021 human reference genome.

1022 **4.2.3 Bioinformatics analysis**

1023 To identify microbial signatures associated with CRC, we employed PathSeq (version 4.1.8.1) (Kostic
1024 et al., 2011; Walker et al., 2018), a computational pipeline designed for metagenomic analysis of high-
1025 throughput sequencing data including the whole-genome sequences. After processing these sequencing
1026 data through the PathSeq pipeline, a comprehensive bioinformatics analyses were conducted to characterize
1027 microbial signatures associated with CRC.

1028 Prevalent taxa identification was performed by determining microbial taxa present in the majority of
1029 the study participants, filtering out low-abundance and rare taxa to ensure robust downstream analyses.

1030 To assess microbial community structure, diversity indices were calculated, including alpha-diversity
1031 to evaluate single-sample diversity and beta-diversity to compare microbial composition between the
1032 tumor tissues and their corresponding adjacent normal tissues. Following alpha-diversity indices were

1033 calculated using the scikit-bio Python package (version 0.6.3) (Rideout et al., 2018), and these alpha-
1034 diversity indices were compared using the MWU test:

- 1035 1. Berger-Parker d (Berger & Parker, 1970)
- 1036 2. Chao1 (Chao, 1984)
- 1037 3. Dominance
- 1038 4. Doubles
- 1039 5. Fisher (Fisher et al., 1943)
- 1040 6. Good's coverage (Good, 1953)
- 1041 7. Margalef (Magurran, 2021)
- 1042 8. McIntosh e (Heip, 1974)
- 1043 9. Observed ASVs (DeSantis et al., 2006)
- 1044 10. Simpson d
- 1045 11. Singles
- 1046 12. Strong (Strong, 2002)

1047 Furthermore, these beta-diversity indices were measured and compared using the PERMANOVA
1048 test (Anderson, 2014; Kelly et al., 2015). To demonstrate multi-dimensional data from the beta-diversity
1049 indices, we utilized the t-SNE algorithm (Van der Maaten & Hinton, 2008).

- 1050 1. Bray-Curtis (Sorensen, 1948)
- 1051 2. Canberra
- 1052 3. Cosine (Ochiai, 1957)
- 1053 4. Hamming (Hamming, 1950)
- 1054 5. Jaccard (Jaccard, 1908)
- 1055 6. Sokal-Sneath (Sokal & Sneath, 1963)

1056 Differentially abundant taxa (DAT) were identified using statistical method, ANCOM (Lin & Peddada,
1057 2020), adjusting for sequencing depth and potential confounders to highlight taxa significantly associated
1058 with categorical clinical information in CRC, such as recurrence. Furthermore, to point attention to
1059 taxa that are substantially linked to continuous clinical measurement in CRC, including OS, DAT were
1060 found using the Spearman correlation and slope from linear regression (Equation 9). Note that both the
1061 Spearman correlation and the slope from linear regression were utilized to provide a more comprehensive
1062 assessment of the relationship between DAT proportions and OS. While the correlation coefficient
1063 measures the strength and direction of a linear relationship between these variables, it does not convey
1064 information about the magnitude of change in independent variable relative to dependent variable. The
1065 slope of the linear regression model, on the other hand, quantifies this change by indicating how much
1066 the dependent variable is expected to increase or decrease per unit change in the independent variable. By
1067 incorporating both the correlation coefficient and the slope from the linear regression, we ensured that
1068 the analysis captured not only whether two variables were associated but also the extent to which one
1069 variable influenced the other. This dual approach enhances the interpretability of results, particularly in
1070 biological and clinical studies where both statistical association and biological effect size are crucial for
1071 meaningful suggestions.

$$\text{slope} = \frac{\Delta \text{OS}}{\Delta \text{DAT proportion}} \quad (9)$$

1072 To assess the predictive potential of microbial signatures in CRC prognosis, we employed a random
1073 forest machine learning model using DAT proportions as input features. Random forest classification was
1074 utilized to predict CRC recurrence, where the classification model was trained to distinguish between
1075 CRC patients with or without recurrence based on the gut microbiome compositions. Additionally,
1076 random forest regression was applied to predict OS by estimating survival time as a continuous clinical
1077 outcome based on microbiome features. This approach allowed for the identification of microbial taxa
1078 that contribute significantly to CRC prognosis, offering insights into potential gut microbiome-based
1079 biomarkers for cancer progression. By integrating these random forest machine learning models, we
1080 aimed to improve CRC risk stratification and precision medicine strategies.

1081 This multi-layered bioinformatics approach enabled a comprehensive investigation of gut microbiome
1082 alteration in CRC, facilitating the identification of potential microbial biomarkers for diagnosis and
1083 prognosis of CRC.

1084 **4.2.4 Data and code availability**

1085 All sequences from the 211 study participants have been published to the Korea Bioinformation Center
1086 (data ID KGD10008857): <https://kbds.re.kr/KGD10008857>. Docker image that employed through-
1087 out this study is available in the DockerHub: <https://hub.docker.com/repository/docker/fumire/unist-crc-copm/general>. Every code used in this study can be found on GitHub: <https://github.com/CompbioLabUnist/CoPM-ColonCancer>.

1090 **4.3 Results**

1091 **4.3.1 Summary of clinical characteristics**

1092 Microsatellite instability (MSI) is one of the key molecular features and risk factors in CRC, resulting
1093 from defects in the DNA mismatch repair system (Boland & Goel, 2010). MSI leads to the accumulation
1094 of mutations in short repetitive DNA sequences (microsatellites), contributing to genomic instability and
1095 tumor development (Søreide, Janssen, Söiland, Körner, & Baak, 2006; Vilar & Gruber, 2010). Therefore,
1096 we compared clinical measurements with MSI status, including microsatellite stable (MSS), MSI-low
1097 (MSI-L), and MSI-high (MSI-H). There were no significant differences in the clinical measurements, *e.g.*
1098 recurrence, sex, OS, and age in diagnosis, in the total of 211 study participants (Table 8).

1099 **4.3.2 Gut microbiome compositions**

1100 In the total of 211 CRC study participants, these ten kingdoms were found in the gut microbiome
1101 composition:

- 1102 1. Archaea kingdom: 31 genera
- 1103 2. Bacteria kingdom: 1508 genera
- 1104 3. Bamfordvirae kingdom: 1 genus
- 1105 4. Eukaryota kingdom: 77 genera
- 1106 5. Fungi kingdom: 137 genera
- 1107 6. Loebvirae kingdom: 2 genera
- 1108 7. Orthornavirae kingdom: 1 genus
- 1109 8. Parnavirae kingdom: 3 genera
- 1110 9. Shotokuvirae kingdom: 6 genera
- 1111 10. Viruses kingdom: 76 genera

1112 Among these kingdoms, the proportions of four major kingdoms, which have at least 50 genera, in
1113 the gut microbiome composition were displayed (Figure 21): Bacteria kingdom, Eukaryota kingdom,
1114 Fungi kingdom, and Viruses kingdom. In the Bacteria kingdom (Figure 21a), *Bacteroides* genus is the
1115 most prevalent genus in the tumor tissue samples, followed by *Fusobacterium* and *Cutibacterium* genera.
1116 *Toxoplasma* and *Malassezia* genera were the dominant genus, which have over 90% of proportions, in
1117 the Eukaryota kingdom (Figure 21b) and the Fungi kingdom (Figure 21c), respectively. On the other
1118 hand, *Roseolovirus* genus is the most popular genus of the Viruses kingdom in the normal tissue samples
1119 (Figure 21d); contrarily, *Lymphocryptovirus* and *Cytomegalovirus* genera had been dominant genera in
1120 the tumor tissue samples. Taken together, these results suggest that the Anna Karenina principle (Ma,
1121 2020; W. Li & Yang, 2025), *i.e.* in human microbiome-associated diseases, every disease-associated
1122 microbiome, including dysbiosis, is unique and patient-specific, whereas all healthy microbiomes are
1123 similar, also applies to CRC.

1124 **4.3.3 Diversity indices**

1125 In alpha-diversity analysis, which measures within-sample microbial community, revealed a significant
1126 increase in tumor tissue samples compared to adjacent normal tissue samples (Figure 22). Alpha-diversity
1127 indices, including Chao1, Fisher α , and observed features, were consistently higher in CRC tumor tissues
1128 (MWU test $p < 0.05$), indicating a more heterogeneous microbial community, *e.g.* the Anna Karenina
1129 principle, potentially influenced by tumor-associated dysbiosis.

1130 To assess the microbial impact on CRC recurrence, alpha-diversity indices compared between normal
1131 and tumor tissue samples in accordance with recurrence information (Figure 23). In the recurrence
1132 patients, most alpha-diversity indices (11 out of 12), except McIntosh index, exhibited increasing in
1133 tumor tissue samples than normal tissue samples (MWU test $p < 0.05$; Figure 23); In the non-recurrence
1134 patients, on the other hand, some alpha-diversity indices (8 out of 12) amplified in tumor tissue samples
1135 than normal tissue samples (MWU test $p < 0.05$; Figure 23). What is interesting about the alpha-diversity
1136 analysis in this figure is that a few indices, namely Fisher α (Figure 28e) and Margalef (Figure 23g),
1137 presented augmentation in normal tissue sample of the recurrence patients than that of the non-recurrence
1138 patients (MWU test $p < 0.05$). Overall, these alpha-diversity results demonstrate that tumor tissue samples
1139 have more diverse microbiome composition than normal tissue samples. Furthermore, although only
1140 two indices significantly increased, the recurrence patients have diversified microbiome compositions
1141 than the non-recurrence patients in normal sample tissue, not in tumor sample tissues, indicating field
1142 cancerization by the gut microbiome leads to unfavorable prognosis such as recurrence (Curtius, Wright,
1143 & Graham, 2018; Rubio, Lang-Schwarz, & Vieth, 2022).

1144 To determine the microbial impact on OS of CRC patients, the Spearman correlation compared
1145 between alpha-diversity indices and OS duration (Figure 24). No significant Spearman correlation was
1146 found between every alpha-diversity indices and OS (Spearman correlation $p \geq 0.1$; Figure 24). However,
1147 a few alpha-diversity indices, *e.g.* Chao1 (Figure 24b), Good's coverage (Figure 24f), and observed
1148 features (Figure 24i), showed negative correlations with OS (Spearman correlation $p < 0.05$). Together
1149 these correlation results provide important insights into heterogeneous microbiome leads to shorter OS,
1150 suggesting the Anna Karenina principle and the field cancerization.

1151 In beta-diversity analysis, which calculates inter-sample microbial community, explain significant
1152 disparity between tumor tissue samples and normal tissue samples (Figure 25). Every six beta-diversity
1153 indices presented discrepancy between normal tissue samples and tumor tissue samples (PERMANOVA
1154 test $p < 0.001$), implying that tumor tissue samples have distinct microbiome compositions from normal
1155 tissue samples.

1156 Beta-diversity indices were evaluated between normal and tumor tissue samples along with recurrence
1157 history in order to evaluate the microbial influence on CRC recurrence (Figure 26). All six beta-diversity
1158 indices examined significant difference in microbial community structure between the recurrence patients
1159 and the non-recurrence patients (PERMANOVA test $p < 0.001$; Figure 26), indicating that tumor-
1160 associated gut microbiome composition varies resulting on recurrence status. tSNE-transformed plots
1161 further illustrated clear clustering patterns (Figure 26), suggesting again that the recurrence patients

1162 harbor dissimilar microbial communities compared to the non-recurrence patients. These observed
1163 differences in beta-diversity represent that microbial shifts, including dysbiosis, may be associated with
1164 CRC progression and recurrence risk, possibly due to specific taxa contributing to a tumor-promoting
1165 microenvironment.

1166 Moreover, beta-diversity analysis suggested a potential associated with OS duration in CRC patients.
1167 In all six beta-diversity indices, tSNE-transformed plots showed clear clustering patterns along OS
1168 duration (Figure 27), implying that possible microbiome composition shifts related to survival outcomes
1169 in CRC. However, since OS is a continuous variable, statistical significance testing could not be directly
1170 performed for these clustering patterns. Despite this limitation, the observed microbial community
1171 variations suggest that alterations in the gut microbiome composition may be associated to CRC prognosis
1172 and survival duration.

1173 Together, diversity indices analyses revealed significant microbial community alterations between
1174 normal and tumor tissue samples, as well as between the recurrence and non-recurrence CRC patients.
1175 Alpha-diversity indices significantly increased in tumor tissue samples than normal tissue samples (MWU
1176 test $p < 0.05$; Figure 22). This increase was more pronounced in the recurrence patients (11 of 12
1177 indices) compared to non-recurrence patients (8 of 12 indices) (Figure 23), indicating a potential link
1178 between microbial diversity and CRC recurrence. Additionally, negative correlation between OS and
1179 alpha-diversity indices were observed in normal samples (Spearman correlation $p < 0.05$; Figure 24),
1180 suggesting that lower microbial diversity may be associated with longer survival in CRC. On the other
1181 hand, beta-diversity indices analysis, showed significant separation between tumor and tumor tissue
1182 samples across all six beta-diversity indices (PERMANOVA test $p < 0.001$; Figure 25). Furthermore,
1183 the recurrence and non-recurrence patients displayed significantly discrete microbial compositions
1184 (PERMONOVA test $p < 0.001$; Figure 26), implying that microbial community shifts may reflect CRC
1185 progression and recurrence risk. These findings highlight the importance of microbiome diversity and
1186 gut microbiome composition in CRC prognosis and warrant further investigation into their potential as
1187 predictive biomarkers.

1188 4.3.4 DAT selection

1189 The selection of differentially abundant taxa (DAT) aimed to identify microbial taxa that exhibit significant
1190 differences in relative abundance between clinical information, such as recurrence history or OS in CRC
1191 patients. Identifying and selection these microbial discrepancies is crucial for understanding the role of
1192 the gut microbiome composition in CRC progression, prognosis, and potential therapeutic interventions.

1193 We identified 19 DAT associated with recurrence history across the total samples by ANCOM (Figure
1194 28a), including 18 non-recurrence-enriched DAT and a recurrence-related DAT. When stratified by sample
1195 type, one DAT was enriched in normal samples of the non-recurrence patients (Figure 28b), whereas six
1196 DAT exhibited significant differential abundance in tumor samples (Figure 28c). These findings suggest
1197 that microbial composition variations in the tumor microenvironment are more pronounced in relation to
1198 recurrence status (Table 9), potentially indicating a microbial signature linked to CRC progression. These

1199 identified DAT may contribute to tumor-associated dysbiosis, influencing the likelihood of CRC recurrence
1200 through mechanisms such as inflammation, metabolic modulation, or immune system interaction.

1201 The non-recurrence-enriched DAT have decreased proportions both in normal and tumor samples of
1202 the recurrence patients than those in the non-recurrence patients (MWU test $p < 0.001$; Figure 28d-h).
1203 What is interesting about these non-recurrence-enriched DAT is that they belong to the *Micrococcus* genus.
1204 Among them, *Micrococcus aloeverae* was consistently identified in all three settings—total (Figure 28a),
1205 normal (Figure 28b), and tumor samples (Figure 28c)—indicating its stable presence regardless of tissue
1206 type. Variation in relative proportions of *Micrococcus aloeverae* (Figure 28d) suggests potential ecological
1207 adaptability within tumor microenvironment of CRC. The remaining *Micrococcus*-related DAT showed
1208 less variation between the recurrence and non-recurrence patients, reinforcing their limited associations
1209 with CRC recurrence. Moreover, only one taxon, *Pseudomonas* sp. *NBRC 111133*, was identified as
1210 recurrence-enriched DAT (Figure 28a). This suggests a potential association between *Pseudomonas* sp.
1211 *NBRC 111133* and CRC recurrence, indicating that its presence may contribute to a tumor-supportive
1212 microbial environment. *Pseudomonas* sp. *NBRC 111133* had higher relative proportions both in normal
1213 and tumor tissue samples of the recurrence patients than those of the non-recurrence patients (Figure
1214 28i). Likewise, *Pseudomonas* sp. *NBRC 111133* were prevalent in tumor tissue samples than normal
1215 tissue samples of the non-recurrence patients (MWU test $p < 0.01$; Figure 28i); however, no significant
1216 difference between normal and tumor tissue samples of the recurrence patients.

1217 These findings imply that while certain species belong to *Micrococcus* genus may be prevalent in CRC
1218 tissues, their roles in cancer progression and recurrence risk remain uncertain. Species of *Pseudomonas*
1219 genus are known for their metabolic involvement in biofilm formation, antibiotic resistance, and immune
1220 modulation, which could play a role in CRC progression.

1221 **4.3.5 ML prediction**

Table 8: Clinical characteristics of CRC study participants.

Statistical significance were assessed using the χ^2 -squared test for categorical values and the Kruskal-Wallis test for continuous values.

	Overall	MSS	MSI-L	MSI-H	p-value
n	211	181	7	18	
Recurrence, n (%)	False	132 (62.6%)	112 (61.9%)	4 (57.1%)	13 (72.2%)
	True	79 (37.4%)	69 (38.1%)	3 (42.9%)	5 (27.8%)
Sex, n (%)	Male	137 (64.9%)	119 (65.7%)	6 (85.7%)	10 (55.6%)
	Female	74 (35.1%)	62 (34.3%)	1 (14.3%)	8 (44.4%)
OS, mean±SD	1248.5±770.3	1268.1±769.5	1416.6±496.3	1097.7±903.2	0.580
Age, mean±SD	61.2±13.1	61.7±12.4	60.1±15.6	60.2±19.4	0.867

Table 9: DAT list for CRC recurrence.

Taxonomy name	Entire-log2FC	Entire-W	Normal-log2FC	Normal-W	Tumor-log2FC	Tumor-W
<i>Cutibacterium acnes</i>	-1.878	10570				
<i>Cutibacterium avidum</i>	-1.383	10266				
<i>Cutibacterium granulosum</i>	-1.476	10271				
<i>Micrococcus aloeverae</i>	-2.280	10740	-1.821	10462	-2.481	10591
<i>Micrococcus luteus</i>	-2.216	10744				
<i>Micrococcus</i> sp. <i>CH3</i>	-2.323	10740				
<i>Micrococcus</i> sp. <i>CH7</i>	-2.321	10740				
<i>Micrococcus</i> sp. <i>HMSC31B01</i>	-2.282	10739				
<i>Micrococcus</i> sp. <i>MS-ASSII-49</i>	-2.284	10740				
<i>Pseudomonas</i> sp. <i>NBRC 111133</i>	1.139	9732				
<i>Pseudonocardia</i> sp. <i>P2</i>	-2.200	10736				
<i>Staphylococcus</i> sp. <i>HMSC034A07</i>	-1.341	10050				
<i>Staphylococcus</i> sp. <i>HMSC063F03</i>	-1.322	10001				
<i>Staphylococcus</i> sp. <i>HMSC064E11</i>	-1.064	10163				
<i>Staphylococcus</i> sp. <i>HMSC067B04</i>	-1.343	9952				
<i>Staphylococcus</i> sp. <i>HMSC068G12</i>	-1.344	10173				
<i>Staphylococcus</i> sp. <i>HMSC072H01</i>	-1.298	10197				
<i>Staphylococcus</i> sp. <i>HMSC077C03</i>	-1.331	10115				
<i>Treponema endosymbiont of Eucomomymptha</i> sp.	-1.629	10472				

Table 10: DAT list for CRC OS.

Taxonomy name	Entire-slope	Entire-r	Normal-slope	Normal-r	Tumor-slope	Tumor-r
<i>Acinetobacter venetianus</i>					3.087	0.203
<i>Actinotalea ferrariae</i>					2.574	0.200
<i>Agaricus bisporus</i>	2.329	0.287	2.925	0.276	2.258	0.306
<i>Bifidobacterium boum</i>					2.096	-0.216
<i>Brevundimonas</i> sp. <i>DS20</i>			2.180	0.279		
<i>Clostridiales bacterium</i>			2.631	-0.203		
<i>Corynebacterium kroppenstedtii</i>	2.117	0.220			2.117	0.302
<i>Corynebacterium lipophiloflavum</i>			2.137	0.227		
<i>Corynebacterium lowii</i>			2.006	-0.216		
<i>Corynebacterium</i> sp. <i>KPL1818</i>	2.101	0.209	2.487	0.220	2.044	0.215
<i>Corynebacterium</i> sp. <i>KPL1824</i>	2.057	0.207	2.511	0.212	2.003	0.226
<i>Corynebacterium</i> sp. <i>KPL1986</i>					2.205	0.202
<i>Corynebacterium</i> sp. <i>KPL1996</i>					2.205	0.202
<i>Corynebacterium</i> sp. <i>KPL1998</i>					2.205	0.202
<i>Corynebacterium</i> sp. <i>KPL2004</i>					2.205	0.202
<i>Kocuria flava</i>			2.729	0.214		
<i>Kytococcus sedentarius</i>					2.267	0.206
<i>Lachnospiraceae bacterium AD3010</i>			2.609	-0.203		
<i>Lachnospiraceae bacterium NK4A136</i>					2.538	-0.220
<i>Methylorum extorquens</i>					2.068	0.295
<i>Microbacterium barkeri</i>			2.071	0.389		
<i>Paracoccus sphaerophysae</i>					2.012	-0.209
<i>Pontibacillus litoralis</i>					2.580	-0.209
<i>Porphyromonas macacae</i>			2.476	-0.200		
<i>Pseudomonas balearica</i>					2.117	0.203
<i>Pseudomonas monteilii</i>					2.183	0.228
<i>Rodentibacter myodis</i>					2.444	0.245
<i>Roseovarius tolerans</i>					2.295	0.221
<i>Staphylococcus epidermidis</i>					2.243	0.214
<i>Staphylococcus</i> sp. <i>HMSC034A07</i>					2.183	0.209
<i>Staphylococcus</i> sp. <i>HMSC034D07</i>	2.278	0.206			2.252	0.253
<i>Staphylococcus</i> sp. <i>HMSC034G11</i>	2.362	0.208			2.357	0.261
<i>Staphylococcus</i> sp. <i>HMSC036A09</i>					2.308	0.239
<i>Staphylococcus</i> sp. <i>HMSC055A10</i>					2.168	0.222
<i>Staphylococcus</i> sp. <i>HMSC055B03</i>	2.134	0.202			2.134	0.266
<i>Staphylococcus</i> sp. <i>HMSC058E12</i>					2.106	0.216
<i>Staphylococcus</i> sp. <i>HMSC061C10</i>					2.882	0.207
<i>Staphylococcus</i> sp. <i>HMSC062B11</i>	2.391	0.203			2.377	0.253
<i>Staphylococcus</i> sp. <i>HMSC062D04</i>	2.278	0.202			2.274	0.259
<i>Staphylococcus</i> sp. <i>HMSC063F03</i>	2.376	0.201			2.367	0.251
<i>Staphylococcus</i> sp. <i>HMSC063F05</i>	2.387	0.210			2.381	0.266
<i>Staphylococcus</i> sp. <i>HMSC064E11</i>					2.276	0.218
<i>Staphylococcus</i> sp. <i>HMSC065D11</i>					2.329	0.245
<i>Staphylococcus</i> sp. <i>HMSC066G04</i>					2.181	0.218
<i>Staphylococcus</i> sp. <i>HMSC067B04</i>	2.332	0.205			2.329	0.260

Table 10 continued from previous page

Taxonomy name	Entire-slope	Entire-r	Normal-slope	Normal-r	Tumor-slope	Tumor-r
<i>Staphylococcus</i> sp. <i>HMSC068G12</i>					2.294	0.226
<i>Staphylococcus</i> sp. <i>HMSC070A07</i>	2.360	0.216			2.362	0.287
<i>Staphylococcus</i> sp. <i>HMSC073C02</i>	2.352	0.205			2.334	0.246
<i>Staphylococcus</i> sp. <i>HMSC073E10</i>					2.366	0.255
<i>Staphylococcus</i> sp. <i>HMSC074D07</i>	2.330	0.218			2.308	0.270
<i>Staphylococcus</i> sp. <i>HMSC076H12</i>					2.200	0.219
<i>Staphylococcus</i> sp. <i>HMSC077C03</i>					2.258	0.207
<i>Staphylococcus</i> sp. <i>HMSC077D09</i>					2.245	0.230
<i>Staphylococcus</i> sp. <i>HMSC077G12</i>	2.335	0.200			2.345	0.276
<i>Staphylococcus</i> sp. <i>HMSC077H01</i>					2.214	0.241
<i>Streptomyces cinnamoneus</i>					2.787	0.208
<i>Thauera terpenica</i>					2.975	0.226

Table 11: Random forest classification and their evaluations.

	Dataset	ACC	AUC	BA	F1	PRE	SEN	SPE
Entire	Total	0.544±0.139	0.667±0.141	0.561±0.141	0.544±0.139	0.559±0.152	0.562±0.192	0.559±0.152
	Normal	0.464±0.214	0.571±0.182	0.484±0.210	0.464±0.214	0.515±0.200	0.454±0.255	0.515±0.200
	Tumor	0.481±0.176	0.615±0.087	0.497±0.181	0.481±0.176	0.464±0.189	0.530±0.212	0.464±0.189
DAT	Total	0.582±0.112	0.656±0.109	0.592±0.120	0.582±0.112	0.558±0.114	0.626±0.167	0.558±0.114
	Normal	0.530±0.117	0.567±0.102	0.553±0.123	0.530±0.117	0.501±0.117	0.604±0.194	0.501±0.117
	Tumor	0.478±0.122	0.570±0.164	0.504±0.143	0.478±0.122	0.527±0.240	0.480±0.119	0.527±0.240

Table 12: **Random forest regression and their evaluations.**

Dataset		MAE	RMSE
Entire	Total	704.909 ± 249.010	894.943 ± 246.192
	Normal	803.487 ± 145.365	979.334 ± 158.813
	Tumor	811.505 ± 204.788	1005.182 ± 197.351
DAT	Total	823.700 ± 141.448	994.698 ± 157.983
	Normal	663.414 ± 147.203	825.461 ± 151.120
	Tumor	729.302 ± 179.940	884.863 ± 181.154

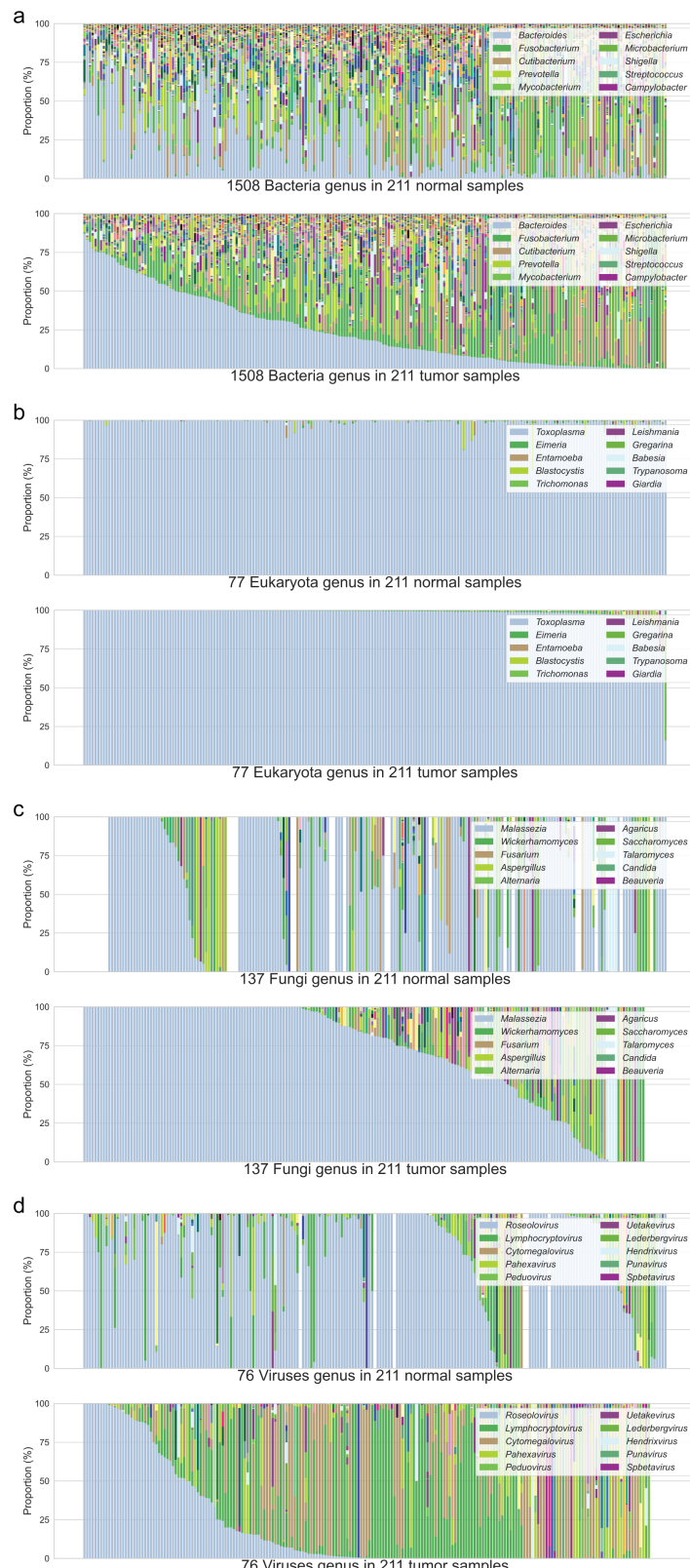


Figure 21: Gut microbiome compositions in genus level.

Taxa were sorted from the most prevalent taxon to the least prevalent taxon. CRC patients were sorted by the most prevalent taxon in descending order. **(a)** Bacteria kingdom **(b)** Eukaryota kingdom **(c)** Fungi kingdom **(d)** Viruses kingdom

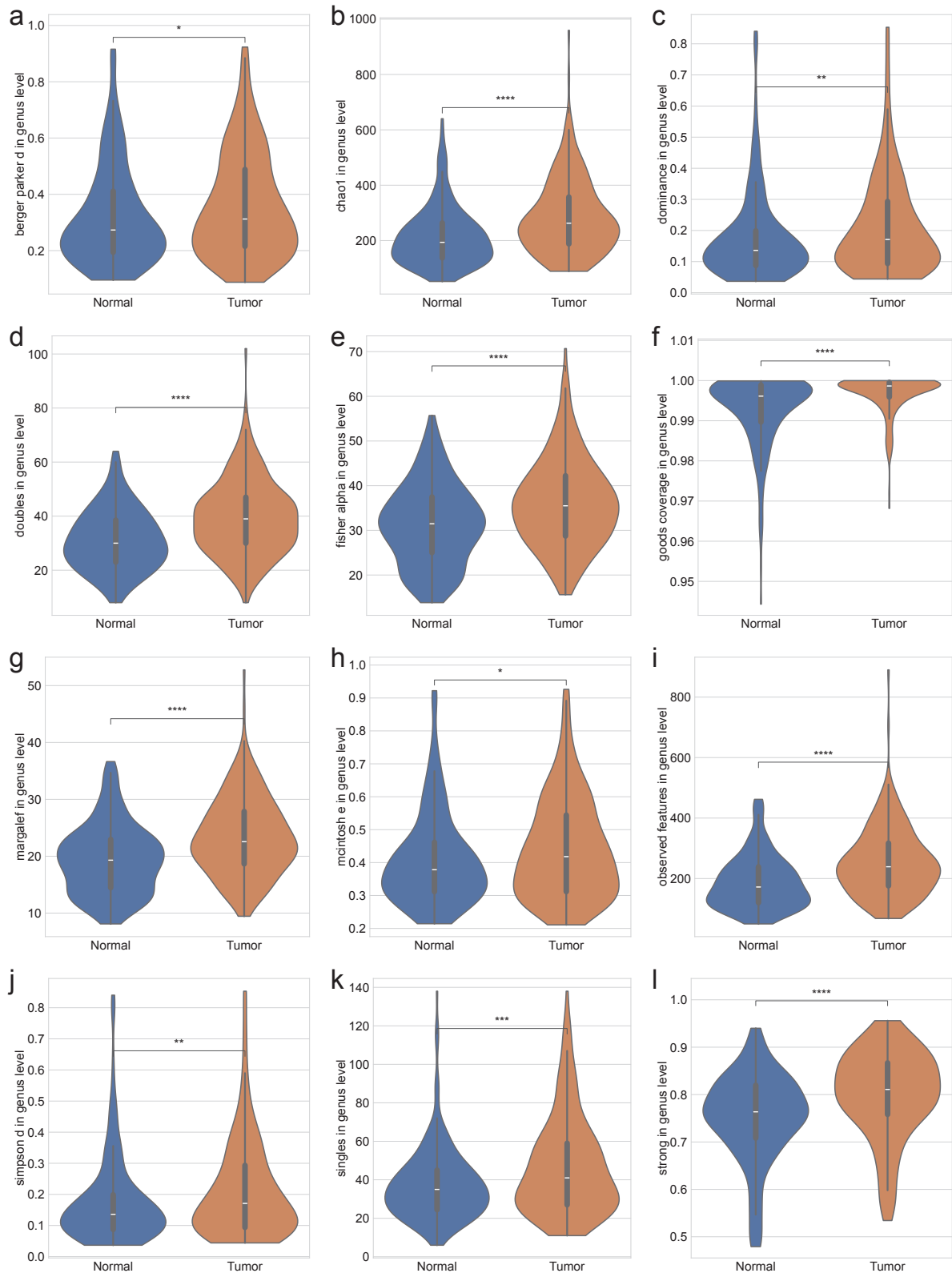


Figure 22: Alpha-diversity indices in genus level.

(a) Berger-Parker d (b) Chao1 (c) Dominance (d) Doubles (e) Fisher α (f) Good's coverage (g) Margalef (h) McIntosh (i) Observed features (j) Simpson d (k) Singles (l) Strong. MWU test: $p < 0.05$ (*), $p < 0.01$ (**), $p < 0.001$ (***), and $p < 0.0001$ (****)

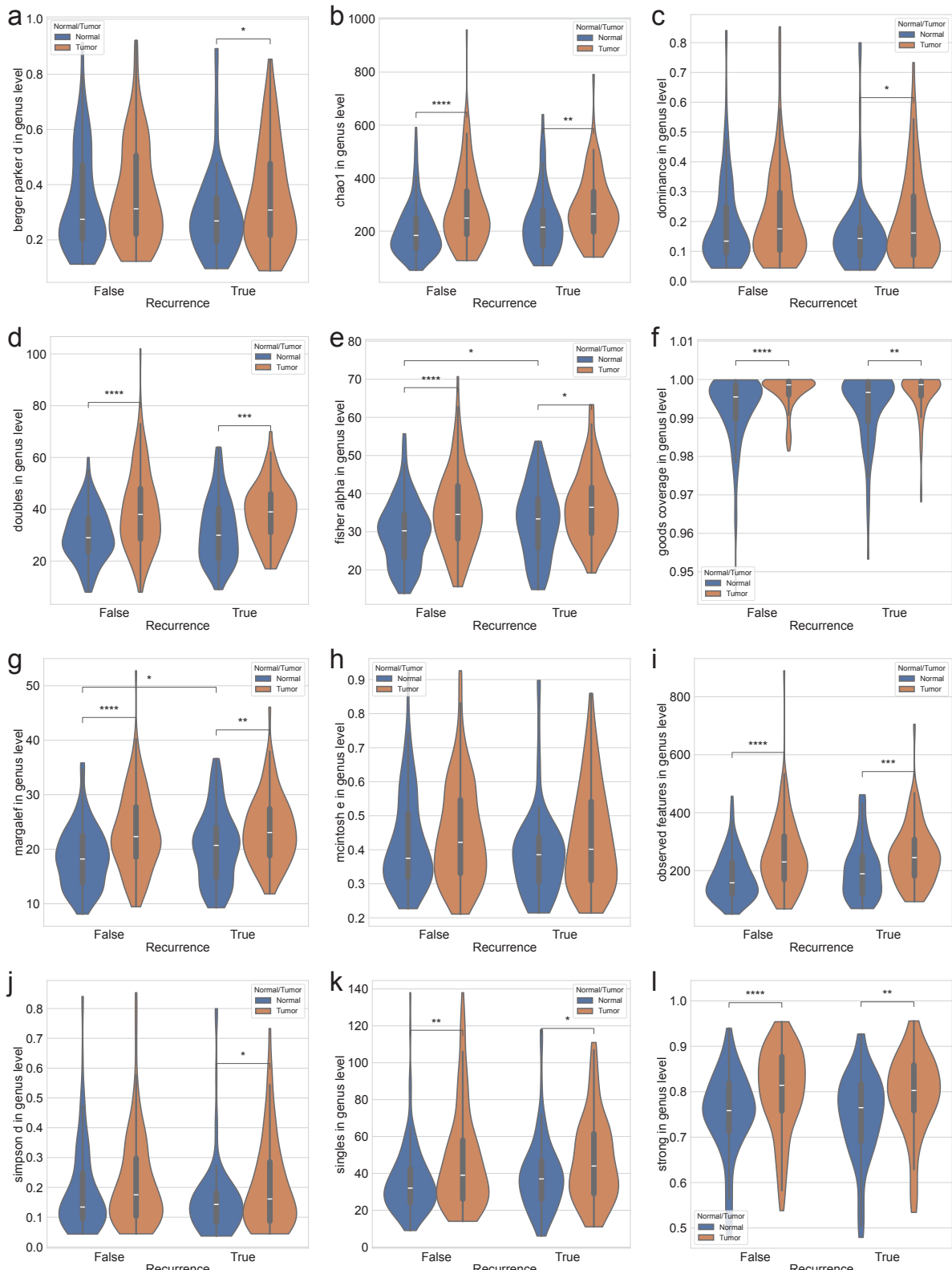


Figure 23: Alpha-diversity indices with recurrence in genus level.

(a) Berger-Parker d (b) Chao1 (c) Dominance (d) Doubles (e) Fisher α (f) Good's coverage (g) Margalef (h) McIntosh (i) Observed features (j) Simpson d (k) Singles (l) Strong. MWU test: $p < 0.05$ (*), $p < 0.01$ (**), $p < 0.001$ (***) $,$ and $p < 0.0001$ (****)

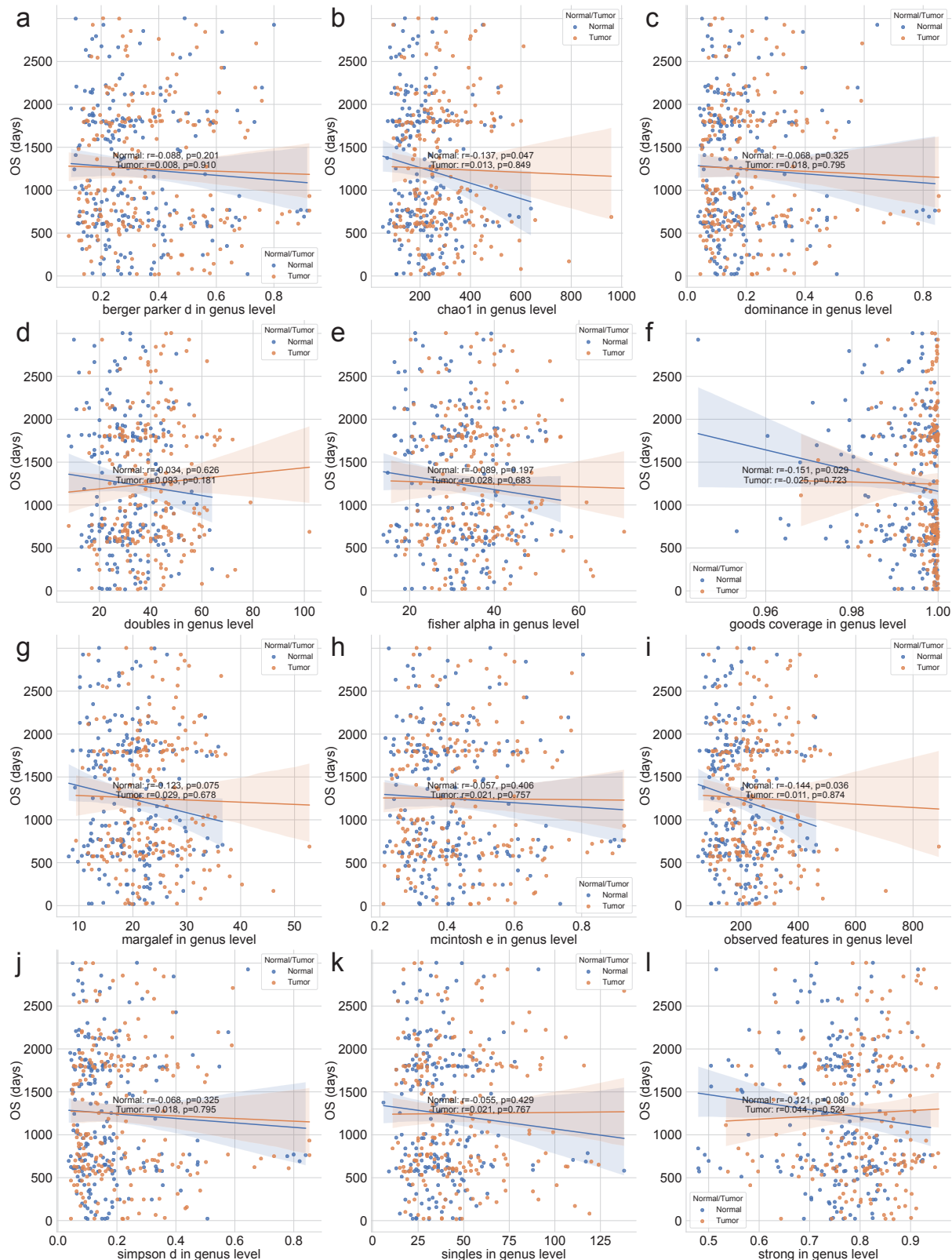


Figure 24: Alpha-diversity indices with OS in genus level.

(a) Berger-Parker d (b) Chao1 (c) Dominance (d) Doubles (e) Fisher α (f) Good's coverage (g) Margalef (h) McIntosh (i) Observed features (j) Simpson d (k) Singles (l) Strong. Statistical significance was calculated by the Spearman correlation.

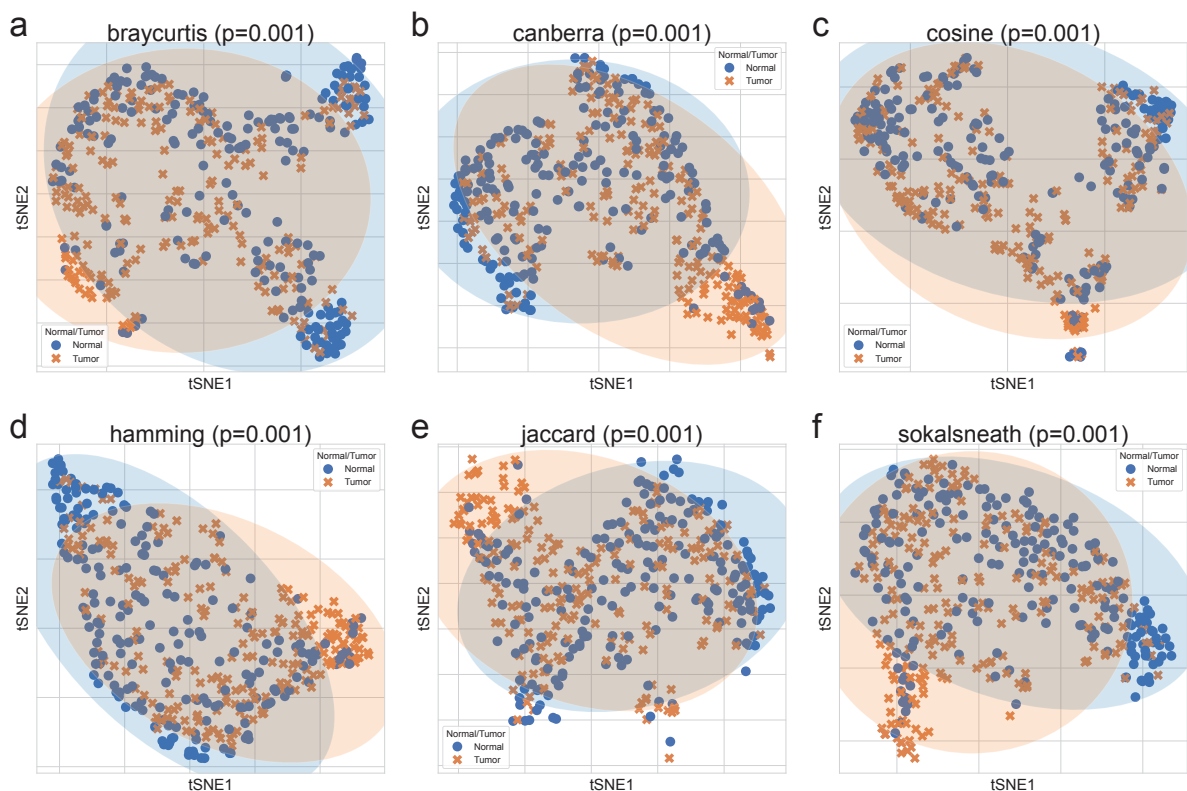


Figure 25: Beta-diversity indices in genus level.

Beta-diversity indices were visualized using a tSNE-transformed plot. The confidence ellipses are shown to display the distribution of each sub-group (Normal or Tumor). **(a)** Bray-Curtis **(b)** Canberra **(c)** Cosine **(d)** Hamming **(e)** Jaccard **(f)** Sokal-Sneath. Statistical significance were determined by PERMANOVA test.

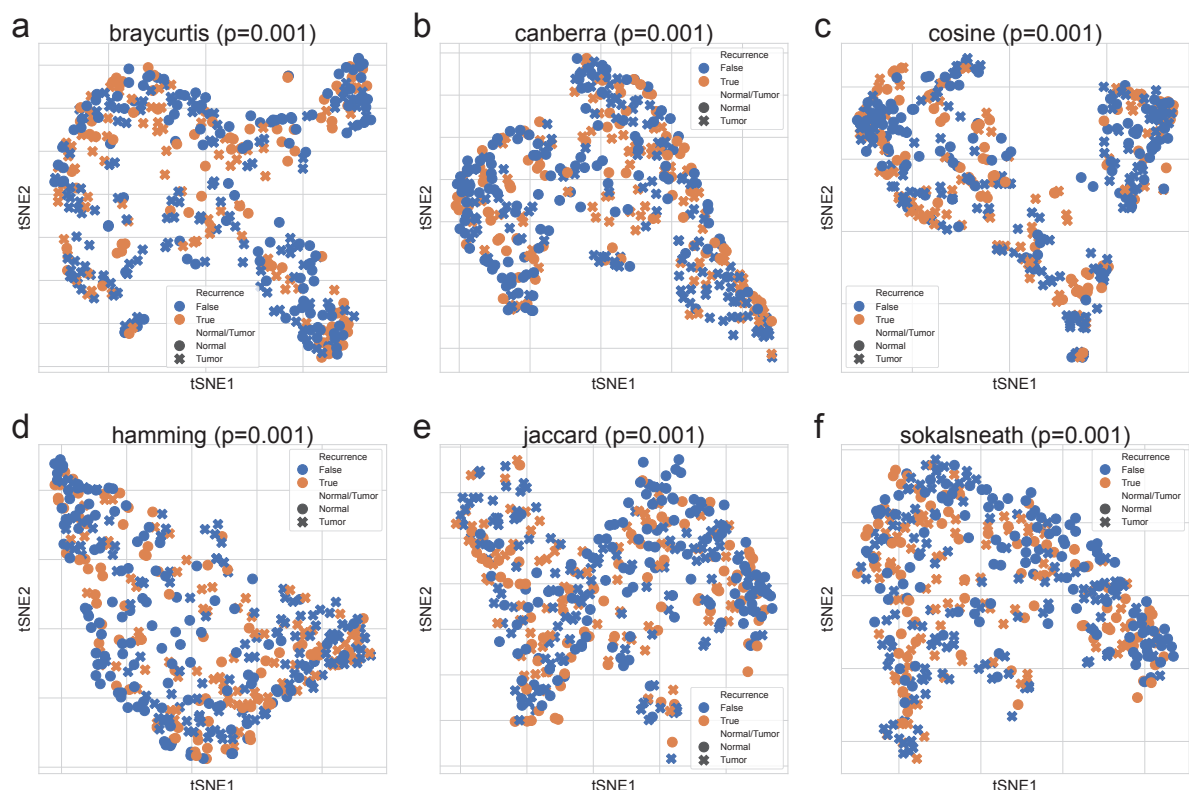


Figure 26: **Beta-diversity indices with recurrence in genus level.**

Beta-diversity indices were visualized using a tSNE-transformed plot. **(a)** Bray-Curtis **(b)** Canberra **(c)** Cosine **(d)** Hamming **(e)** Jaccard **(f)** Sokal-Sneath. Statistical significance were determined by PERMANOVA test.

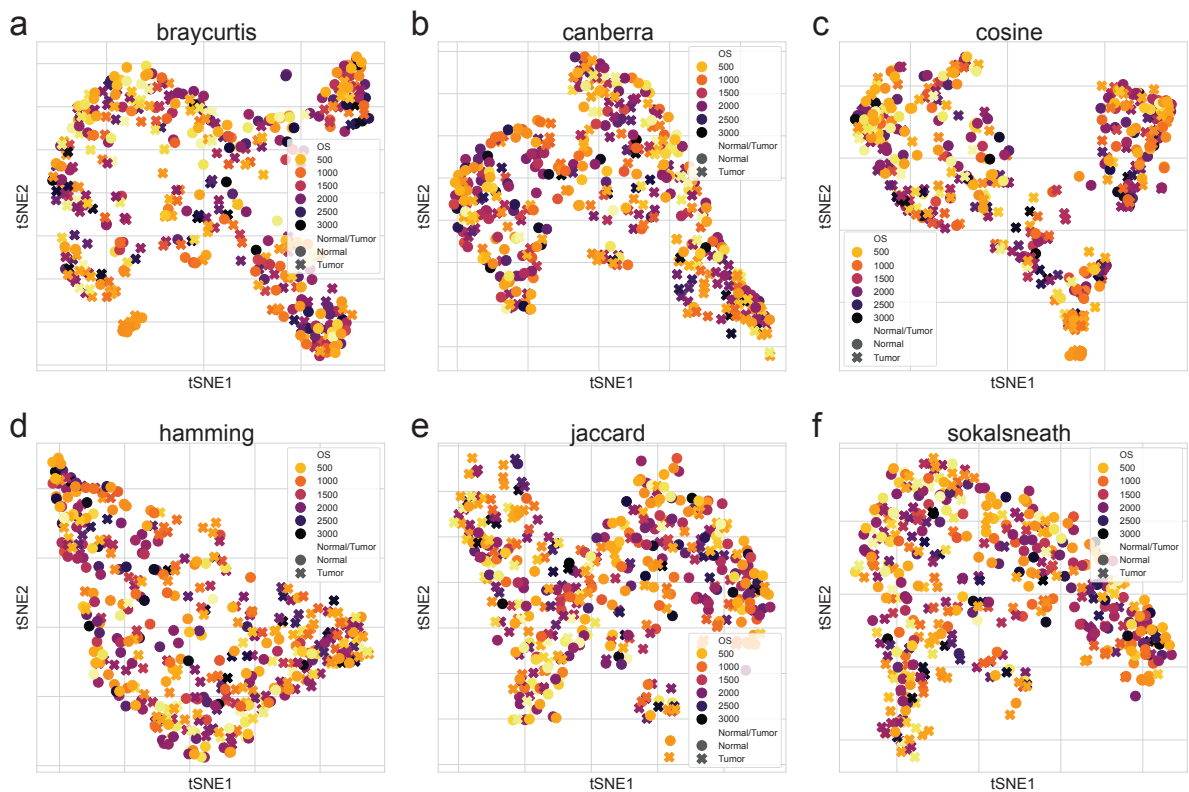


Figure 27: Beta-diversity indices with OS in genus level.

Beta-diversity indices were visualized using a tSNE-transformed plot. (a) Bray-Curtis (b) Canberra (c) Cosine (d) Hamming (e) Jaccard (f) Sokal-Sneath.

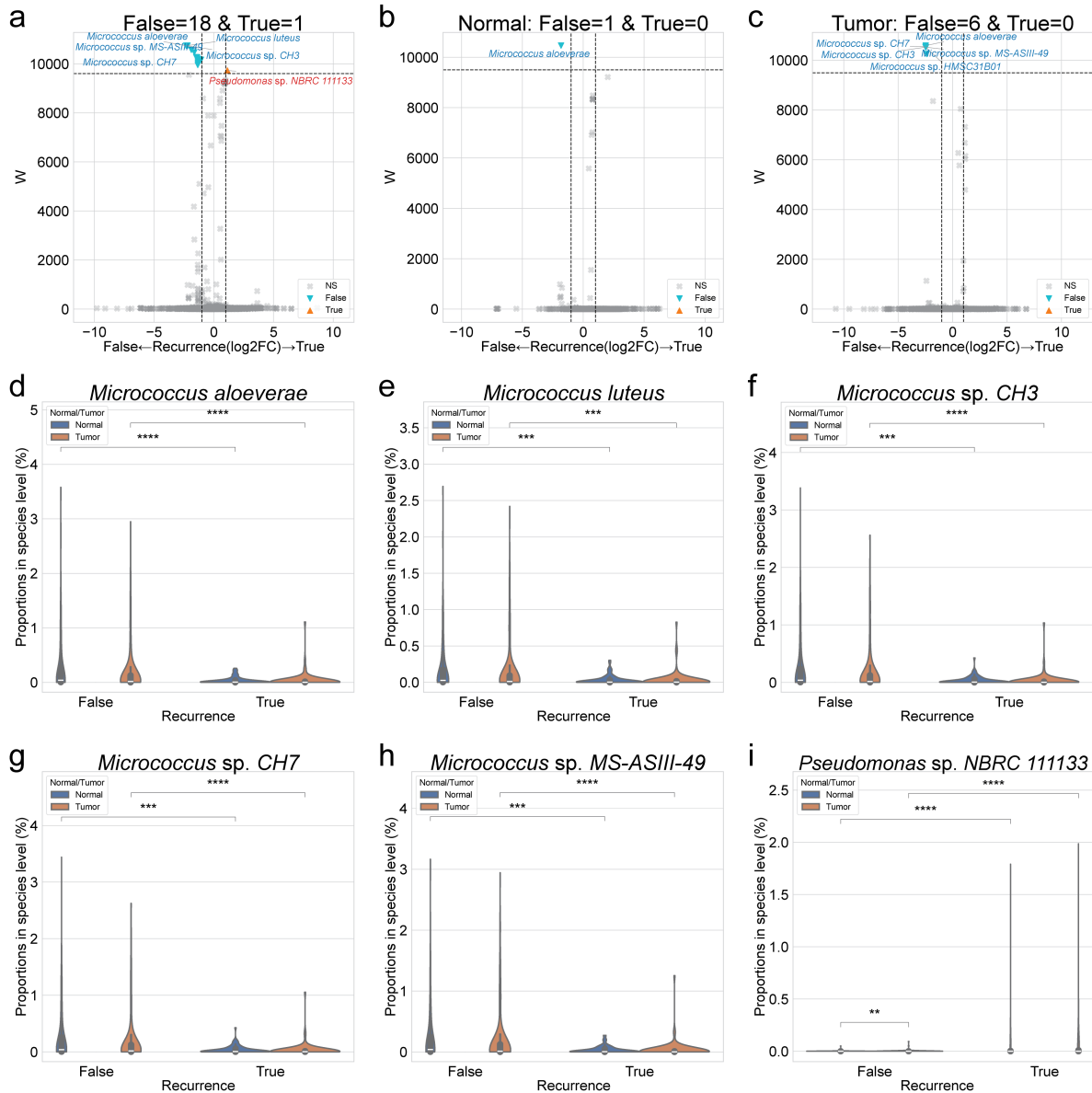


Figure 28: DAT with recurrence in species level.

(a-c) Volcano plots with recurrence. x-axis indicates \log_2 (Fold Change) on recurrence, and y-axis indicates ANCOM significance (W). **(a)** Total **(b)** Normal samples **(c)** Tumor samples. **(d-i)** Violin plots of each taxon proportion with recurrence. **(d)** *Micrococcus aloeverae* **(e)** *Micrococcus luteus* **(f)** *Micrococcus* sp. *CH3* **(g)** *Micrococcus* sp. *CH7* **(h)** *Micrococcus* sp. *MS-ASIII-49* **(i)** *Pseudomonas* sp. *NBRC 111133*. MWU test: $p < 0.05$ (*), $p < 0.01$ (**), $p < 0.001$ (***) , and $p < 0.0001$ (****)

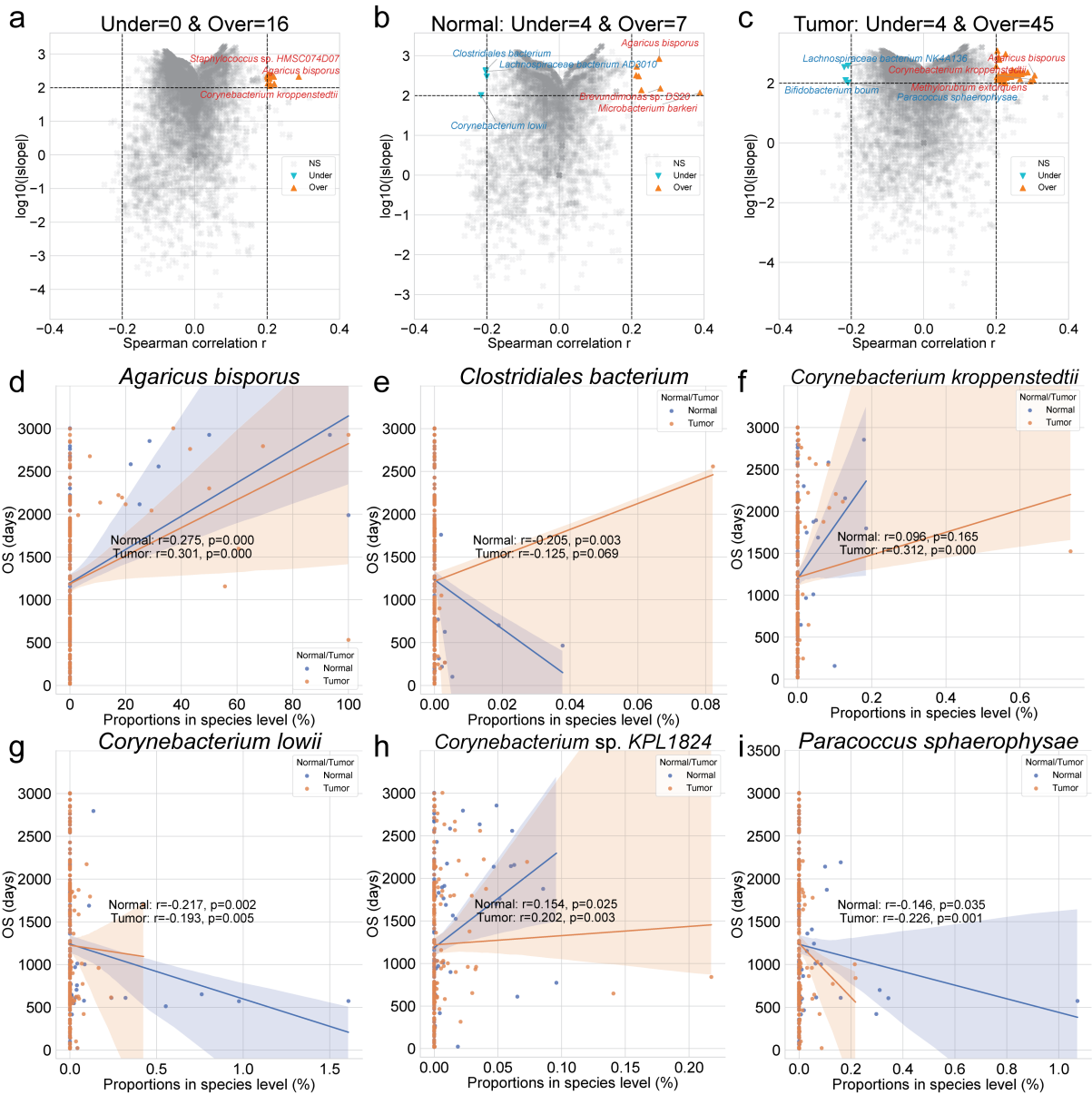


Figure 29: DAT with OS in species level.

(a-c) Volcano plots with OS. x-axis indicates Spearman correlation coefficient (r), and y-axis indicates $\log_{10}(|\text{slope}|)$. **(a)** Total **(b)** Normal samples **(c)** Tumor samples. **(d-l)** Scatter plots of each taxon proportion with OS. **(d)** *Agaricus bisporus* **(e)** *Corynebacterium jeikeium* **(f)** *Corynebacterium kroppenstedtii* **(g)** *Corynebacterium lowii* **(h)** *Kocuria flava* **(i)** *Paracoccus sphaerophysae* **(j)** *Propionibacterium virus Stormborn* **(k)** *Sphingomonas phyllosphaerae* **(l)** *Staphylococcus phage StB20-like*. Statistical significance were calculated with Spearman correlation (r and p).

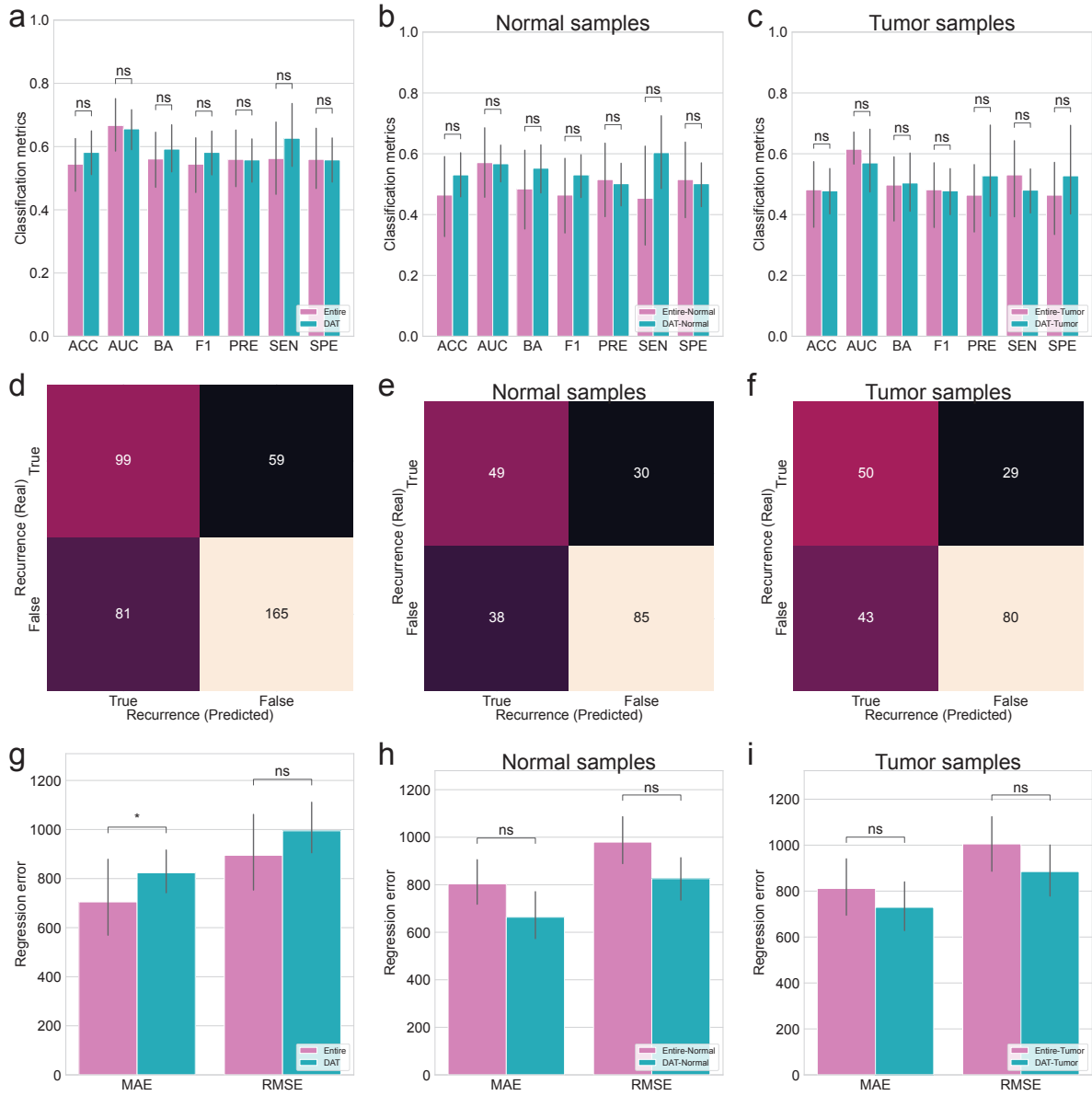


Figure 30: **Random forest classification and regression.**

(a-c) Random forest classification metrics for recurrence. **(a)** Total **(b)** Normal samples **(c)** Tumor samples. **(d-f)** Random forest classification confusion matrices for recurrence. **(d)** Total **(e)** Normal samples **(f)** Tumor samples. **(g-i)** Random forest regression errors for OS. **(g)** Total **(h)** Normal samples **(i)** Tumor samples. MWU test: $p < 0.05$ (*), $p < 0.01$ (**), $p < 0.001$ (***) $p < 0.0001$ (****)

1222 **4.4 Discussion**

₁₂₂₃ **5 Conclusion**

₁₂₂₄ In conclusion, the research described in this doctoral dissertation was conducted to identify significant ...

₁₂₂₅ In the section 2, I show that

¹²²⁶ References

- ¹²²⁷ Aagaard, K., Ma, J., Antony, K. M., Ganu, R., Petrosino, J., & Versalovic, J. (2014). The placenta harbors
¹²²⁸ a unique microbiome. *Science translational medicine*, 6(237), 237ra65–237ra65.
- ¹²²⁹ Abu-Ghazaleh, N., Chua, W. J., & Gopalan, V. (2021). Intestinal microbiota and its association with
¹²³⁰ colon cancer and red/processed meat consumption. *Journal of gastroenterology and hepatology*,
¹²³¹ 36(1), 75–88.
- ¹²³² Abusleme, L., Hoare, A., Hong, B.-Y., & Diaz, P. I. (2021). Microbial signatures of health, gingivitis,
¹²³³ and periodontitis. *Periodontology 2000*, 86(1), 57–78.
- ¹²³⁴ Aitchison, J., Barceló-Vidal, C., Martín-Fernández, J. A., & Pawlowsky-Glahn, V. (2000). Logratio
¹²³⁵ analysis and compositional distance. *Mathematical geology*, 32, 271–275.
- ¹²³⁶ Aja, E., Mangar, M., Fletcher, H., & Mishra, A. (2021). Filifactor alocis: recent insights and advances.
¹²³⁷ *Journal of dental research*, 100(8), 790–797.
- ¹²³⁸ Alelyani, S. (2021). Stable bagging feature selection on medical data. *Journal of Big Data*, 8(1), 11.
- ¹²³⁹ Altabtbaei, K., Maney, P., Ganesan, S. M., Dabdoub, S. M., Nagaraja, H. N., & Kumar, P. S. (2021). Anna
¹²⁴⁰ karenina and the subgingival microbiome associated with periodontitis. *Microbiome*, 9, 1–15.
- ¹²⁴¹ Altingöz, S. M., Kurgan, Ş., Önder, C., Serdar, M. A., Ünlütürk, U., Uyanık, M., ... Günhan, M.
¹²⁴² (2021). Salivary and serum oxidative stress biomarkers and advanced glycation end products in
¹²⁴³ periodontitis patients with or without diabetes: A cross-sectional study. *Journal of periodontology*,
¹²⁴⁴ 92(9), 1274–1285.
- ¹²⁴⁵ Alverdy, J., Hyoju, S., Weigerinck, M., & Gilbert, J. (2017). The gut microbiome and the mechanism of
¹²⁴⁶ surgical infection. *Journal of British Surgery*, 104(2), e14–e23.
- ¹²⁴⁷ An, S., & Park, S. (2022). Association of physical activity and sedentary behavior with the risk of
¹²⁴⁸ colorectal cancer. *Journal of Korean Medical Science*, 37(19).
- ¹²⁴⁹ Anderson, M. J. (2014). Permutational multivariate analysis of variance (permanova). *Wiley statsref:
1250 statistics reference online*, 1–15.
- ¹²⁵¹ Aruni, A. W., Mishra, A., Dou, Y., Chioma, O., Hamilton, B. N., & Fletcher, H. M. (2015). Filifactor
¹²⁵² alocis—a new emerging periodontal pathogen. *Microbes and infection*, 17(7), 517–530.
- ¹²⁵³ Aziz, Q., & Thompson, D. G. (1998). Brain-gut axis in health and disease. *Gastroenterology*, 114(3),
¹²⁵⁴ 559–578.
- ¹²⁵⁵ Bai, X., Wei, H., Liu, W., Coker, O. O., Gou, H., Liu, C., ... others (2022). Cigarette smoke promotes
¹²⁵⁶ colorectal cancer through modulation of gut microbiota and related metabolites. *Gut*, 71(12),

- 1257 2439–2450.
- 1258 Baldelli, V., Scaldaferri, F., Putignani, L., & Del Chierico, F. (2021). The role of enterobacteriaceae in
1259 gut microbiota dysbiosis in inflammatory bowel diseases. *Microorganisms*, 9(4), 697.
- 1260 Bardou, M., Rouland, A., Martel, M., Loffroy, R., Barkun, A. N., & Chapelle, N. (2022). Obesity and
1261 colorectal cancer. *Alimentary Pharmacology & Therapeutics*, 56(3), 407–418.
- 1262 Barlow, G. M., Yu, A., & Mathur, R. (2015). Role of the gut microbiome in obesity and diabetes mellitus.
1263 *Nutrition in clinical practice*, 30(6), 787–797.
- 1264 Basavaprabhu, H., Sonu, K., & Prabha, R. (2020). Mechanistic insights into the action of probiotics
1265 against bacterial vaginosis and its mediated preterm birth: An overview. *Microbial pathogenesis*,
1266 141, 104029.
- 1267 Belstrøm, D., Constancias, F., Drautz-Moses, D. I., Schuster, S. C., Veleba, M., Mahé, F., & Givskov, M.
1268 (2021). Periodontitis associates with species-specific gene expression of the oral microbiota. *npj
1269 Biofilms and Microbiomes*, 7(1), 76.
- 1270 Berger, W. H., & Parker, F. L. (1970). Diversity of planktonic foraminifera in deep-sea sediments.
1271 *Science*, 168(3937), 1345–1347.
- 1272 Berghella, V. (2012). Universal cervical length screening for prediction and prevention of preterm birth.
1273 *Obstetrical & gynecological survey*, 67(10), 653–657.
- 1274 Blencowe, H., Cousens, S., Oestergaard, M. Z., Chou, D., Moller, A.-B., Narwal, R., ... others (2012).
1275 National, regional, and worldwide estimates of preterm birth rates in the year 2010 with time trends
1276 since 1990 for selected countries: a systematic analysis and implications. *The lancet*, 379(9832),
1277 2162–2172.
- 1278 Boland, C. R., & Goel, A. (2010). Microsatellite instability in colorectal cancer. *Gastroenterology*,
1279 138(6), 2073–2087.
- 1280 Boleij, A., Hechenbleikner, E. M., Goodwin, A. C., Badani, R., Stein, E. M., Lazarev, M. G., ... others
1281 (2015). The bacteroides fragilis toxin gene is prevalent in the colon mucosa of colorectal cancer
1282 patients. *Clinical Infectious Diseases*, 60(2), 208–215.
- 1283 Bolstad, A., Jensen, H. B., & Bakken, V. (1996). Taxonomy, biology, and periodontal aspects of
1284 fusobacterium nucleatum. *Clinical microbiology reviews*, 9(1), 55–71.
- 1285 Bolyen, E., Rideout, J. R., Dillon, M. R., Bokulich, N. A., Abnet, C. C., Al-Ghalith, G. A., ... others
1286 (2019). Reproducible, interactive, scalable and extensible microbiome data science using qiime 2.
1287 *Nature biotechnology*, 37(8), 852–857.
- 1288 Bombin, A., Yan, S., Bombin, S., Mosley, J. D., & Ferguson, J. F. (2022). Obesity influences composition
1289 of salivary and fecal microbiota and impacts the interactions between bacterial taxa. *Physiological
1290 reports*, 10(7), e15254.
- 1291 Bonnet, M., Buc, E., Sauvanet, P., Darcha, C., Dubois, D., Pereira, B., ... Darfeuille-Michaud, A. (2014).
1292 Colonization of the human gut by e. coli and colorectal cancer risk. *Clinical Cancer Research*,
1293 20(4), 859–867.
- 1294 Breiman, L. (2001). Random forests. *Machine learning*, 45, 5–32.
- 1295 Brennan, C. A., & Garrett, W. S. (2019). Fusobacterium nucleatum—symbiont, opportunist and

- 1296 oncobacterium. *Nature Reviews Microbiology*, 17(3), 156–166.
- 1297 Broom, L. J., & Kogut, M. H. (2018). The role of the gut microbiome in shaping the immune system of
1298 chickens. *Veterinary immunology and immunopathology*, 204, 44–51.
- 1299 Bryll, R., Gutierrez-Osuna, R., & Quek, F. (2003). Attribute bagging: improving accuracy of classifier
1300 ensembles by using random feature subsets. *Pattern recognition*, 36(6), 1291–1302.
- 1301 Bullman, S., Pedamallu, C. S., Sicinska, E., Clancy, T. E., Zhang, X., Cai, D., ... others (2017). Analysis
1302 of fusobacterium persistence and antibiotic response in colorectal cancer. *Science*, 358(6369),
1303 1443–1448.
- 1304 Burt, R. W., Leppert, M. F., Slattery, M. L., Samowitz, W. S., Spirio, L. N., Kerber, R. A., ... others
1305 (2004). Genetic testing and phenotype in a large kindred with attenuated familial adenomatous
1306 polyposis. *Gastroenterology*, 127(2), 444–451.
- 1307 Cai, Y., Li, Y., Xiong, Y., Geng, X., Kang, Y., & Yang, Y. (2024). Diabetic foot exacerbates gut
1308 mycobiome dysbiosis in adult patients with type 2 diabetes mellitus: revealing diagnostic markers.
1309 *Nutrition & Diabetes*, 14(1), 71.
- 1310 Callahan, B. J., McMurdie, P. J., Rosen, M. J., Han, A. W., Johnson, A. J. A., & Holmes, S. P. (2016).
1311 Dada2: High-resolution sample inference from illumina amplicon data. *Nature methods*, 13(7),
1312 581–583.
- 1313 Canakci, V., & Canakci, C. F. (2007). Pain levels in patients during periodontal probing and mechanical
1314 non-surgical therapy. *Clinical oral investigations*, 11, 377–383.
- 1315 Cappellato, M., Baruzzo, G., & Di Camillo, B. (2022). Investigating differential abundance methods in
1316 microbiome data: A benchmark study. *PLoS computational biology*, 18(9), e1010467.
- 1317 Castaner, O., Goday, A., Park, Y.-M., Lee, S.-H., Magkos, F., Shiow, S.-A. T. E., & Schröder, H. (2018).
1318 The gut microbiome profile in obesity: a systematic review. *International journal of endocrinology*,
1319 2018(1), 4095789.
- 1320 Center, M. M., Jemal, A., Smith, R. A., & Ward, E. (2009). Worldwide variations in colorectal cancer.
1321 *CA: a cancer journal for clinicians*, 59(6), 366–378.
- 1322 Centor, R. M. (1991). Signal detectability: the use of roc curves and their analyses. *Medical decision
1323 making*, 11(2), 102–106.
- 1324 Cerqueira, F. M., Photenhauer, A. L., Pollet, R. M., Brown, H. A., & Koropatkin, N. M. (2020). Starch
1325 digestion by gut bacteria: crowdsourcing for carbs. *Trends in Microbiology*, 28(2), 95–108.
- 1326 Champagne, C., McNairn, H., Daneshfar, B., & Shang, J. (2014). A bootstrap method for assessing
1327 classification accuracy and confidence for agricultural land use mapping in canada. *International
1328 Journal of Applied Earth Observation and Geoinformation*, 29, 44–52.
- 1329 Chao, A. (1984). Nonparametric estimation of the number of classes in a population. *Scandinavian
1330 Journal of statistics*, 265–270.
- 1331 Chao, A., & Lee, S.-M. (1992). Estimating the number of classes via sample coverage. *Journal of the
1332 American statistical Association*, 87(417), 210–217.
- 1333 Chapple, I. L., Mealey, B. L., Van Dyke, T. E., Bartold, P. M., Dommisch, H., Eickholz, P., ... others
1334 (2018). Periodontal health and gingival diseases and conditions on an intact and a reduced

- 1335 periodontium: Consensus report of workgroup 1 of the 2017 world workshop on the classification
1336 of periodontal and peri-implant diseases and conditions. *Journal of periodontology*, 89, S74–S84.
- 1337 Chen, T., Marsh, P., & Al-Hebshi, N. (2022). Smdi: an index for measuring subgingival microbial
1338 dysbiosis. *Journal of dental research*, 101(3), 331–338.
- 1339 Chen, T., Yu, W.-H., Izard, J., Baranova, O. V., Lakshmanan, A., & Dewhirst, F. E. (2010). The human
1340 oral microbiome database: a web accessible resource for investigating oral microbe taxonomic and
1341 genomic information. *Database*, 2010.
- 1342 Chen, X., D’Souza, R., & Hong, S.-T. (2013). The role of gut microbiota in the gut-brain axis: current
1343 challenges and perspectives. *Protein & cell*, 4, 403–414.
- 1344 Chen, X., Jansen, L., Guo, F., Hoffmeister, M., Chang-Claude, J., & Brenner, H. (2021). Smoking,
1345 genetic predisposition, and colorectal cancer risk. *Clinical and translational gastroenterology*,
1346 12(3), e00317.
- 1347 Chen, X., Li, H., Guo, F., Hoffmeister, M., & Brenner, H. (2022). Alcohol consumption, polygenic risk
1348 score, and early-and late-onset colorectal cancer risk. *EClinicalMedicine*, 49.
- 1349 Chew, R. J. J., Tan, K. S., Chen, T., Al-Hebshi, N. N., & Goh, C. E. (2024). Quantifying periodontitis-
1350 associated oral dysbiosis in tongue and saliva microbiomes—an integrated data analysis. *Journal
1351 of Periodontology*.
- 1352 Čižmárová, B., Tomečková, V., Hubková, B., Hurajtová, A., Ohlasová, J., & Birková, A. (2022). Salivary
1353 redox homeostasis in human health and disease. *International Journal of Molecular Sciences*,
1354 23(17), 10076.
- 1355 Cullin, N., Antunes, C. A., Straussman, R., Stein-Thoeringer, C. K., & Elinav, E. (2021). Microbiome
1356 and cancer. *Cancer Cell*, 39(10), 1317–1341.
- 1357 Curtius, K., Wright, N. A., & Graham, T. A. (2018). An evolutionary perspective on field cancerization.
1358 *Nature Reviews Cancer*, 18(1), 19–32.
- 1359 Dabke, K., Hendrick, G., Devkota, S., et al. (2019). The gut microbiome and metabolic syndrome. *The
1360 Journal of clinical investigation*, 129(10), 4050–4057.
- 1361 DeSantis, T. Z., Hugenholtz, P., Larsen, N., Rojas, M., Brodie, E. L., Keller, K., … Andersen, G. L.
1362 (2006). Greengenes, a chimera-checked 16s rrna gene database and workbench compatible with
1363 arb. *Applied and environmental microbiology*, 72(7), 5069–5072.
- 1364 Doyle, R., Alber, D., Jones, H., Harris, K., Fitzgerald, F., Peebles, D., & Klein, N. (2014). Term and
1365 preterm labour are associated with distinct microbial community structures in placental membranes
1366 which are independent of mode of delivery. *Placenta*, 35(12), 1099–1101.
- 1367 Fahmy, C. A., Gamal-Eldeen, A. M., El-Hussieny, E. A., Raafat, B. M., Mehanna, N. S., Talaat, R. M., &
1368 Shaaban, M. T. (2019). *Bifidobacterium longum* suppresses murine colorectal cancer through the
1369 modulation of oncomirs and tumor suppressor mirnas. *Nutrition and cancer*, 71(4), 688–700.
- 1370 Faith, D. P. (1992). Conservation evaluation and phylogenetic diversity. *Biological conservation*, 61(1),
1371 1–10.
- 1372 Fettweis, J. M., Serrano, M. G., Brooks, J. P., Edwards, D. J., Girerd, P. H., Parikh, H. I., … others
1373 (2019). The vaginal microbiome and preterm birth. *Nature medicine*, 25(6), 1012–1021.

- 1374 Fisher, R. A., Corbet, A. S., & Williams, C. B. (1943). The relation between the number of species and
1375 the number of individuals in a random sample of an animal population. *The Journal of Animal*
1376 *Ecology*, 42–58.
- 1377 Flanagan, L., Schmid, J., Ebert, M., Soucek, P., Kunicka, T., Liska, V., ... others (2014). Fusobacterium
1378 nucleatum associates with stages of colorectal neoplasia development, colorectal cancer and disease
1379 outcome. *European journal of clinical microbiology & infectious diseases*, 33, 1381–1390.
- 1380 Fortenberry, J. D. (2013). The uses of race and ethnicity in human microbiome research. *Trends in*
1381 *microbiology*, 21(4), 165–166.
- 1382 Francescone, R., Hou, V., & Grivennikov, S. I. (2014). Microbiome, inflammation, and cancer. *The*
1383 *Cancer Journal*, 20(3), 181–189.
- 1384 Friedman, J. H. (2002). Stochastic gradient boosting. *Computational statistics & data analysis*, 38(4),
1385 367–378.
- 1386 Fushiki, T. (2011). Estimation of prediction error by using k-fold cross-validation. *Statistics and*
1387 *Computing*, 21, 137–146.
- 1388 Gambin, D. J., Vitali, F. C., De Carli, J. P., Mazzon, R. R., Gomes, B. P., Duque, T. M., & Trentin, M. S.
1389 (2021). Prevalence of red and orange microbial complexes in endodontic-periodontal lesions: a
1390 systematic review and meta-analysis. *Clinical Oral Investigations*, 1–14.
- 1391 Gao, J., Yin, J., Xu, K., Li, T., & Yin, Y. (2019). What is the impact of diet on nutritional diarrhea
1392 associated with gut microbiota in weaning piglets: a system review. *BioMed research international*,
1393 2019(1), 6916189.
- 1394 Geurts, P., Ernst, D., & Wehenkel, L. (2006). Extremely randomized trees. *Machine learning*, 63, 3–42.
- 1395 Ghanavati, R., Akbari, A., Mohammadi, F., Asadollahi, P., Javadi, A., Talebi, M., & Rohani, M. (2020).
1396 Lactobacillus species inhibitory effect on colorectal cancer progression through modulating the
1397 wnt/β-catenin signaling pathway. *Molecular and Cellular Biochemistry*, 470, 1–13.
- 1398 Ghajogh, B., & Crowley, M. (2019). The theory behind overfitting, cross validation, regularization,
1399 bagging, and boosting: tutorial. *arXiv preprint arXiv:1905.12787*.
- 1400 Ghorbani, E., Avan, A., Ryzhikov, M., Ferns, G., Khazaei, M., & Soleimanpour, S. (2022). Role of
1401 lactobacillus strains in the management of colorectal cancer: An overview of recent advances.
1402 *Nutrition*, 103, 111828.
- 1403 Gilbert, J. A., Blaser, M. J., Caporaso, J. G., Jansson, J. K., Lynch, S. V., & Knight, R. (2018). Current
1404 understanding of the human microbiome. *Nature medicine*, 24(4), 392–400.
- 1405 Gini, C. (1912). Variabilità e mutabilità (variability and mutability). *Tipografia di Paolo Cuppini,*
1406 *Bologna, Italy*, 156.
- 1407 Goldenberg, R. L., Culhane, J. F., Iams, J. D., & Romero, R. (2008). Epidemiology and causes of preterm
1408 birth. *The lancet*, 371(9606), 75–84.
- 1409 Gonçalves, L., Subtil, A., Oliveira, M. R., & de Zea Bermudez, P. (2014). Roc curve estimation: An
1410 overview. *REVSTAT-Statistical journal*, 12(1), 1–20.
- 1411 Good, I. J. (1953). The population frequencies of species and the estimation of population parameters.
1412 *Biometrika*, 40(3-4), 237–264.

- 1413 Goodyear, M. D., Krleza-Jeric, K., & Lemmens, T. (2007). *The declaration of helsinki* (Vol. 335) (No. 1414 7621). British Medical Journal Publishing Group.
- 1415 Haffajee, A., Teles, R., & Socransky, S. (2006). Association of eubacterium nodatum and treponema 1416 denticola with human periodontitis lesions. *Oral microbiology and immunology*, 21(5), 269–282.
- 1417 Hajishengallis, G. (2015). Periodontitis: from microbial immune subversion to systemic inflammation. 1418 *Nature reviews immunology*, 15(1), 30–44.
- 1419 Hamjane, N., Mechita, M. B., Nourouti, N. G., & Barakat, A. (2024). Gut microbiota dysbiosis-associated 1420 obesity and its involvement in cardiovascular diseases and type 2 diabetes. a systematic review. 1421 *Microvascular Research*, 151, 104601.
- 1422 Hamming, R. W. (1950). Error detecting and error correcting codes. *The Bell system technical journal*, 1423 29(2), 147–160.
- 1424 Hampel, H., Frankel, W. L., Martin, E., Arnold, M., Khanduja, K., Kuebler, P., ... others (2008). 1425 Feasibility of screening for lynch syndrome among patients with colorectal cancer. *Journal of Clinical Oncology*, 26(35), 5783–5788.
- 1427 Han, Y. W. (2015). Fusobacterium nucleatum: a commensal-turned pathogen. *Current opinion in 1428 microbiology*, 23, 141–147.
- 1429 Han, Y. W., & Wang, X. (2013). Mobile microbiome: oral bacteria in extra-oral infections and 1430 inflammation. *Journal of dental research*, 92(6), 485–491.
- 1431 Hand, D. J. (2012). Assessing the performance of classification methods. *International Statistical Review*, 1432 80(3), 400–414.
- 1433 Hartstra, A. V., Bouter, K. E., Bäckhed, F., & Nieuwdorp, M. (2015). Insights into the role of the 1434 microbiome in obesity and type 2 diabetes. *Diabetes care*, 38(1), 159–165.
- 1435 Hashemi Goradel, N., Heidarzadeh, S., Jahangiri, S., Farhood, B., Mortezaee, K., Khanlarkhani, N., & 1436 Negahdari, B. (2019). Fusobacterium nucleatum and colorectal cancer: A mechanistic overview. 1437 *Journal of Cellular Physiology*, 234(3), 2337–2344.
- 1438 Heip, C. (1974). A new index measuring evenness. *Journal of the Marine Biological Association of the 1439 United Kingdom*, 54(3), 555–557.
- 1440 Helmink, B. A., Khan, M. W., Hermann, A., Gopalakrishnan, V., & Wargo, J. A. (2019). The microbiome, 1441 cancer, and cancer therapy. *Nature medicine*, 25(3), 377–388.
- 1442 Hill, M. O. (1973). Diversity and evenness: a unifying notation and its consequences. *Ecology*, 54(2), 1443 427–432.
- 1444 Hiranmayi, K. V., Sirisha, K., Rao, M. R., & Sudhakar, P. (2017). Novel pathogens in periodontal 1445 microbiology. *Journal of Pharmacy and Bioallied Sciences*, 9(3), 155–163.
- 1446 Honda, K., & Littman, D. R. (2012). The microbiome in infectious disease and inflammation. *Annual 1447 review of immunology*, 30(1), 759–795.
- 1448 Honest, H., Forbes, C., Durée, K., Norman, G., Duffy, S., Tsourapas, A., ... others (2009). Screening to 1449 prevent spontaneous preterm birth: systematic reviews of accuracy and effectiveness literature with 1450 economic modelling. *Health Technol Assess*, 13(43), 1–627.
- 1451 Hong, Y. M., Lee, J., Cho, D. H., Jeon, J. H., Kang, J., Kim, M.-G., ... J. K. (2023). Predicting preterm

- 1452 birth using machine learning techniques in oral microbiome. *Scientific Reports*, 13(1), 21105.
- 1453 Hossin, M., & Sulaiman, M. N. (2015). A review on evaluation metrics for data classification evaluations.
1454 *International journal of data mining & knowledge management process*, 5(2), 1.
- 1455 Huang, R.-Y., Lin, C.-D., Lee, M.-S., Yeh, C.-L., Shen, E.-C., Chiang, C.-Y., ... Fu, E. (2007). Mandibular
1456 disto-lingual root: a consideration in periodontal therapy. *Journal of periodontology*, 78(8), 1485–
1457 1490.
- 1458 Iams, J. D., & Berghella, V. (2010). Care for women with prior preterm birth. *American journal of
1459 obstetrics and gynecology*, 203(2), 89–100.
- 1460 Ide, M., & Papapanou, P. N. (2013). Epidemiology of association between maternal periodontal
1461 disease and adverse pregnancy outcomes—systematic review. *Journal of clinical periodontology*,
1462 40, S181–S194.
- 1463 Iniesta, M., Chamorro, C., Ambrosio, N., Marín, M. J., Sanz, M., & Herrera, D. (2023). Subgingival
1464 microbiome in periodontal health, gingivitis and different stages of periodontitis. *Journal of
1465 Clinical Periodontology*, 50(7), 905–920.
- 1466 Inra, J. A., Steyerberg, E. W., Grover, S., McFarland, A., Syngal, S., & Kastrinos, F. (2015). Racial
1467 variation in frequency and phenotypes of apc and mutyh mutations in 6,169 individuals undergoing
1468 genetic testing. *Genetics in Medicine*, 17(10), 815–821.
- 1469 Jaccard, P. (1908). Nouvelles recherches sur la distribution florale. *Bull. Soc. Vaud. Sci. Nat.*, 44,
1470 223–270.
- 1471 Janda, J. M., & Abbott, S. L. (2007). 16s rrna gene sequencing for bacterial identification in the diagnostic
1472 laboratory: pluses, perils, and pitfalls. *Journal of clinical microbiology*, 45(9), 2761–2764.
- 1473 Jiang, W., & Simon, R. (2007). A comparison of bootstrap methods and an adjusted bootstrap approach
1474 for estimating the prediction error in microarray classification. *Statistics in medicine*, 26(29),
1475 5320–5334.
- 1476 John, G. K., & Mullin, G. E. (2016). The gut microbiome and obesity. *Current oncology reports*, 18,
1477 1–7.
- 1478 Johnson, J. S., Spakowicz, D. J., Hong, B.-Y., Petersen, L. M., Demkowicz, P., Chen, L., ... others (2019).
1479 Evaluation of 16s rrna gene sequencing for species and strain-level microbiome analysis. *Nature
1480 communications*, 10(1), 5029.
- 1481 Jorth, P., Turner, K. H., Gumus, P., Nizam, N., Buduneli, N., & Whiteley, M. (2014). Metatranscriptomics
1482 of the human oral microbiome during health and disease. *MBio*, 5(2), 10–1128.
- 1483 Joscelyn, J., & Kasper, L. H. (2014). Digesting the emerging role for the gut microbiome in central
1484 nervous system demyelination. *Multiple Sclerosis Journal*, 20(12), 1553–1559.
- 1485 Kang, Y., Kang, X., Yang, H., Liu, H., Yang, X., Liu, Q., ... others (2022). Lactobacillus acidophilus ame-
1486 liorates obesity in mice through modulation of gut microbiota dysbiosis and intestinal permeability.
1487 *Pharmacological research*, 175, 106020.
- 1488 Karched, M., Bhardwaj, R. G., Qudeimat, M., Al-Khabbaz, A., & Ellepol, A. (2022). Proteomic analysis
1489 of the periodontal pathogen prevotella intermedia secretomes in biofilm and planktonic lifestyles.
1490 *Scientific Reports*, 12(1), 5636.

- 1491 Katz, J., Chegini, N., Shiverick, K., & Lamont, R. (2009). Localization of *p. gingivalis* in preterm delivery
1492 placenta. *Journal of dental research*, 88(6), 575–578.
- 1493 Kau, A. L., Ahern, P. P., Griffin, N. W., Goodman, A. L., & Gordon, J. I. (2011). Human nutrition, the
1494 gut microbiome and the immune system. *Nature*, 474(7351), 327–336.
- 1495 Kelly, B. J., Gross, R., Bittinger, K., Sherrill-Mix, S., Lewis, J. D., Collman, R. G., ... Li, H. (2015).
1496 Power and sample-size estimation for microbiome studies using pairwise distances and permanova.
1497 *Bioinformatics*, 31(15), 2461–2468.
- 1498 Kennedy, J., Alexander, P., Taillie, L. S., & Jaacks, L. M. (2024). Estimated effects of reductions in
1499 processed meat consumption and unprocessed red meat consumption on occurrences of type 2
1500 diabetes, cardiovascular disease, colorectal cancer, and mortality in the usa: a microsimulation
1501 study. *The Lancet Planetary Health*, 8(7), e441–e451.
- 1502 Kim, B.-R., Shin, J., Guevarra, R. B., Lee, J. H., Kim, D. W., Seol, K.-H., ... Isaacson, R. E. (2017).
1503 Deciphering diversity indices for a better understanding of microbial communities. *Journal of
1504 Microbiology and Biotechnology*, 27(12), 2089–2093.
- 1505 Kim, C. H. (2018). Immune regulation by microbiome metabolites. *Immunology*, 154(2), 220–229.
- 1506 Kim, E.-H., Kim, S., Kim, H.-J., Jeong, H.-o., Lee, J., Jang, J., ... others (2020). Prediction of chronic
1507 periodontitis severity using machine learning models based on salivary bacterial copy number.
1508 *Frontiers in Cellular and Infection Microbiology*, 10, 571515.
- 1509 Kim, J.-H. (2009). Estimating classification error rate: Repeated cross-validation, repeated hold-out and
1510 bootstrap. *Computational statistics & data analysis*, 53(11), 3735–3745.
- 1511 Kinane, D. F., Stathopoulou, P. G., & Papapanou, P. N. (2017). Periodontal diseases. *Nature reviews
1512 Disease primers*, 3(1), 1–14.
- 1513 Kindinger, L. M., Bennett, P. R., Lee, Y. S., Marchesi, J. R., Smith, A., Caciato, S., ... MacIntyre,
1514 D. A. (2017). The interaction between vaginal microbiota, cervical length, and vaginal progesterone
1515 treatment for preterm birth risk. *Microbiome*, 5, 1–14.
- 1516 Kogut, M. H., Lee, A., & Santin, E. (2020). Microbiome and pathogen interaction with the immune
1517 system. *Poultry science*, 99(4), 1906–1913.
- 1518 Kostic, A. D., Ojesina, A. I., Pedamallu, C. S., Jung, J., Verhaak, R. G., Getz, G., & Meyerson, M. (2011).
1519 Pathseq: software to identify or discover microbes by deep sequencing of human tissue. *Nature
1520 biotechnology*, 29(5), 393–396.
- 1521 Kotsiantis, S. B., Zaharakis, I. D., & Pintelas, P. E. (2006). Machine learning: a review of classification
1522 and combining techniques. *Artificial Intelligence Review*, 26, 159–190.
- 1523 Kuipers, E. J., Grady, W. M., Lieberman, D., Seufferlein, T., Sung, J. J., Boelens, P. G., ... Watanabe, T.
1524 (2015). Colorectal cancer. *Nature reviews. Disease primers*, 1, 15065.
- 1525 Lafaurie, G. I., Neuta, Y., Ríos, R., Pacheco-Montealegre, M., Pianeta, R., Castillo, D. M., ... oth-
1526 ers (2022). Differences in the subgingival microbiome according to stage of periodontitis: A
1527 comparison of two geographic regions. *PloS one*, 17(8), e0273523.
- 1528 Lamont, R. J., & Jenkinson, H. F. (2000). Subgingival colonization by *porphyromonas gingivalis*. *Oral
1529 Microbiology and Immunology: Mini-review*, 15(6), 341–349.

- 1530 Lamont, R. J., Koo, H., & Hajishengallis, G. (2018). The oral microbiota: dynamic communities and
1531 host interactions. *Nature reviews microbiology*, 16(12), 745–759.
- 1532 Leitich, H., & Kaider, A. (2003). Fetal fibronectin—how useful is it in the prediction of preterm birth?
1533 *BJOG: An International Journal of Obstetrics & Gynaecology*, 110, 66–70.
- 1534 Le Leu, R. K., Hu, Y., Brown, I. L., Woodman, R. J., & Young, G. P. (2010). Synbiotic intervention of
1535 bifidobacterium lactis and resistant starch protects against colorectal cancer development in rats.
1536 *Carcinogenesis*, 31(2), 246–251.
- 1537 León, R., Silva, N., Ovalle, A., Chaparro, A., Ahumada, A., Gajardo, M., ... Gamonal, J. (2007).
1538 Detection of porphyromonas gingivalis in the amniotic fluid in pregnant women with a diagnosis
1539 of threatened premature labor. *Journal of periodontology*, 78(7), 1249–1255.
- 1540 Li, H., & Durbin, R. (2009). Fast and accurate short read alignment with burrows–wheeler transform.
1541 *bioinformatics*, 25(14), 1754–1760.
- 1542 Li, N., Lu, B., Luo, C., Cai, J., Lu, M., Zhang, Y., ... Dai, M. (2021). Incidence, mortality, survival,
1543 risk factor and screening of colorectal cancer: A comparison among china, europe, and northern
1544 america. *Cancer letters*, 522, 255–268.
- 1545 Li, R., Miao, Z., Liu, Y., Chen, X., Wang, H., Su, J., & Chen, J. (2024). The brain–gut–bone axis in
1546 neurodegenerative diseases: insights, challenges, and future prospects. *Advanced Science*, 11(38),
1547 2307971.
- 1548 Li, W., & Yang, J. (2025). Investigating the anna karenina principle of the breast microbiome. *BMC
1549 microbiology*, 25(1), 1–10.
- 1550 Li, X., Yu, D., Wang, Y., Yuan, H., Ning, X., Rui, B., ... Li, M. (2021). The intestinal dysbiosis of
1551 mothers with gestational diabetes mellitus (gdm) and its impact on the gut microbiota of their
1552 newborns. *Canadian Journal of Infectious Diseases and Medical Microbiology*, 2021(1), 3044534.
- 1553 Li, Y., Qian, F., Cheng, X., Wang, D., Wang, Y., Pan, Y., ... Tian, Y. (2023). Dysbiosis of oral microbiota
1554 and metabolite profiles associated with type 2 diabetes mellitus. *Microbiology spectrum*, 11(1),
1555 e03796–22.
- 1556 Lim, J. W., Park, T., Tong, Y. W., & Yu, Z. (2020). The microbiome driving anaerobic digestion and
1557 microbial analysis. In *Advances in bioenergy* (Vol. 5, pp. 1–61). Elsevier.
- 1558 Lin, H., Eggesbø, M., & Peddada, S. D. (2022). Linear and nonlinear correlation estimators unveil
1559 undescribed taxa interactions in microbiome data. *Nature communications*, 13(1), 4946.
- 1560 Lin, H., & Peddada, S. D. (2020). Analysis of compositions of microbiomes with bias correction. *Nature
1561 communications*, 11(1), 3514.
- 1562 Lin, H., & Peddada, S. D. (2024). Multigroup analysis of compositions of microbiomes with covariate
1563 adjustments and repeated measures. *Nature Methods*, 21(1), 83–91.
- 1564 Listgarten, M. A. (1986). Pathogenesis of periodontitis. *Journal of clinical periodontology*, 13(5),
1565 418–425.
- 1566 Lloyd-Price, J., Abu-Ali, G., & Huttenhower, C. (2016). The healthy human microbiome. *Genome
1567 medicine*, 8, 1–11.
- 1568 López-Aladid, R., Fernández-Barat, L., Alcaraz-Serrano, V., Bueno-Freire, L., Vázquez, N., Pastor-

- 1569 Ibáñez, R., ... Torres, A. (2023). Determining the most accurate 16s rrna hypervariable region for
1570 taxonomic identification from respiratory samples. *Scientific reports*, 13(1), 3974.
- 1571 Love, M. I., Huber, W., & Anders, S. (2014). Moderated estimation of fold change and dispersion for
1572 rna-seq data with deseq2. *Genome biology*, 15, 1–21.
- 1573 Ma, Z. S. (2020). Testing the anna karenina principle in human microbiome-associated diseases. *Iscience*,
1574 23(4).
- 1575 Magnúsdóttir, S., & Thiele, I. (2018). Modeling metabolism of the human gut microbiome. *Current
1576 opinion in biotechnology*, 51, 90–96.
- 1577 Magurran, A. E. (2021). Measuring biological diversity. *Current Biology*, 31(19), R1174–R1177.
- 1578 Mandic, M., Safizadeh, F., Niedermaier, T., Hoffmeister, M., & Brenner, H. (2023). Association of
1579 overweight, obesity, and recent weight loss with colorectal cancer risk. *JAMA network Open*, 6(4),
1580 e239556–e239556.
- 1581 Mann, H. B., & Whitney, D. R. (1947). On a test of whether one of two random variables is stochastically
1582 larger than the other. *The annals of mathematical statistics*, 50–60.
- 1583 Manolis, A. A., Manolis, T. A., Melita, H., & Manolis, A. S. (2022). Gut microbiota and cardiovascular
1584 disease: symbiosis versus dysbiosis. *Current Medicinal Chemistry*, 29(23), 4050–4077.
- 1585 Martin, C. R., Osadchiy, V., Kalani, A., & Mayer, E. A. (2018). The brain-gut-microbiome axis. *Cellular
1586 and molecular gastroenterology and hepatology*, 6(2), 133–148.
- 1587 Maulud, D., & Abdulazeez, A. M. (2020). A review on linear regression comprehensive in machine
1588 learning. *Journal of Applied Science and Technology Trends*, 1(2), 140–147.
- 1589 Mayer, E. A., Tillisch, K., Gupta, A., et al. (2015). Gut/brain axis and the microbiota. *The Journal of
1590 clinical investigation*, 125(3), 926–938.
- 1591 Melguizo-Rodríguez, L., Costela-Ruiz, V. J., Manzano-Moreno, F. J., Ruiz, C., & Illescas-Montes, R.
1592 (2020). Salivary biomarkers and their application in the diagnosis and monitoring of the most
1593 common oral pathologies. *International journal of molecular sciences*, 21(14), 5173.
- 1594 Merrill, L. C., & Mangano, K. M. (2023). Racial and ethnic differences in studies of the gut microbiome
1595 and osteoporosis. *Current Osteoporosis Reports*, 21(5), 578–591.
- 1596 Miller, C. S., Ding, X., Dawson III, D. R., & Ebersole, J. L. (2021). Salivary biomarkers for discriminating
1597 periodontitis in the presence of diabetes. *Journal of clinical periodontology*, 48(2), 216–225.
- 1598 Morita, T., Yamazaki, Y., Mita, A., Takada, K., Seto, M., Nishinoue, N., ... Maeno, M. (2010). A cohort
1599 study on the association between periodontal disease and the development of metabolic syndrome.
1600 *Journal of periodontology*, 81(4), 512–519.
- 1601 Na, H. S., Kim, S. Y., Han, H., Kim, H.-J., Lee, J.-Y., Lee, J.-H., & Chung, J. (2020). Identification of
1602 potential oral microbial biomarkers for the diagnosis of periodontitis. *Journal of clinical medicine*,
1603 9(5), 1549.
- 1604 Nemoto, T., Shiba, T., Komatsu, K., Watanabe, T., Shimogishi, M., Shibasaki, M., ... others (2021).
1605 Discrimination of bacterial community structures among healthy, gingivitis, and periodontitis
1606 statuses through integrated metatranscriptomic and network analyses. *Msystems*, 6(6), e00886–21.
- 1607 Nesbitt, M. J., Reynolds, M. A., Shiau, H., Choe, K., Simonsick, E. M., & Ferrucci, L. (2010). Association

- of periodontitis and metabolic syndrome in the baltimore longitudinal study of aging. *Aging clinical and experimental research*, 22, 238–242.
- Network, C. G. A., et al. (2012). Comprehensive molecular characterization of human colon and rectal cancer. *Nature*, 487(7407), 330.
- Nibali, L., Sousa, V., Davrandi, M., Spratt, D., Alyahya, Q., Dopico, J., & Donos, N. (2020). Differences in the periodontal microbiome of successfully treated and persistent aggressive periodontitis. *Journal of Clinical Periodontology*, 47(8), 980–990.
- Novaković, J. D., Veljović, A., Ilić, S. S., Papić, Ž., & Tomović, M. (2017). Evaluation of classification models in machine learning. *Theory and Applications of Mathematics & Computer Science*, 7(1), 39.
- Obuchowski, N. A., & Bullen, J. A. (2018). Receiver operating characteristic (roc) curves: review of methods with applications in diagnostic medicine. *Physics in Medicine & Biology*, 63(7), 07TR01.
- Ochiai, A. (1957). Zoogeographic studies on the soleoid fishes found in japan and its neighbouring regions. *Bulletin of Japanese Society of Scientific Fisheries*, 22, 526–530.
- Offenbacher, S., Katz, V., Fertik, G., Collins, J., Boyd, D., Maynor, G., ... Beck, J. (1996). Periodontal infection as a possible risk factor for preterm low birth weight. *Journal of periodontology*, 67, 1103–1113.
- Ojesina, A. I., Pedamallu, C. S., Kostic, A., Jung, J., Auclair, D., Lohr, J., ... Meyerson, M. (2013). High throughput sequencing-based pathogen discovery in multiple myeloma. *Blood*, 122(21), 5322.
- Omondiagbe, D. A., Veeramani, S., & Sidhu, A. S. (2019). Machine learning classification techniques for breast cancer diagnosis. In *Iop conference series: materials science and engineering* (Vol. 495, p. 012033).
- O'Sullivan, D. E., Sutherland, R. L., Town, S., Chow, K., Fan, J., Forbes, N., ... Brenner, D. R. (2022). Risk factors for early-onset colorectal cancer: a systematic review and meta-analysis. *Clinical gastroenterology and hepatology*, 20(6), 1229–1240.
- Paganini, D., & Zimmermann, M. B. (2017). The effects of iron fortification and supplementation on the gut microbiome and diarrhea in infants and children: a review. *The American journal of clinical nutrition*, 106, 1688S–1693S.
- Pan, A. Y. (2021). Statistical analysis of microbiome data: the challenge of sparsity. *Current Opinion in Endocrine and Metabolic Research*, 19, 35–40.
- Papapanou, P. N., Sanz, M., Buduneli, N., Dietrich, T., Feres, M., Fine, D. H., ... others (2018). Periodontitis: Consensus report of workgroup 2 of the 2017 world workshop on the classification of periodontal and peri-implant diseases and conditions. *Journal of periodontology*, 89, S173–S182.
- Parizadeh, M., & Arrieta, M.-C. (2023). The global human gut microbiome: genes, lifestyles, and diet. *Trends in Molecular Medicine*.
- Park, J., Park, S. H., Lee, D., Lee, J. E., Lee, D., Na, K. J., ... Im, H.-J. (2024). Detecting cancer microbiota using unmapped rna reads on spatial transcriptomics. *Cancer Research*, 84(6_Supplement), 4881–4881.
- Payne, M. S., Newnham, J. P., Doherty, D. A., Furfarro, L. L., Pendal, N. L., Loh, D. E., & Keelan, J. A.

- 1647 (2021). A specific bacterial dna signature in the vagina of australian women in midpregnancy
1648 predicts high risk of spontaneous preterm birth (the predict1000 study). *American journal of*
1649 *obstetrics and gynecology*, 224(2), 206–e1.
- 1650 Peirce, J. M., & Alviña, K. (2019). The role of inflammation and the gut microbiome in depression and
1651 anxiety. *Journal of neuroscience research*, 97(10), 1223–1241.
- 1652 Peltomaki, P. (2003). Role of dna mismatch repair defects in the pathogenesis of human cancer. *Journal*
1653 *of clinical oncology*, 21(6), 1174–1179.
- 1654 Pezzino, S., Sofia, M., Greco, L. P., Litrico, G., Filippello, G., Sarvà, I., ... Latteri, S. (2023). Microbiome
1655 dysbiosis: a pathological mechanism at the intersection of obesity and glaucoma. *International*
1656 *Journal of Molecular Sciences*, 24(2), 1166.
- 1657 Pollard, T. J., Johnson, A. E., Raffa, J. D., & Mark, R. G. (2018). tableone: An open source python
1658 package for producing summary statistics for research papers. *JAMIA open*, 1(1), 26–31.
- 1659 Premaraj, T. S., Vella, R., Chung, J., Lin, Q., Hunter, P., Underwood, K., ... Zhou, Y. (2020). Ethnic
1660 variation of oral microbiota in children. *Scientific reports*, 10(1), 14788.
- 1661 Raut, J. R., Schöttker, B., Holleczek, B., Guo, F., Bhardwaj, M., Miah, K., ... Brenner, H. (2021).
1662 A microrna panel compared to environmental and polygenic scores for colorectal cancer risk
1663 prediction. *Nature Communications*, 12(1), 4811.
- 1664 Rebersek, M. (2021). Gut microbiome and its role in colorectal cancer. *BMC cancer*, 21(1), 1325.
- 1665 Redanz, U., Redanz, S., Treerat, P., Prakasam, S., Lin, L.-J., Merritt, J., & Kreth, J. (2021). Differential
1666 response of oral mucosal and gingival cells to corynebacterium durum, streptococcus sanguinis, and
1667 porphyromonas gingivalis multispecies biofilms. *Frontiers in cellular and infection microbiology*,
1668 11, 686479.
- 1669 Relvas, M., Regueira-Iglesias, A., Balsa-Castro, C., Salazar, F., Pacheco, J., Cabral, C., ... Tomás, I.
1670 (2021). Relationship between dental and periodontal health status and the salivary microbiome:
1671 bacterial diversity, co-occurrence networks and predictive models. *Scientific reports*, 11(1), 929.
- 1672 Renson, A., Jones, H. E., Beghini, F., Segata, N., Zolnik, C. P., Usyk, M., ... others (2019). Sociodemo-
1673 graphic variation in the oral microbiome. *Annals of epidemiology*, 35, 73–80.
- 1674 Renvert, S., & Persson, G. (2002). A systematic review on the use of residual probing depth, bleeding on
1675 probing and furcation status following initial periodontal therapy to predict further attachment and
1676 tooth loss. *Journal of clinical periodontology*, 29, 82–89.
- 1677 Rideout, J. R., Caporaso, G., Bolyen, E., McDonald, D., Baeza, Y. V., Alastuey, J. C., ... Sharma, K.
1678 (2018, December). *biocore/scikit-bio: scikit-bio 0.5.5: More compositional methods added*. Zenodo.
1679 Retrieved from <https://doi.org/10.5281/zenodo.2254379> doi: 10.5281/zenodo.2254379
- 1680 Rôças, I. N., Siqueira Jr, J. F., Santos, K. R., Coelho, A. M., & de Janeiro, R. (2001). “red com-
1681 plex”(bacteroides forsythus, porphyromonas gingivalis, and treponema denticola) in endodontic
1682 infections: a molecular approach. *Oral Surgery, Oral Medicine, Oral Pathology, Oral Radiology,*
1683 *and Endodontology*, 91(4), 468–471.
- 1684 Romero, R., Dey, S. K., & Fisher, S. J. (2014). Preterm labor: one syndrome, many causes. *Science*,
1685 345(6198), 760–765.

- 1686 Romero, R., Hassan, S. S., Gajer, P., Tarca, A. L., Fadrosh, D. W., Nikita, L., ... others (2014). The
1687 composition and stability of the vaginal microbiota of normal pregnant women is different from
1688 that of non-pregnant women. *Microbiome*, 2, 1–19.
- 1689 Rosan, B., & Lamont, R. J. (2000). Dental plaque formation. *Microbes and infection*, 2(13), 1599–1607.
- 1690 Rubio, C. A., Lang-Schwarz, C., & Vieth, M. (2022). Further study on field cancerization in the human
1691 colon. *Anticancer Research*, 42(12), 5891–5895.
- 1692 Schwabe, R. F., & Jobin, C. (2013). The microbiome and cancer. *Nature Reviews Cancer*, 13(11),
1693 800–812.
- 1694 Segata, N., Izard, J., Waldron, L., Gevers, D., Miropolsky, L., Garrett, W. S., & Huttenhower, C. (2011).
1695 Metagenomic biomarker discovery and explanation. *Genome biology*, 12, 1–18.
- 1696 Sen, P. C., Hajra, M., & Ghosh, M. (2020). Supervised classification algorithms in machine learning: A
1697 survey and review. In *Emerging technology in modelling and graphics: Proceedings of iem graph
1698 2018* (pp. 99–111).
- 1699 Sepich-Poore, G. D., Zitvogel, L., Straussman, R., Hasty, J., Wargo, J. A., & Knight, R. (2021). The
1700 microbiome and human cancer. *Science*, 371(6536), eabc4552.
- 1701 Sharma, S., & Tripathi, P. (2019). Gut microbiome and type 2 diabetes: where we are and where to go?
1702 *The Journal of nutritional biochemistry*, 63, 101–108.
- 1703 Shi, N., Li, N., Duan, X., & Niu, H. (2017). Interaction between the gut microbiome and mucosal
1704 immune system. *Military Medical Research*, 4, 1–7.
- 1705 Simpson, E. (1949). Measurement of diversity. *Nature*, 163.
- 1706 Sokal, R. R., & Sneath, P. H. (1963). Principles of numerical taxonomy.
- 1707 Song, M., Chan, A. T., & Sun, J. (2020). Influence of the gut microbiome, diet, and environment on risk
1708 of colorectal cancer. *Gastroenterology*, 158(2), 322–340.
- 1709 Söreide, K., Janssen, E., Söiland, H., Körner, H., & Baak, J. (2006). Microsatellite instability in colorectal
1710 cancer. *Journal of British Surgery*, 93(4), 395–406.
- 1711 Sørensen, T. (1948). A method of establishing groups of equal amplitude in plant sociology based on
1712 similarity of species content and its application to analyses of the vegetation on danish commons.
1713 *Biologiske skrifter*, 5, 1–34.
- 1714 Sotiriadis, A., Papatheodorou, S., Kavvadias, A., & Makrydimas, G. (2010). Transvaginal cervical
1715 length measurement for prediction of preterm birth in women with threatened preterm labor: a
1716 meta-analysis. *Ultrasound in Obstetrics and Gynecology: The Official Journal of the International
1717 Society of Ultrasound in Obstetrics and Gynecology*, 35(1), 54–64.
- 1718 Spss, I., et al. (2011). Ibm spss statistics for windows, version 20.0. *New York: IBM Corp*, 440, 394.
- 1719 Stafford, G., Roy, S., Honma, K., & Sharma, A. (2012). Sialic acid, periodontal pathogens and tannerella
1720 forsythia: stick around and enjoy the feast! *Molecular Oral Microbiology*, 27(1), 11–22.
- 1721 Stout, M. J., Conlon, B., Landeau, M., Lee, I., Bower, C., Zhao, Q., ... Mysorekar, I. U. (2013).
1722 Identification of intracellular bacteria in the basal plate of the human placenta in term and preterm
1723 gestations. *American journal of obstetrics and gynecology*, 208(3), 226–e1.
- 1724 Strong, W. (2002). Assessing species abundance unevenness within and between plant communities.

- 1725 *Community Ecology*, 3(2), 237–246.
- 1726 Sultan, S., El-Mowafy, M., Elgaml, A., Ahmed, T. A., Hassan, H., & Mottawea, W. (2021). Metabolic
1727 influences of gut microbiota dysbiosis on inflammatory bowel disease. *Frontiers in physiology*, 12,
1728 715506.
- 1729 Suzuki, N., Nakano, Y., Yoneda, M., Hirofumi, T., & Hanioka, T. (2022). The effects of cigarette
1730 smoking on the salivary and tongue microbiome. *Clinical and Experimental Dental Research*, 8(1),
1731 449–456.
- 1732 Swidsinski, A., Khilkin, M., Kerjaschki, D., Schreiber, S., Ortner, M., Weber, J., & Lochs, H. (1998).
1733 Association between intraepithelial escherichia coli and colorectal cancer. *Gastroenterology*,
1734 115(2), 281–286.
- 1735 Swift, D., Cresswell, K., Johnson, R., Stilianoudakis, S., & Wei, X. (2023). A review of normalization
1736 and differential abundance methods for microbiome counts data. *Wiley Interdisciplinary Reviews: Computational Statistics*, 15(1), e1586.
- 1737 Tanner, A. C., Kent Jr, R., Kanasi, E., Lu, S. C., Paster, B. J., Sonis, S. T., ... Van Dyke, T. E. (2007).
1738 Clinical characteristics and microbiota of progressing slight chronic periodontitis in adults. *Journal of clinical periodontology*, 34(11), 917–930.
- 1739 Tanner, A. C., Paster, B. J., Lu, S. C., Kanasi, E., Kent Jr, R., Van Dyke, T., & Sonis, S. T. (2006).
1740 Subgingival and tongue microbiota during early periodontitis. *Journal of dental research*, 85(4),
1741 318–323.
- 1742 Tejeda, M., Farrell, J., Zhu, C., Haines, J. L., Wang, L.-S., Schellenberg, G. D., ... others (2021). Multiple
1743 viruses detected in human dna are associated with alzheimer disease risk. *Alzheimer's & Dementia*,
1744 17, e054585.
- 1745 Teles, F., Wang, Y., Hajishengallis, G., Hasturk, H., & Marchesan, J. T. (2021). Impact of systemic
1746 factors in shaping the periodontal microbiome. *Periodontology 2000*, 85(1), 126–160.
- 1747 Thaiss, C. A., Zmora, N., Levy, M., & Elinav, E. (2016). The microbiome and innate immunity. *Nature*,
1748 535(7610), 65–74.
- 1749 Tian, R., Liu, H., Feng, S., Wang, H., Wang, Y., Wang, Y., ... Zhang, S. (2021). Gut microbiota dysbiosis
1750 in stable coronary artery disease combined with type 2 diabetes mellitus influences cardiovascular
1751 prognosis. *Nutrition, Metabolism and Cardiovascular Diseases*, 31(5), 1454–1466.
- 1752 Tilg, H., Kaser, A., et al. (2011). Gut microbiome, obesity, and metabolic dysfunction. *The Journal of
1753 clinical investigation*, 121(6), 2126–2132.
- 1754 Tonetti, M. S., Greenwell, H., & Kornman, K. S. (2018). Staging and grading of periodontitis: Framework
1755 and proposal of a new classification and case definition. *Journal of periodontology*, 89, S159–S172.
- 1756 Tringe, S. G., & Hugenholtz, P. (2008). A renaissance for the pioneering 16s rRNA gene. *Current opinion
1757 in microbiology*, 11(5), 442–446.
- 1758 Tucker, C. M., Cadotte, M. W., Carvalho, S. B., Davies, T. J., Ferrier, S., Fritz, S. A., ... others (2017). A
1759 guide to phylogenetic metrics for conservation, community ecology and macroecology. *Biological
1760 Reviews*, 92(2), 698–715.
- 1761 Ulger Toprak, N., Yagci, A., Gulluoglu, B., Akin, M., Demirkalem, P., Celenk, T., & Soyletir, G. (2006).

- 1764 A possible role of bacteroides fragilis enterotoxin in the aetiology of colorectal cancer. *Clinical*
1765 *microbiology and infection*, 12(8), 782–786.
- 1766 Ursell, L. K., Metcalf, J. L., Parfrey, L. W., & Knight, R. (2012). Defining the human microbiome.
1767 *Nutrition reviews*, 70(suppl_1), S38–S44.
- 1768 Utzschneider, K. M., Kratz, M., Damman, C. J., & Hullarg, M. (2016). Mechanisms linking the gut
1769 microbiome and glucose metabolism. *The Journal of Clinical Endocrinology & Metabolism*,
1770 101(4), 1445–1454.
- 1771 Vander Haar, E. L., So, J., Gyamfi-Bannerman, C., & Han, Y. W. (2018). Fusobacterium nucleatum and
1772 adverse pregnancy outcomes: epidemiological and mechanistic evidence. *Anaerobe*, 50, 55–59.
- 1773 Van der Maaten, L., & Hinton, G. (2008). Visualizing data using t-sne. *Journal of machine learning*
1774 *research*, 9(11).
- 1775 Vasen, H. F., Mecklin, J.-P., Khan, P. M., & Lynch, H. T. (1991). The international collaborative group
1776 on hereditary non-polyposis colorectal cancer (icg-hnpcc). *Diseases of the Colon & Rectum*, 34(5),
1777 424–425.
- 1778 Vilar, E., & Gruber, S. B. (2010). Microsatellite instability in colorectal cancer—the stable evidence.
1779 *Nature reviews Clinical oncology*, 7(3), 153–162.
- 1780 Walker, M. A., Pedamallu, C. S., Ojesina, A. I., Bullman, S., Sharpe, T., Whelan, C. W., & Meyerson, M.
1781 (2018). Gatk pathseq: a customizable computational tool for the discovery and identification of
1782 microbial sequences in libraries from eukaryotic hosts. *Bioinformatics*, 34(24), 4287–4289.
- 1783 Weaver, W. (1963). *The mathematical theory of communication*. University of Illinois Press.
- 1784 Whiteside, S. A., Razvi, H., Dave, S., Reid, G., & Burton, J. P. (2015). The microbiome of the urinary
1785 tract—a role beyond infection. *Nature Reviews Urology*, 12(2), 81–90.
- 1786 Witkin, S. (2019). Vaginal microbiome studies in pregnancy must also analyse host factors. *BJOG: An*
1787 *International Journal of Obstetrics & Gynaecology*, 126(3), 359–359.
- 1788 Wong, T.-T., & Yeh, P.-Y. (2019). Reliable accuracy estimates from k-fold cross validation. *IEEE*
1789 *Transactions on Knowledge and Data Engineering*, 32(8), 1586–1594.
- 1790 Wyss, C., Moter, A., Choi, B.-K., Dewhirst, F., Xue, Y., Schüpbach, P., ... Guggenheim, B. (2004).
1791 *Treponema putidum* sp. nov., a medium-sized proteolytic spirochaete isolated from lesions of
1792 human periodontitis and acute necrotizing ulcerative gingivitis. *International journal of systematic*
1793 *and evolutionary microbiology*, 54(4), 1117–1122.
- 1794 Xia, Y. (2023). Statistical normalization methods in microbiome data with application to microbiome
1795 cancer research. *Gut Microbes*, 15(2), 2244139.
- 1796 Yaman, E., & Subasi, A. (2019). Comparison of bagging and boosting ensemble machine learning methods
1797 for automated emg signal classification. *BioMed research international*, 2019(1), 9152506.
- 1798 Yang, I., Claussen, H., Arthur, R. A., Hertzberg, V. S., Geurs, N., Corwin, E. J., & Dunlop, A. L. (2022).
1799 Subgingival microbiome in pregnancy and a potential relationship to early term birth. *Frontiers in*
1800 *cellular and infection microbiology*, 12, 873683.
- 1801 Yildiz, B., Bilbao, J. I., & Sproul, A. B. (2017). A review and analysis of regression and machine learning
1802 models on commercial building electricity load forecasting. *Renewable and Sustainable Energy*

- 1803 *Reviews*, 73, 1104–1122.
- 1804 Yoshimura, F., Murakami, Y., Nishikawa, K., Hasegawa, Y., & Kawaminami, S. (2009). Surface
1805 components of *porphyromonas gingivalis*. *Journal of periodontal research*, 44(1), 1–12.
- 1806 Zhang, C.-Z., Cheng, X.-Q., Li, J.-Y., Zhang, P., Yi, P., Xu, X., & Zhou, X.-D. (2016). Saliva in the
1807 diagnosis of diseases. *International journal of oral science*, 8(3), 133–137.
- 1808 Zhou, X., Wang, L., Xiao, J., Sun, J., Yu, L., Zhang, H., ... others (2022). Alcohol consumption,
1809 dna methylation and colorectal cancer risk: Results from pooled cohort studies and mendelian
1810 randomization analysis. *International journal of cancer*, 151(1), 83–94.
- 1811 Zhu, W., & Lee, S.-W. (2016). Surface interactions between two of the main periodontal pathogens:
1812 *Porphyromonas gingivalis* and *tannerella forsythia*. *Journal of periodontal & implant science*,
1813 46(1), 2–9.
- 1814 Zhu, X., Han, Y., Du, J., Liu, R., Jin, K., & Yi, W. (2017). Microbiota-gut-brain axis and the central
1815 nervous system. *Oncotarget*, 8(32), 53829.
- 1816 Zhuang, Y., Wang, H., Jiang, D., Li, Y., Feng, L., Tian, C., ... others (2021). Multi gene mutation
1817 signatures in colorectal cancer patients: predict for the diagnosis, pathological classification, staging
1818 and prognosis. *BMC cancer*, 21, 1–16.

Acknowledgments

1820 I would like to disclose my earnest appreciation for my advisor, Professor **Semin Lee**, who provided
 1821 solicitous supervision and cherished opportunities throughout the course of my research. His advice and
 1822 consultation encouraged me to become as a researcher and to receive all humility and gentleness. I am also
 1823 grateful to all of my committee members, Professor **Taejoon Kwon**, Professor **Eunhee Kim**, Professor
 1824 **Kyemyung Park**, and Professor **Min Hyuk Lim**, for their meaningful mentions and suggestions.

1825 I extend my deepest gratitude to my Lord, **the Flying Spaghetti Monster**, His Noodly Appendage
 1826 has guided me through the twist and turns of this academic journey. His presence, ever comforting and
 1827 mysterious, has been a source of strength and humor during both highs and lows. In moments of doubt, I
 1828 found solace in the belief that you were there, gently reminding me to keep faith in the process. His Holy
 1829 Noodle has nourished my mind, and for that, I am truly overwhelmed. May His Holy Noodle continue to
 1830 guide me in all my future endeavors. *R’Amen.*

1831 I would like to extend my heartfelt gratitude to Professor **You Mi Hong** for her invaluable guidance
 1832 and insightful advice on PTB study. Her expertise in maternal and fetal health, along with her deep under-
 1833 standing of statistical and clinical interpretations, greatly contributed to refining the analytical framework
 1834 of this study. Her constructive feedback and thoughtful discussions provided critical perspectives that
 1835 enhanced the robustness and relevance of the research findings. I sincerely appreciate her generosity
 1836 in sharing her knowledge and effort, as well as her encouragement throughout my Ph.D. journey. Her
 1837 support has been instrumental in strengthening this work, and I am truly grateful for her contributions.

1838 I also would like to express my sincere gratitude for Professor **Jun Hyeok Lim** for his invaluable
 1839 guidance and insightful advice on lung cancer study. His expertise in cancer genomics and data interpreta-
 1840 tion provided essential perspectives that greatly enriched the analytical approach of my Ph.D. journey. His
 1841 constructive feedback and thoughtful discussion helped refine methodologies and enhance the scientific
 1842 rigor of the research. I deeply appreciate his willingness to share his knowledge and expertise, which has
 1843 been instrumental in shaping key aspects of this work. His support and encouragement have been truly
 1844 inspiring, and I am grateful for the opportunity to have benefited from his mentorship.

1845 I would like to extend my heartfelt gratitude to my colleagues of the **Computational Biology Lab @**
 1846 **UNIST**, whose collaboration, friendship, brotherhood, and support have been an invaluable part of my
 1847 journey. Your willingness to share insights, engage in thoughtful discussions, and offer encouragement
 1848 during the challenging moments of research has significantly shaped my academic experience. The
 1849 camaraderie in Computational Biology Lab made even the most demanding days more enjoyable, and I
 1850 am deeply grateful for the collaborative environment we created together. I appreciate you for standing
 1851 by my side throughout this Ph.D. journey.

1852 I would like to express my heartfelt gratitude to **my family**, whose unwavering support has been the
 1853 foundation of everything I have achieved. Your love, encouragement, and belief in me have sustained me
 1854 through every challenge, and I could not have come this far without you. From your words of wisdom to
 1855 your patience and understanding, each of you has played a vital role in helping me navigate this journey.
 1856 The strength and comfort I have drawn from our family bond have been my greatest source of resilience.

1857 Your presence, both near and far, has filled my life with warmth and motivation. I am deeply grateful for
1858 your unconditional love and for always being there when I needed you the most. Thank you for being my
1859 constant source of strength and inspiration.

1860 I am incredibly pleased to my friends, especially my GSHS alumni (**이망특**), for their unwavering
1861 support and encouragement throughout this journey. The bonds we formed back in our school days have
1862 only grown stronger over the years, and I am fortunate to have had such loyal and understanding friends
1863 by my side. Your constant words of motivation, and even moments of levity during stressful times have
1864 helped keep me grounded. Whether it was a late-night conversations, a shared laugh, or a simple message
1865 of reassurance, you all have played a vital role in keeping me focused and motivated. I am relieved for the
1866 ways you celebrated each small achievement with me and how you patiently listened to my worries. The
1867 memories of our shared past provided me with comfort and a sense of stability when the road ahead felt
1868 uncertain. I could not have reached this point without the love and friendship that you all have generously
1869 given. Each of your, in your unique way, has contributed to this dissertation, even if indirectly, and for
1870 that, I am forever beholden. I look forward to continuing our friendship as we all grow in our individual
1871 paths, knowing that the support we share is something truly special.

1872 I would like to express my deepest recognition to **my girlfriend (expected)** for her unwavering
1873 support, patience, and companionship throughout my Ph.D. journey. Her presence has been a constant
1874 source of comfort and motivation, helping me navigate the challenges of research and writing with
1875 renewed energy. Through moments of frustration and accomplishment alike, her encouragement has
1876 reminded me of the importance of balance and perseverance. Her kindness, understanding, and belief
1877 in me have been invaluable, making even the most difficult days feel lighter. I am truly grateful for her
1878 support and for sharing this journey with me, and I look forward to all the moments we will continue to
1879 experience together.

1880 I would like to express my sincere gratitude to the amazing members of my animal protection groups,
1881 DRDR (**두루두루**) and UNIMALS (**유니멀스**), whose dedication and compassion have been a constant
1882 source of motivation. Your unwavering commitment to improving the lives of animals has inspired me
1883 throughout this journey. I am also thankful for the beautiful cats we have cared for, whose presence
1884 brought both joy and purpose to our allegiance. Their playful spirits and gentle companionship served as
1885 daily reminders of why we continue to fight for animal rights. The bond we share, both with each other
1886 and with the animals we protect, has enriched my life in countless ways. I appreciate you all again for
1887 your support, dedication, and for being part of this meaningful cause.

1888 I would like to express my deepest gratitude to **everyone** I have had the honor of meeting throughout
1889 this journey. Your kindness, encouragement, and support have carried me through both the challenging
1890 and rewarding moments of my life. Whether through a kind word, thoughtful advice, or simply being
1891 there when I needed it most, your presence has made all the difference. I am incredibly fortunate to have
1892 received such generosity and warmth from those around me, and I do not take it for granted. Every act
1893 of kindness, no matter how big or small, has been a source of strength and motivation for me. To all
1894 my friends, colleagues, mentors, and beloved ones, thank you for your unwavering support. I am truly
1895 grateful for each of you, and your kindness has left an indelible mark on my journey.

1896 My Lord, *the Flying Spaghetti Monster*,
1897 give us grace to accept with serenity the things that cannot be changed,
1898 courage to change the things that should be changed,
1899 and the wisdom to distinguish the one from the other.

1900
1901 Glory be to *the Meatball*, to *the Sauce*, and to *the Holy Noodle*.
1902 As it was in the beginning, is now, and ever shall be.

1903 *R'Amen.*



May your progress be evident to all

